Medicinal Research Reviews

WILEY

REVIEW ARTICLE OPEN ACCESS

Boronic Acid Inhibitors of β-Lactamases: A Promising Strategy Against Antimicrobial Resistance

Nicolò Santi[1] | Federico Corsini[1,2] | Robert A. Bonomo[3,4,5,6,7] | Emilia Caselli[1] | Fabio Prati[1]

[1]Department of Life Sciences, Università degli Studi di Modena e Reggio Emilia (UNIMORE), Modena, Italy | [2]Department of Life Sciences, Health Innovative Products and Technologies (HIP-TECH) PhD Program, Università degli Studi di Modena e Reggio Emilia (UNIMORE), Modena, Italy | [3]Department of Molecular Biology and Microbiology, Case Western Reserve University School of Medicine, Cleveland, Ohio, USA | [4]CWRU-Cleveland VAMC Center for Antimicrobial Resistance and Epidemiology (Case VA CARES), Cleveland, Ohio, USA | [5]Louis Stokes Cleveland Department of Veterans Affairs Medical Center, Cleveland, Ohio, USA | [6]Department of Medicine, Case Western Reserve University School of Medicine, Cleveland, Ohio, USA | [7]Departments of Pharmacology, Biochemistry, and Proteomics and Bioinformatics, Case Western Reserve University School of Medicine, Cleveland, Ohio, USA

Correspondence: Fabio Prati (fabio.prati@unimore.it)

Received: 19 September 2025 | **Revised:** 23 July 2026 | **Accepted:** 29 July 2026

Funding: European Union's Horizon Europe research and innovation programme under the Marie Sklodowska-Curie, Grant/Award Number: 101068156; Ministero dell'Università e della Ricerca, Grant/Award Number: 2022WBPFSC; National Institutes of Health (NIH), Grant/Award Number: R01AI072219

Keywords: antimicrobial resistance | BATSI | boronic acids | β-lactamase inhibitors | β-lactamases

ABSTRACT

The rise of antimicrobial resistance (AMR) poses a critical threat to global health, mostly due to the proliferation of β-lactamases, a class of enzymes responsible for the inactivation of β-lactam antibiotics. Among the most promising strategies to restore β-lactam efficacy is the use of β-lactamase inhibitors (BLIs), with boronic acid derivatives emerging as a pivotal and chemically versatile class. These compounds act as transition-state analogs, forming reversible covalent bonds with the catalytic serine of serine β-lactamases (SBLs), effectively mimicking the tetrahedral intermediate of β-lactam hydrolysis. Their electron-deficient boron atom, combined with a tunable scaffold, allows fine modulation of potency, selectivity, and pharmacokinetic properties. This review traces the evolution of boronic acid-based BLIs from early phenylboronic acids to next-generation acyclic and cyclic derivatives, highlighting key structure-activity relationships, binding mechanisms, and microbiological profiles. Clinically approved agents such as vaborbactam, as well as investigational compounds including taniborbactam, xeruborbactam, and benzoxaboroles, are discussed in the context of their therapeutic relevance and spectrum of activity. Particular attention is given to their ability to inhibit class A and C enzymes, with ongoing efforts aimed at extending coverage to class D and metallo-β-lactamases. Additionally, the review explores innovative approaches such as kinetic target-guided synthesis and fragment-based design to expand the chemical space of boronic acid pharmacophores. Together, these advances underscore the potential of boronic acid-based BLIs as powerful tools in overcoming β-lactamase-mediated resistance and developing next-generation antimicrobial therapies.

1 | Introduction

1.1 | β-Lactamase-Mediated Resistance

The alarming rise of antimicrobial resistance (AMR) is pushing modern medicine toward a post-antibiotic era, an undesirable scenario in which antibiotics may no longer be effective for the treatment of common bacterial infections [1, 2]. Among the pathogens driving this crisis, resistant Gram-negative bacteria are of particular concern, as both genetic mutations and horizontal gene transfer (HGT) have contributed to the emergence of multidrug-resistant, extensively drug-resistant, and pandrug-resistant (MDR, XDR, and PDR) pathogens [3]. These organisms are responsible for a substantial proportion of healthcare-associated infections and an increasing number of community-

acquired infections [4]. Notably, carbapenem-resistant *Acinetobacter baumannii* [5], oxyimino-cephalosporin-resistant Enterobacterales [6], particularly *Klebsiella pneumoniae* and *Escherichia coli*, and carbapenem-resistant Enterobacterales are among the pathogens most frequently associated with severe and difficult-to-treat infections, often accompanied by high morbidity and mortality [7–9]. These resistant bacteria compromise the efficacy of multiple chemically distinct classes of antibiotics, including β-lactams, which remain the most widely used agents for the treatment of both common and severe bacterial infections [10]. β-Lactams exert their antibacterial effect through *quasi*-irreversible acylation of the catalytic serine residue of penicillin-binding proteins (PBPs, EC 3.4.16.4), a family of bacterial *DD*-transpeptidases essential for peptidoglycan biosynthesis and cell-wall integrity [11–14]. Gram-negative bacteria can counteract β-lactam antibiotic activity through several mechanisms, including reduced outer-membrane permeability (porin mutation) [13, 15], active efflux (overexpression of efflux pumps), target modification (PBP mutation), and, most importantly, enzymatic drug hydrolysis by β-lactamases (Figure 1) [16–21].

β-Lactamases (EC 3.5.2.6) are a conserved yet evolutionarily diverse family of bacterial hydrolases capable of inactivating β-lactam antibiotics by cleaving their characteristic four-membered ring [22]. By efficiently neutralizing β-lactams before target engagement, β-lactamases represent the most successful bacterial strategy for overcoming this antibiotic class and are therefore a central focus of inhibitor development [23]. In Gram-positive bacteria, β-lactamases are typically secreted into the extracellular milieu or associated with the cell surface [24], whereas in Gram-negative organisms they are generally localized in the periplasm, where they can intercept β-lactams before the antibiotics reach the PBP targets [25]. Notably, some enzymes, such as NDM-1 and selected OXA-type carbapenemases, deviate from this pattern, as they can be lipidated, associated with the outer membrane, and exported in outer membrane vesicles, thereby contributing to enzyme stability and dissemination of resistance [26, 27].

Given broad-spectrum penicillins and cephalosporins remain among the most widespread antibiotics, the extensive dissemination of β-lactamase-producing Gram-negative bacteria poses a major threat to human and animal health, complicating antimicrobial stewardship and resistance containment across clinical, veterinary, and agricultural settings [28]. This threat is further amplified by the spread of extended-spectrum β-lactamases (ESBLs), which hydrolyze oxyimino-cephalosporins [29], and by the emergence of carbapenemases, which confer resistance to penicillins, cephalosporins, monobactams, and carbapenems [30].

β-Lactamases can be classified according to the Ambler scheme into four distinct classes (A, B, C, and D) based on amino acid sequence homology and active-site architecture [31, 32]. A further macro-categorization originates from the active site residue/atoms responsible for the catalytic properties of these hydrolases and defines classes A, C, and D as serine

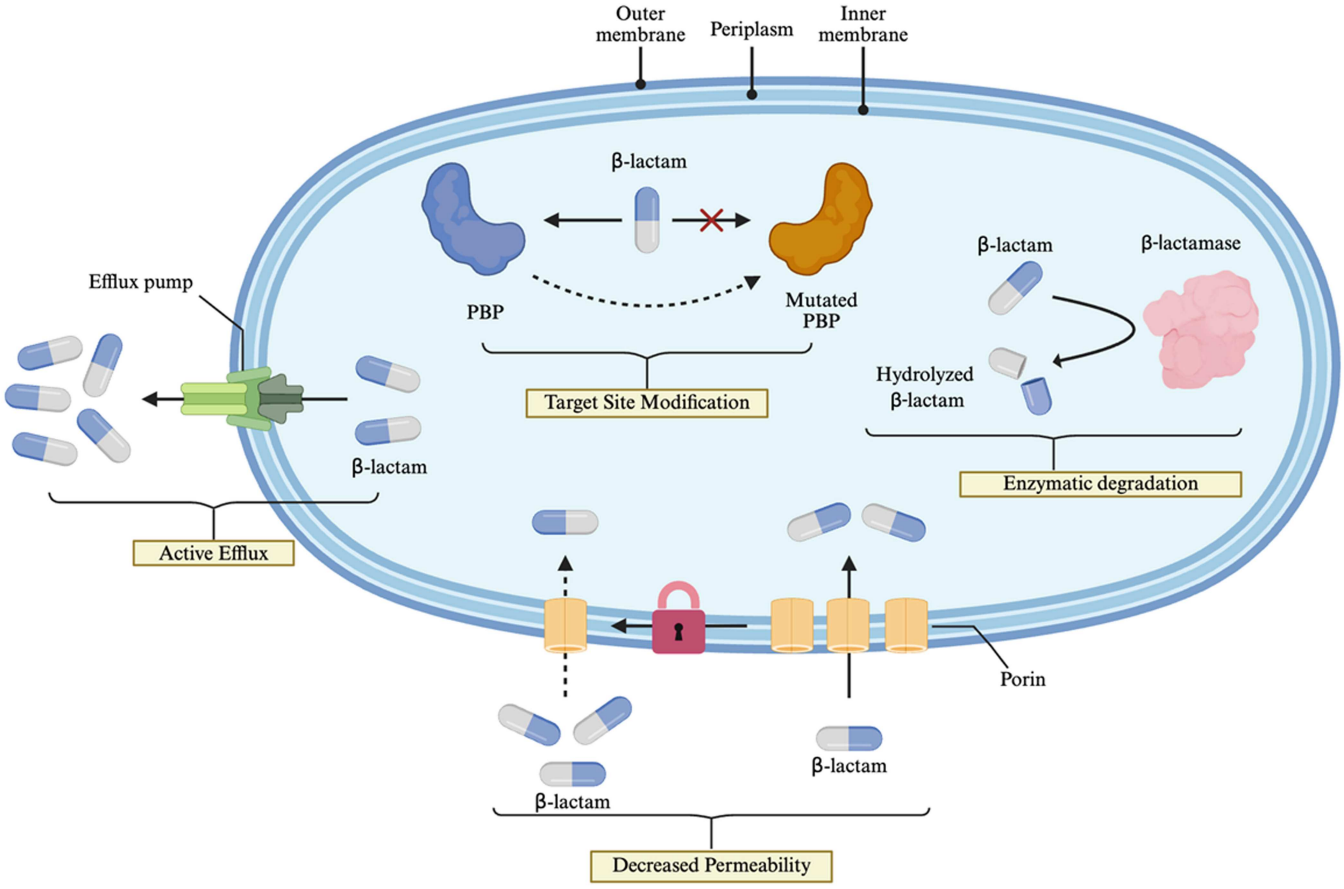

FIGURE 1 | Schematic representation for the main molecular mechanisms associated with β-lactams resistance in Gram-negative bacteria. Figure 1 was prepared by the authors based on a relevant reference [16]. [Color figure can be viewed at wileyonlinelibrary.com]

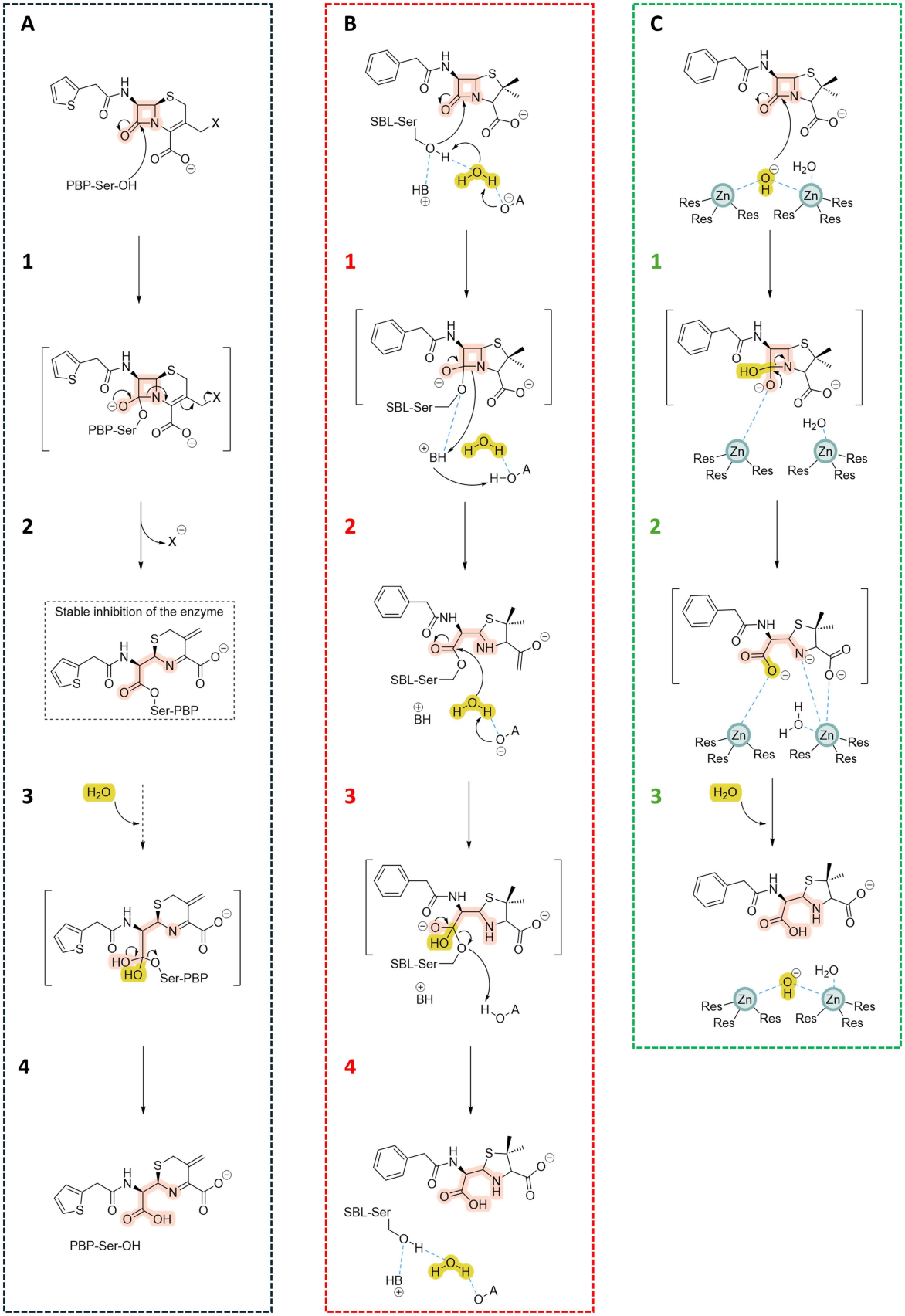

SCHEME 1 | Legend on next page.

β-lactamases (SBLs), whereas class B enzymes comprise the entire metallo-β-lactamases (MBLs) domain [31]. This distinction is mechanistically important as SBLs share key catalytic and evolutionary features with PBPs, the physiological targets of β-lactam antibiotics. Both PBPs and SBLs react with β-lactams through acylation of an active-site serine residue, reflecting their common evolutionary origin from ancestral *DD*-peptidases [22, 33–35]. However, whereas in PBPs the resulting acyl-enzyme complex is long-lived and undergoes very slow deacylation, thereby blocking peptidoglycan cross-linking and impairing cell-wall biosynthesis, SBLs have acquired the ability to efficiently catalyze the hydrolysis of β-lactams by accelerating the breakdown of the acyl-enzyme intermediate [33]. In contrast, MBLs catalyze β-lactam hydrolysis via a metal-dependent mechanism, wherein one or two zinc ions coordinate and activate a water molecule responsible for attack on the β-lactam ring [23, 36]. The mechanistic relationships between PBPs, serine β-lactamases, and metallo-β-lactamases are summarized in Scheme 1. This mechanistic divergence is highly relevant for inhibitor design, since most classical β-lactamase inhibitors primarily target SBLs, whereas the development of compounds active against both SBLs and MBLs remains a major challenge.

In addition to the Ambler classification, the Bush-Jacoby (also known as Bush-Jacoby-Medeiros) functional classification groups β-lactamases according to substrate profile and inhibitor susceptibility (Figure 2) [42]. In the context of this review, Ambler classification is used as the primary organizational framework because it aligns more directly with catalytic mechanism and inhibitor design, while the corresponding Bush-Jacoby groups for the principal enzymes discussed are summarized in Table 1 [42].

Excellent reviews comprehensively covering the evolution, clinical relevance, structural diversity, localization and biogenesis of β-lactamases have been published, offering valuable insights into their role in antibiotic resistance and therapeutic challenges [22, 23, 27, 30, 36, 38, 42, 44, 45].

1.2 | β-Lactamase Inhibitors: Current and Evolving Landscape

To overcome the hydrolytic activity of β-lactamases, two main strategies have been pursued [46, 47]. The first involves designing novel or structurally optimized β-lactam antibiotics with improved resistance to enzymatic degradation [23, 38, 47, 48]. While this approach has led to significant advances, such as the development of expanded-spectrum cephalosporins and carbapenems, it is inherently constrained by the limited chemical space that can be explored, due to structural modifications being confined to the same region of the β-lactam scaffold. This limitation, in turn, contributes to the ongoing challenge of resistance mediated by β-lactamases [49]. Moreover, the high costs, extended timelines, and substantial resources required for the R&D efforts often render this strategy not very practical and viable [49].

A more targeted and widely adopted strategy to combat β-lactamase-mediated resistance involves the development of specific inhibitors directed against β-lactamases [28, 50]. These molecules, known as β-lactamase inhibitors (BLIs), typically exhibit little to no intrinsic antibacterial activity on their own and function as adjuvants [47]. When co-administered with β-lactam antibiotics, they protect the antibiotic from enzymatic degradation, thereby restoring its antibacterial efficacy [28, 50, 51]. These inhibitors have become a cornerstone of treatment strategies against multidrug-resistant Gram-negative bacteria, leading to various approved β-lactam/BLI combinations and several others currently in clinical trials as summarized in Chart 1 [46, 52–54]. These inhibitors are generally classified into three major classes based on their structure and mechanism of action [47].

1.2.1 | β-Lactam-Derived BLIs

The "first generation" of BLIs, initially reported in 1976 with the discovery of clavulanic acid, also includes sulbactam, and tazobactam (see Chart 1, orange dash-dot box) [47]. Recently, enmetazobactam, a *N*-methylated derivative of tazobactam (formerly known as AAI101, Allecra Therapeutics), has also been approved [55]. These β-lactam-derived molecules act as mechanism-based inhibitors of serine β-lactamases by acylating the catalytic serine residue to form covalent acyl-enzyme complexes. These intermediates can subsequently rearrange into stabilized inhibitory species, including bridged or conjugated forms, that are poorly susceptible to deacylation [47, 56, 57]. Though they offered significant clinical benefit when first introduced, these classical inhibitors primarily target class A β-lactamases and are less effective against class C and class D enzymes [49]. Structurally related to penicillins or cephalosporins, these compounds therefore act as "suicide substrates," trapping the enzyme in long-lived inactive forms [38]. For example, clavulanic acid, a naturally occurring oxapenem, has been widely used in combination with amoxicillin, while sulbactam and tazobactam have been co-formulated with ampicillin and piperacillin, respectively [49]. While classical inhibitors laid the foundation, the emergence of ESBLs and carbapenemases, such as KPCs and MBLs, necessitated the development of broader-spectrum and more structurally diverse inhibitors [49]. More recently, cefepime/enmetazobactam has demonstrated efficacy against ESBL- and OXA-48-producing

SCHEME 1 | Comparison of the catalytic mechanism of β-lactams in PBPs, class A serine β-lactamases, and metallo-β-lactamases (MBLs). (A) PBPs are acylated by β-lactams at the catalytic serine, generating a long-lived acyl-enzyme complex, which undergoes slow deacylation relative to SBLs, ultimately resulting in inhibition of peptidoglycan cross-linking. (B) Class A SBLs also form a serine-linked acyl-enzyme intermediate, but efficiently deacylate it through activation of a catalytic water molecule, thereby hydrolyzing and inactivating the antibiotic. (C) Class B β-lactamases hydrolyze β-lactams through a Zn(II)-dependent mechanism in which an activated water/hydroxide nucleophile attacks the β-lactam carbonyl directly, without formation of a serine-linked acyl-enzyme intermediate and proceeds through an anionic intermediate [37]. B = General basic residue; A = General acidic residue; Res = General residue. Scheme 1 was prepared by the authors based on relevant references [38–41]. [Color figure can be viewed at wileyonlinelibrary.com]

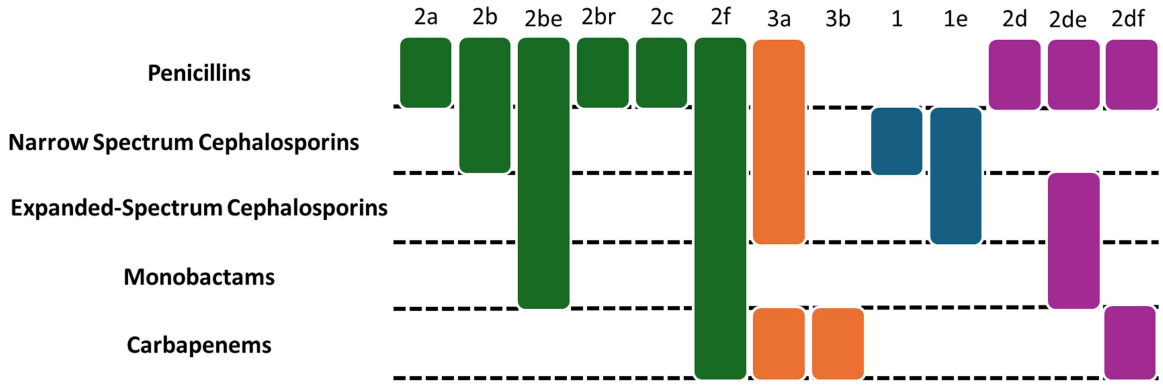

FIGURE 2 | Spectrum of activity for the β-lactamase groups subdivided by the Bush-Jacoby classification. Ambler's class A: green; class B: orange; class C: blue; class D: purple. [Color figure can be viewed at wileyonlinelibrary.com]

Enterobacterales, with improved activity relative to piperacillin/tazobactam [49, 55, 58].

1.2.2 | *Diazabicyclooctane (DBO)-Based BLIs*

A major breakthrough in β-lactamase inhibition came with the development of diazabicyclooctane (DBO)-based β-lactamase inhibitors (Chart 1, blue dash-dot box) [59]. Avibactam (AVE1330A and NXL104), the first approved DBO in 2015, pioneered a novel inhibitory mechanism by forming a reversible covalent bond with the catalytic serine of SBLs [60]. This reversibility indicates the pharmacophore is not hydrolyzed during inhibition, allowing avibactam to retain its inhibitory activity over multiple catalytic cycles, although irreversible inhibition occurs in class D enzymes and desulfation in class A KPC-2 [61–63]. Avibactam exhibits broad-spectrum activity against class A (i.e., TEM, SHV, and KPCs), some class C (AmpC), and limited class D enzymes (no inhibition on OXA-24/40) [49, 64]. It is approved in combination with ceftazidime, and aztreonam/avibactam also extends coverage against MBL-producing Enterobacterales [53, 65]. Subsequent DBOs developed include relebactam (MK-7655), nacubactam (OP0595, RO7079901, or RG6080), and zidebactam (WCK5107) [49]. Relebactam, featuring a piperidine moiety, is used in combination with imipenem-cilastatin and targets mainly class A and C enzymes [66–68]. Nacubactam and zidebactam display dual modes of action, combining β-lactamase inhibition with direct binding to PBPs, thereby enhancing antibacterial activity. Notably, zidebactam is characterized primarily by high-affinity binding to PBP2, which underpins its distinctive β-lactam enhancer profile [69–71]. Both are under clinical development: nacubactam with meropenem (Phase 1), and zidebactam with cefepime (Phase 3) for cUTIs and pyelonephritis [46, 72]. Durlobactam (formerly ETX2514) is a next-generation DBO engineered for enhanced rigidity and affinity, especially toward class D carbapenemases, while retaining its inhibitory spectrum against class A and C β-lactamases [73–75]. Combined with sulbactam (Xacduro, FDA approved), is approved for hospital-acquired and ventilator-associated bacterial pneumonia caused by the *A. baumannii-calcoaceticus* complex, although its complex synthesis presents manufacturing challenges [49, 53, 75]. New-generation DBOs in clinical pipelines include ETX1317 (prodrug ETX0282) [76, 77], funobactam (XNW4107) [78, 79], pralurbactam (FL058) [80], and ANT3310 [81]. These agents demonstrate promising broad-spectrum inhibition of class A, C, and D enzymes, with some showing activity against *Mycobacterium abscessus* and KPC- or OXA-producing Enterobacterales [46, 82–85]. Most are under phase 1-3 trials in combination with β-lactams to treat serious Gram-negative infections [46, 52, 78, 79, 81, 85]. Despite their major clinical impact, resistance to DBO-based inhibitors is an emerging concern, particularly in class A enzymes. In KPC enzymes, resistance-associated substitutions include D179N and S130G in KPC-2, as well as D179Y in KPC-2 and KPC-3-derived variants identified in *K. pneumoniae* [86]. In addition, the combined L169Q/S130G substitutions in CTX-M-15, evaluated in an *E. coli* background, markedly impaired inhibition by avibactam. These alterations can reduce DBO susceptibility by affecting inhibitor recognition or acylation. Importantly, however, these substitutions often impose a fitness or catalytic cost on the enzyme, so the resulting resistance phenotype may be accompanied by reduced β-lactam hydrolytic efficiency or partial restoration of β-lactam susceptibility [86].

1.2.3 | *Boronic Acid-Based BLIs*

Boronic acid derivatives represent a key advancement in the field of BLIs, owing to their distinctive mechanism of action (Figure 3) [47]. These compounds act as acylation or deacylation transition-state analogs, mimicking the high-energy tetrahedral intermediate formed during β-lactam hydrolysis [38]. Through this mimicry, boronic acid inhibitors establish a reversible covalent (dative) bond with the catalytic serine residue of SBLs, effectively blocking the enzyme active site [87, 88]. Importantly, despite this covalent mode of action, boronic acids can achieve remarkable selectivity for β-lactamases over other serine hydrolases, including mammalian serine proteases, owing to the complementary architecture of the β-lactamase active site and the tailored interactions established by the inhibitor scaffold [89]. Several structural features contribute to the effectiveness of boronic acids. First, boron shares strategic chemical characteristics with the β-lactam carbonyl group: both function as electrophilic centers susceptible to nucleophilic attack [90]. Second, the geometry and stereochemical arrangement of the substituent corresponding to the R_1 side chain relative to the reactive center are often closely conserved between β-lactams and boronic acids. In many boronic acids mimicking the β-lactam scaffold, the carbon adjacent to the electrophilic boron center bears an amide functionality closely resembling the C(6) or C(7) side chains of penicillins and cephalosporins respectively, including their stereochemical configuration. This structural and stereochemical

TABLE 1 | Ambler and Bush-Jacoby classes categorization for the principal β-lactamases discussed in this review.

Ambler class	Bush-Jacoby class	Substrates	β-lactamase	Organism	UniProt ID
A	2a	P	PC1*	Not reported in this review	
	2b	P, NSC	TEM-1	*Escherichia coli*	P62593
			SHV-1	*Klebsiella pneumoniae*	P0AD64
	2be	P, NSC, ESC, M	SHV-5	*K. pneumoniae*	P0A3M1
			SHV-12	*K. pneumoniae*	H6UQL7
			CTX-M-9	*E. coli*	Q9L5C8
			CTX-M-14	*E. coli*	Q9L5C7
			CTX-M-15	*E. coli*	A0A223A5J4
			CTX-M-96	*K. pneumoniae*	Q6ZXB6
			TEM-10	*Klebsiella oxytoca*	Q48388
			TEM-43	*K. pneumoniae*	O34176
			TEM-116	*E. coli*	Q79DR3
	2br	P	SHV-10*	Not reported in this review	
	2c	P, CR	CARB-1*	Not reported in this review	
	2f	P, NSC, ESC, CB, M	KPC-2	*K. pneumoniae*	Q9F663
			KPC-3 [43]	*K. pneumoniae*	Q93DC4
			SME-2	*Serratia marcescens*	P52682
			GES-5	*K. pneumoniae*	Q09HD0
			FRI-1	*Enterobacter cloacae*	N.A.
			BKC-1	*K. pneumoniae*	A0A0F6QEY8
B	3a	P, NSC, ESC, CB	IMP-1	*S. marcescens*	P52699
			NDM-1	*K. pneumoniae*	C7C422
			VIM-1	*K. pneumoniae*	Q5GN09
			VIM-2	*Pseudomonas aeruginosa*	Q9K2N0
			L1	*Stenotrophomonas maltophilia*	P52700
			GOB-18	*Elizabethkingia meningoseptica*	Q4JRB6
	3b	CB	Sfh-I	*Serratia fonticola*	Q9RMI1
			CphA	*Aeromonas hydrophila*	P26918
C	1	NSC	AmpC	*E. coli*	P00811
			AmpC (PAO1)	*P. aeruginosa*	P24735
			P99	*E. cloacae*	P05364
			CMY-2	*K. pneumoniae*	Q48434
			ADC-7	*Acinetobacter baumannii*	Q6DRA1
			ADC-30	*A. baumannii*	A7XM81
			ADC-33	*A. baumannii*	A7Y407
			PDC-3	*P. aeruginosa*	P24735
			PDC-11	*P. aeruginosa*	D0EJY2
			MOX-1	*E. coli*	Q51578
	1e	NSC, ESC	GC1*	Not reported in this review	
D	2d	P	OXA-1	*E. coli*	P13661
			OXA-10	*P. aeruginosa*	P14489
	2de	P, ESC, M	OXA-15*	Not reported in this review	
	2df	P, CB	OXA-23	*A. baumannii*	Q9L4P2
			OXA-24/40	*A. baumannii*	Q8RLA6

(Continues)

TABLE 1 | (Continued)

Ambler class	Bush-Jacoby class	Substrates	β-lactamase	Organism	UniProt ID
			OXA-48	*K. pneumoniae*	Q6XEC0

Abbreviations: CB = Carbapenems, CR = Carbenicillin, ESC = expanded-spectrum cephalosporin, L1 = is a tetramer, M = Monobactam, NSC = Narrow-Spectrum Cephalosporins, P = Penicillins.
*Not reported in this review.

conservation enables boronic acids to faithfully reproduce the orientation with which β-lactam side chains are presented to the enzyme active site, thereby preserving the recognition elements required for productive binding. These parallels make boronic acids well-suited to occupy and inhibit the active site of β-lactamases. From a chemical standpoint, boron is an electron-deficient Lewis acid with an empty *p* orbital, rendering it highly electrophilic. In boronic acids, the B-O bond displays partial double bond character and a short bond length, contributing to overall molecular stability. Unlike peptide bonds or β-lactam rings, B-O bonds are not readily hydrolyzed by bacterial enzymes, making boronic acids more resistant to enzymatic degradation [91]. In solution, boronic acids typically exist in a trigonal planar geometry (sp^2 hybridization), with the empty *p* orbital positioned perpendicular to the plane. Upon nucleophilic attack, such as that mediated by the hydroxyl group of the catalytic serine, boron undergoes rehybridization to an sp^3 state, forming a tetrahedral anionic intermediate. This transition enables boronic acids to mimic both the electrophilic β-lactam carbonyl group and the tetrahedral intermediate formed during β-lactam hydrolysis, thereby underpinning the potent inhibitory activity and selectivity of boron-based inhibitors [91]. Notably, a growing body of biochemical, pharmacological, and clinical evidence accumulated over the past decades has also helped to dispel earlier concerns regarding boron-associated toxicity, supporting boronic acid derivatives as a viable and generally well-tolerated class of compounds for β-lactamase inhibitor development [92].

Unlike β-lactam-based inhibitors or DBOs, boronic acid inhibitors possess flexible chemical scaffolds, which allows for fine-tuning of pharmacodynamic properties and broad-spectrum coverage [87, 93]. The approval of vaborbactam (herein compound **59**), a cyclic boronate used in combination with meropenem (Vabomere) [94], marked a major milestone, particularly due to its high efficacy against class A β-lactamases like KPC and some class C enzymes (see Chart 1) [95]. While vaborbactam does not inhibit metallo-β-lactamases, its ability to restore carbapenem efficacy in KPC-producing Enterobacterales highlights the clinical value of boronates. The design, properties, and activity profiles of all clinically relevant and investigational boronic acid-based BLIs will be comprehensively described and discussed in detail in the following sections of this review.

2 | Discussion

2.1 | Acyclic Boronic Acid Derivatives

2.1.1 | *Acetamide, Carboxamido, and Glycineboronic Acid*

A biomimetic approach to design potent inhibitors: The concept of using acyclic boronic acids as BLIs (Chart 2) was first introduced in the 1990s, when Martin et al. rationally designed a novel inhibitor by incorporating functional groups from β-lactam antibiotics into an acyclic boronic acid scaffold [96–98]. Leveraging crystallographic data of the *E. coli* TEM-1:PenG acyl-enzyme complex (Figure 4A, PDB: 1FQG) [98–100], structure-based design led to the development of (1*R*)−1-acetamido-2-(3-carboxyphenyl)ethane boronic acid (**1**), a transition-state analogue of the high energy intermediate observed in the SBLs catalytic mechanism of β-lactam hydrolysis [101]. Compound **1** exhibited potent inhibition of class A TEM-1, with a K_i of 110 nM [97]. Authors proposed that one of the oxygen atoms linked to the boron adduct sits in the oxyanion hole forming a direct H-bond interaction with S70 and the nitrogen from the main chain of A237, therefore resembling the position of the carbonyl oxygen atom in the acyl-enzyme complex (Figure 4B, PDB: 1ERM) [97]. The second oxygen has the role to replace the deacylating water and to form strong hydrogen bonds to the E166 carboxylate and N170 amide side chains. Furthermore, a detailed review of the mechanism of acyclic boronic acid as class A β-lactamase covalent inhibitors was provided in this manuscript, suggesting a central role for K73 in the deacylation step of β-lactam hydrolysis [97]. In detail, K73 acts as a proton shuttle between E166 and S70 during deacylation, as evidenced by a strong hydrogen bond (2.7 Å) with E166. That is also supported by the distance greater than 4 Å between E166 and S70.

Although the inhibitory profile of compound **1** was not initially evaluated against other β-lactamases, and microbiological data were lacking, this seminal work laid the foundation for subsequent scaffold optimization by the same group [102]. Using a rational design approach, Ness and coworker developed two deacylation transition state analogue derivatives: (1*R*)−1-phenylacetamido-2-(3-carboxyphenyl)ethylboronic acid (compound **2**) and (1*R*)−1-acetamido-2-(3-carboxy-2-hydroxyphenyl)ethylboronic acid (compound **3**). To enhance the potency of the parent compound **1**, structural modifications were introduced to strengthen energetically favorable interactions within the TEM-1 active site. In compound **2**, the side chain acetamido group was replaced with a phenylacetamido moiety, mimicking the R-group of PenG and enhancing van der Waals and hydrophobic contacts with residues 235-238. This modification resulted in a 20-fold improvement in inhibitory potency ($K_i = 5.9$ nM). Instead, compound **3** resembles the structure of **1**, with the incorporation of a phenolic hydroxyl group in *o*-position to increase hydrogen bonding, particularly with residue S130, leading to a 10-fold improvement in activity ($K_i = 13$ nM) relative to its parent compound. This biomimetic approach capitalizes on the structural and electronic similarities between the β-lactam carbonyl group and the boron atom (as discussed in Section 1.2.3), effectively combining the boronic acid pharmacophore ability to target the nucleophilic serine of class A SBLs with the well-established side chain recognition features

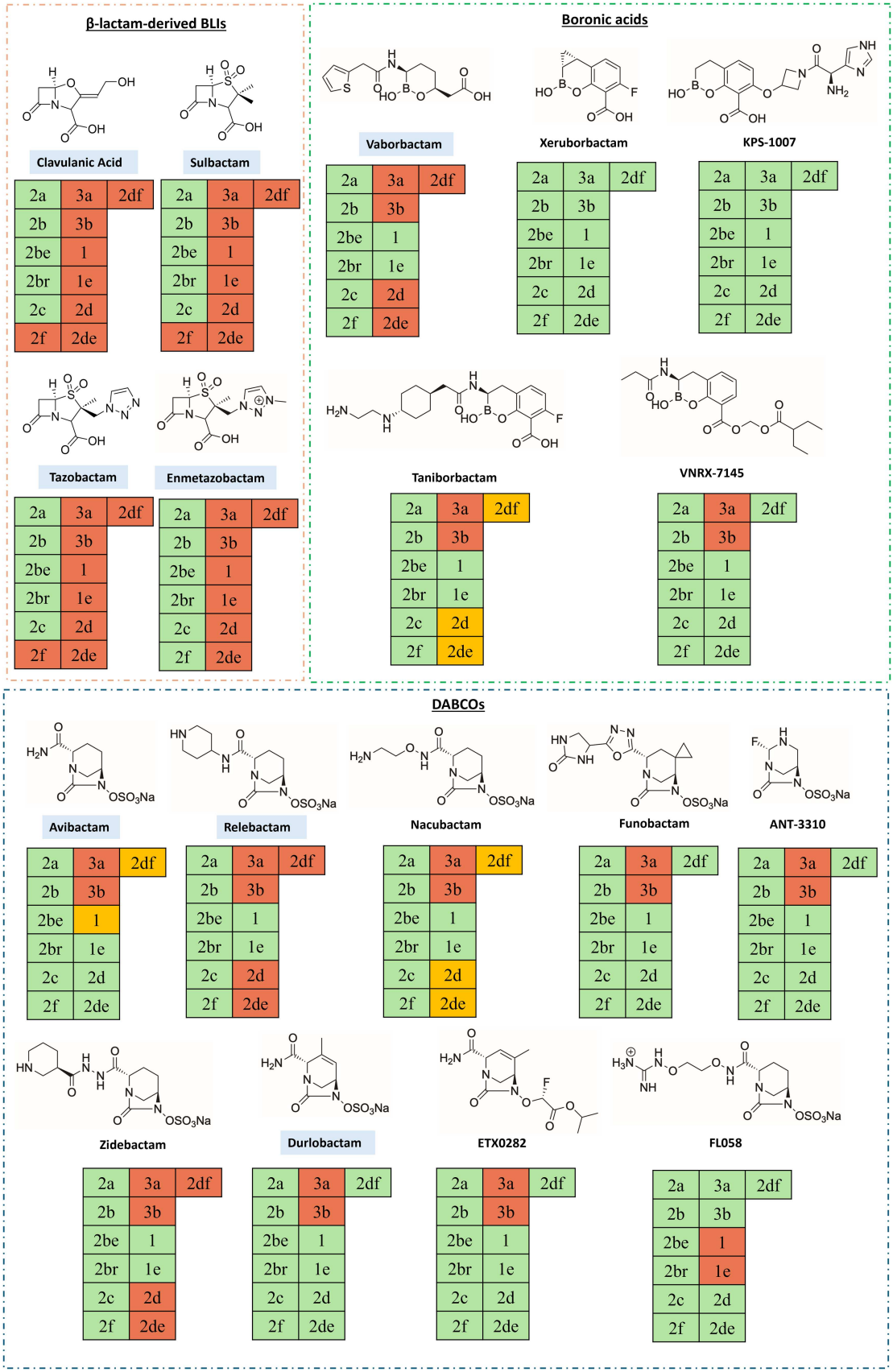

CHART 1 | Chemical structures of clinically approved BLIs (light blue box) and derivatives currently in clinical trials divided by chemical class. Within each box, the spectrum of action for each BLIs against β-lactamases (Bush-Jacoby classification). Red = Inactive; Orange = Partially active; Green = Active. [Color figure can be viewed at wileyonlinelibrary.com]

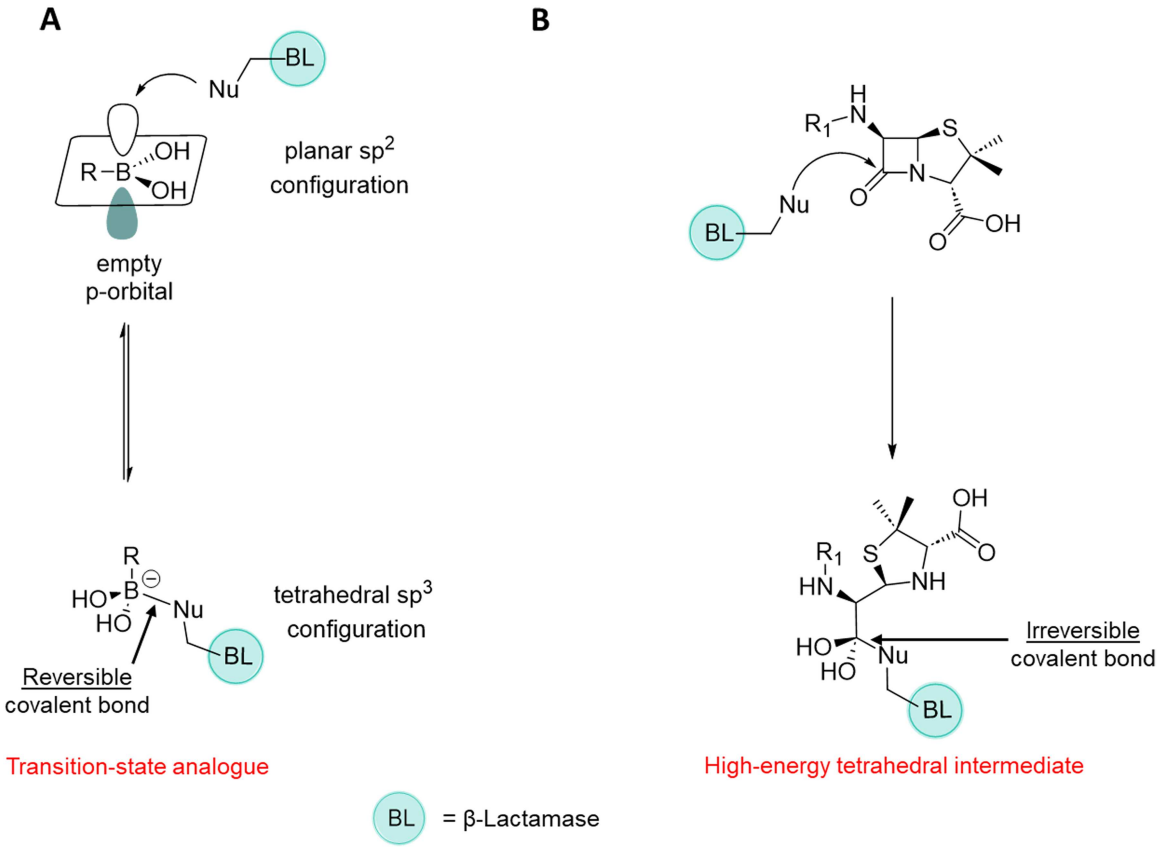

FIGURE 3 | Comparison between (A) boronic acids and (B) β-lactams chemical rehybridization and mechanism after binding with a nucleophilic entity. [Color figure can be viewed at wileyonlinelibrary.com]

of β-lactam substrates. Crystallographic analysis of the TEM-1 complexes with compounds **2** and **3** (PDBs: 1ERO and 1ERQ, respectively) revealed additional unanticipated interactions, including hydrogen bond formation, displacement of active-site water molecules, and side chain rearrangements (Figure 5A). Interestingly, this study was the first to propose compound **3** might induce formation of a cyclic boronate ester, thereby laying the groundwork for subsequent work on bicyclic boronates described in Section 2.3.3. However, the crystal structure shown in Figure 5B did not reveal the bicyclic boronate form of compound **3**. Compound **2** inhibitory profile against class A β-lactamases was further confirmed by Rojas et al., demonstrating potent inhibition towards clinically relevant SHV-1 ($IC_{50} = 200$ nM) and KPC-2 ($IC_{50} = 70$ nM) [103].

In a seminal study, Caselli et al. investigated the energetic factors governing β-lactamase recognition of β-lactam by correlating affinities of properly derivatized acylglycineboronic acids with binding energy [89]. By decorating eight acylglycineboronic acids with side chains from penicillins and cephalosporins, they generated a series of potent boronic acid transition state inhibitors (BATSIs) and laid the basis for future inhibitors design (Table 2). Interestingly, the differential binding energies ($\Delta\Delta G$) among the BATSIs provided insights into key enzyme-inhibitor interactions, as confirmed by X-ray crystal structures. To quantify the contribution of different R_1 side chains to enzyme binding, $\Delta\Delta G$ values were calculated by comparing each boronic acid derivative to the reference compound (acetamidomethyl)boronic acid. This approach allowed the authors to assess how individual side chains enhance or weaken binding affinity. The reversible nature of boronic acid inhibition enabled structural comparisons with acyl-enzyme intermediates, revealing how R_1 recognition evolves from the transition state to the covalently bound ground state. These binding differences were functionally validated by evaluating the inhibitory activity of each derivative against a representative class C SBL, *E. coli* AmpC.

Crystal structures of *E. coli* AmpC in complex with glycineboronic acids bearing cloxacillin (compound **4**) and cephalothin (compound **5**) R_1-side chains suggested the amide group (C6-C7 in β-lactams) is essential for binding, contributing 3.2 kcal/mol to the free energy (Figure 6). Interestingly, compounds **6** and **7**, carrying the nafcillin and ceftazidime side chains respectively, were the most potent. Compound **6** had a K_i of 33 nM for AmpC, while compound **7** reached 20 nM for AmpC and 390 nM for TEM-1. Both enhanced ceftazidime and cefotaxime activity against resistant *E. cloacae* and *S. aureus* strains, demonstrating a promising spectrum of activity against both Gram-negative and -positive bacteria. These boronic acids also showed high selectivity over serine proteases like α-chymotrypsin, β-trypsin, and elastase.

An additional study by Chen et al. employed boronic acids as powerful molecular probes to uncover key details of β-lactamase recognition and catalytic mechanisms [104]. Whereas glycineboronic acids bearing penicillin and cephalosporins R_1 side chains can act as acylation transition-state analogues, chiral glycineboronic

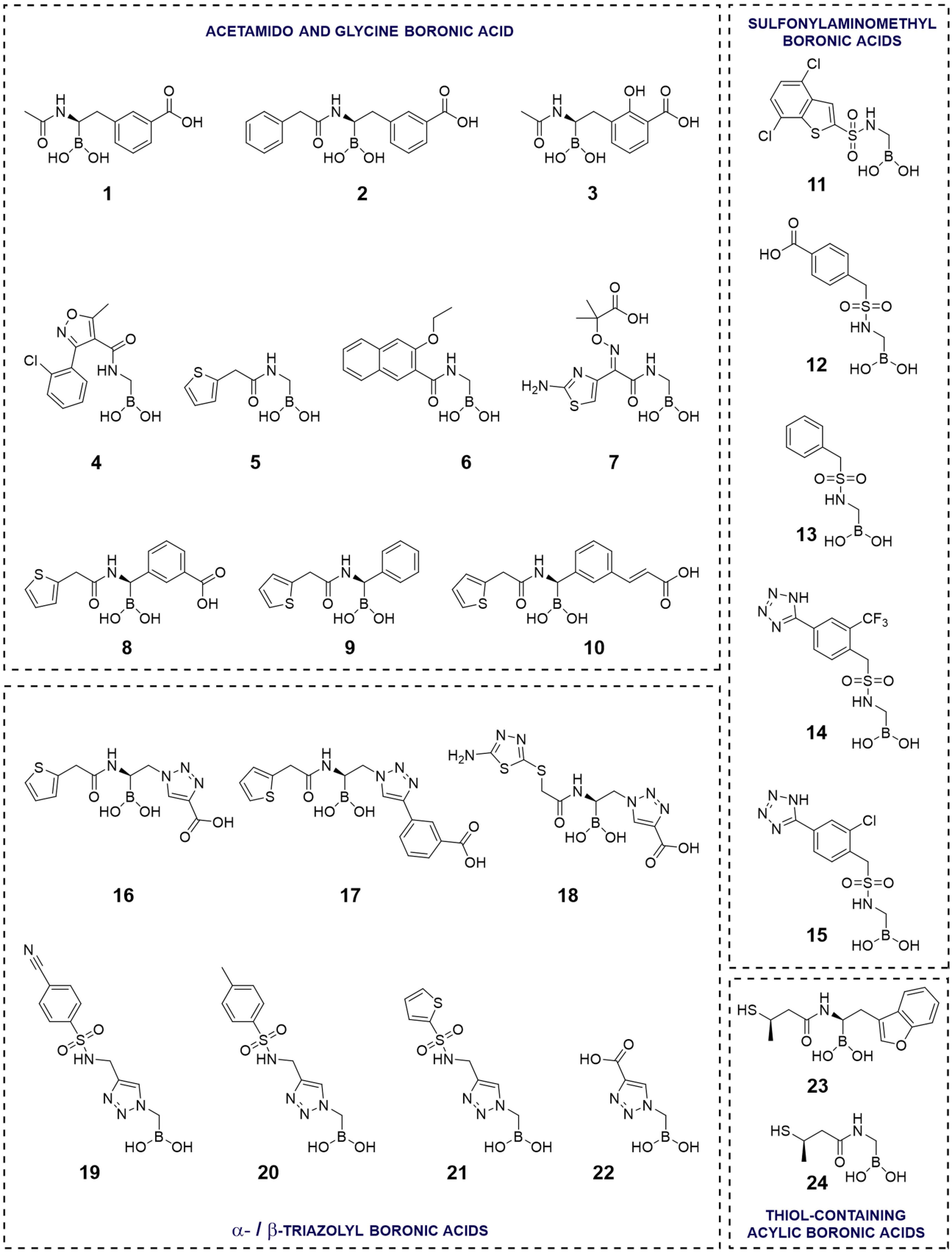

CHART 2 | List of acyclic boronic acids presented in Section 2.1. [Color figure can be viewed at wileyonlinelibrary.com]

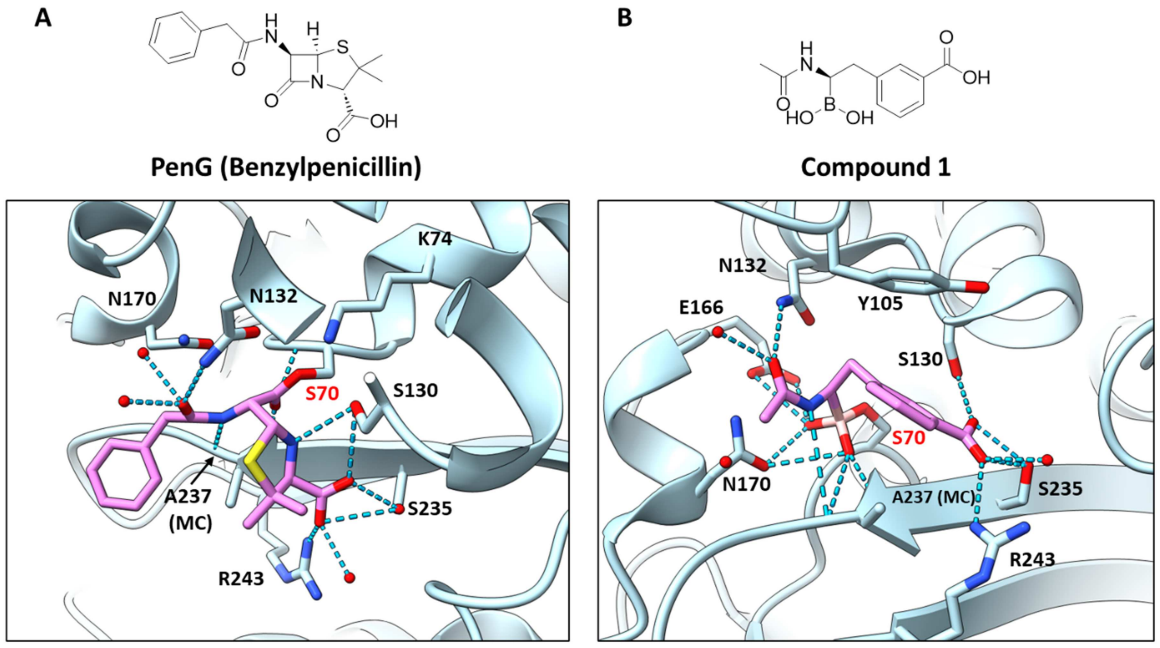

FIGURE 4 | (A) Crystal structures of PenG (PDB: 1FQG) in complex with *Escherichia coli* TEM-1 (UniProt ID: P62593); (B) Crystal structures of compound **1** (PDB: 1ERM) in complex with *E. coli* TEM-1. TEM-1 ribbon and carbon atoms depicted in light blue, ligand carbon atoms in magenta, oxygen in red, nitrogen in blue, sulfur in yellow, boron in amaranth pink. Blue dashes represent hydrogen bonds, water molecules are represented by red spheres. MC indicates the protein main chain. [Color figure can be viewed at wileyonlinelibrary.com]

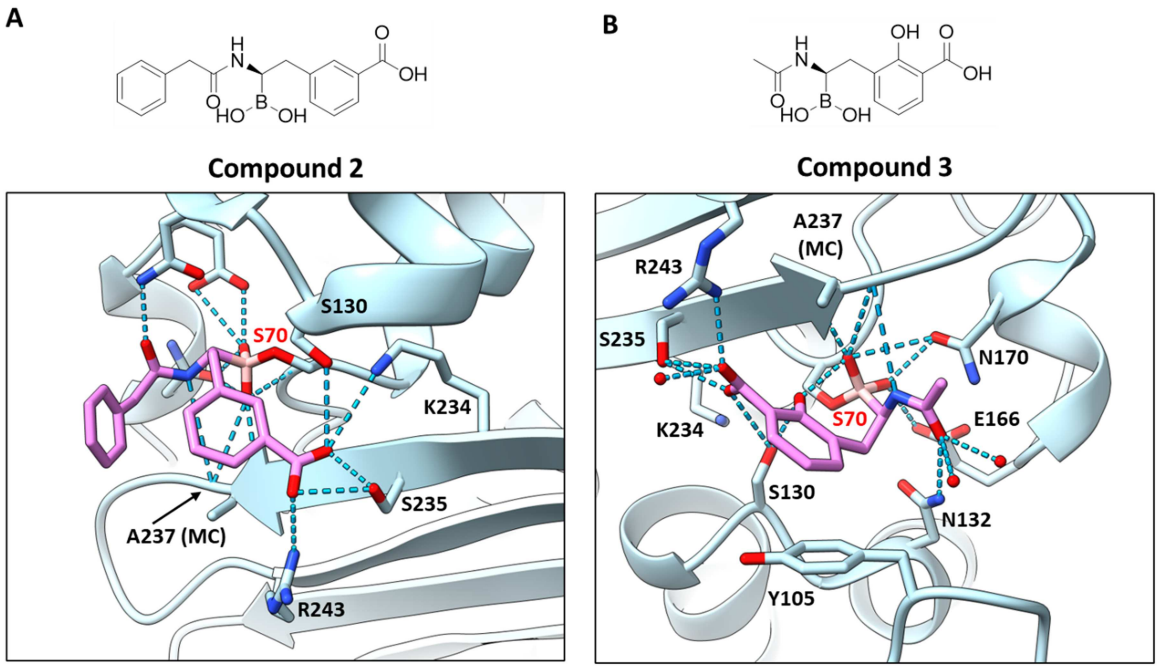

FIGURE 5 | Crystal structures *Escherichia coli* TEM-1 (UniProt ID: P62593) in complex with: (A) compound **2** (PDB: 1ERO) and (B) compound **3** (PDB: 1ERQ). Color code and graphical conventions are as in Figure 4. [Color figure can be viewed at wileyonlinelibrary.com]

acids with a supplementary R_2 side chains behave as deacylation transition-state analogues (Scheme 2). Moreover, in this report it was confirmed these derivatives form reversible, fast-on/fast-off adducts with SBLs.

Further advances in BATSI design against class C β-lactamases were later achieved using a structure-based approach. Building on prior work that identified key AmpC "hot spots" [105], and pursuing a biomimetic approach, a series of *m*-carboxyphenylglycylboronic acids were developed to enhance inhibitor binding [106]. Following the same rationale as for glycineboronic acids, side chains (R_1) from cephalothin and cloxacillin were introduced, while a *m*-carboxyphenyl group (R_2) was placed at the same boron-bearing carbon atom. This led to compound **8**, a highly potent AmpC inhibitor ($K_i = 1$ nM), showing a 300-fold improvement over the parent molecule

TABLE 2 | Some of the most relevant BATSIs reported in Caselli et al. [89] ΔΔG= Differential free energy of binding relative to (acetamidomethyl)boronic acid at 25°C.

Compound	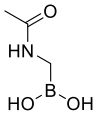	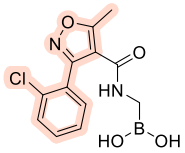 4	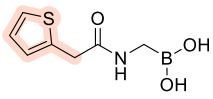 5	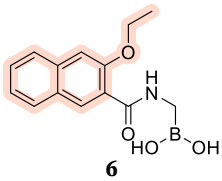 6	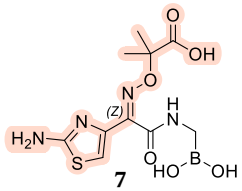 7
β-Lactam side chain		Cloxacillin	Cephalothin	Nafcillin	Ceftazidime
K_i AmpC (μM)		0.15	0.32	0.033	0.020
$\Delta\Delta G_{R1}$ (kcal/mol)		2.85	2.40	3.75	4.04

Note: A positive value indicates improved affinity. In pink are highlighted the scaffold portions relevant to the ΔΔG calculations.

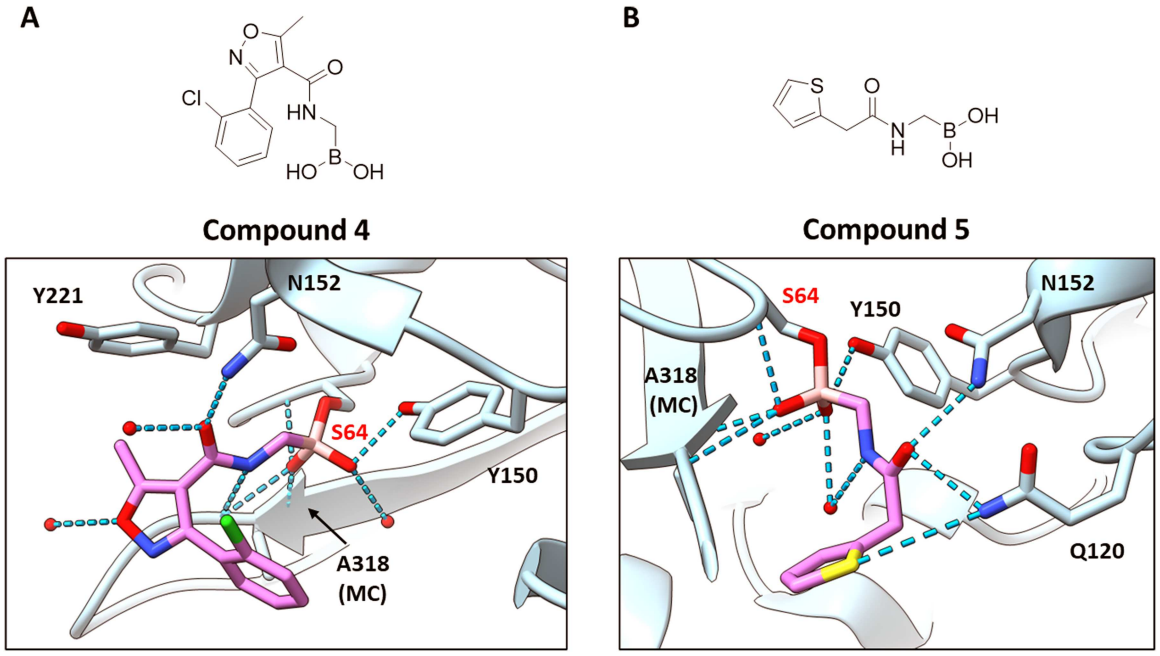

FIGURE 6 | Crystal structures *Escherichia coli* AmpC (UniProt ID: P00811) in complex with: (A) compound **4** (PDB: 1FSY) and (B) compound **5** (PDB: 1FSW). Color code and graphical conventions are as in Figure 4. [Color figure can be viewed at wileyonlinelibrary.com]

lacking the R_2 group. Crystal structure analysis of the AmpC-**8** complex highlights the critical role of the C3(4)′ acidic group in target recognition (Figure 7A). The carboxylate contributes significantly to binding, as confirmed by comparison with compound **9**, which lacks the group and exhibits a K_i of 35 nM (Figure 7B). Although structural differences between the **8**- and **9**-AmpC complexes are minimal, the carboxylate enhances binding free energy by 2.1 kcal/mol, underlining its key role in inhibitor recognition. In microbiological assays, compound **8** slightly outperformed **9**, reducing ceftazidime MIC values by 8- to 32-fold against strains from *C. freundii*, *E. coli*, *E. cloacae*, and *Pseudomonas aeruginosa*. Compound **8**, and more broadly this inhibitor series, also displayed high selectivity for AmpC over representative serine proteases, being 5 orders of magnitude more selective than versus α-chymotrypsin and showing no measurable inhibition of β-trypsin below 1 mM. Since residue N289 is not conserved across class C β-lactamases, as in P99 enzyme from *E. cloacae*, Morandi et al. investigated whether mutations at this position would affect compound **8** inhibitory activity. Compound **8** showed a slightly reduced potency ($K_i = 17$ nM) against the AmpC N289A mutant. To address this, a structure-based optimization was undertaken using **8** as the starting point, resulting in compound **10** [107]. The design of compound **10** was aimed to generate a scaffold that could interact with the carboxylate subsite formed by N343, N346 and T316, replacing the interaction with N289. Although **10** retained high affinity for wt AmpC ($K_i = 1$ nM) and improved binding to the N289A mutant ($K_i = 2.8$ nM), it did not outperform **8**. Crystal structure of the AmpC-**10** complex revealed that the inhibitor carboxylate interacted only with N343 (Figure 7C).

In the years that followed, boronic acids gained increasing attention as BLIs. While initially employed as molecular probes to investigate the mechanistic details of β-lactamase catalysis, their role evolved significantly once it became evident that boron-containing compounds were not inherently toxic to humans [92]. As a result, boronic acids transitioned from academic curiosities to viable drug candidates, sparking interest from the pharmaceutical industry and prompting the development of more potent, selective, and pharmacologically optimized inhibitors. This

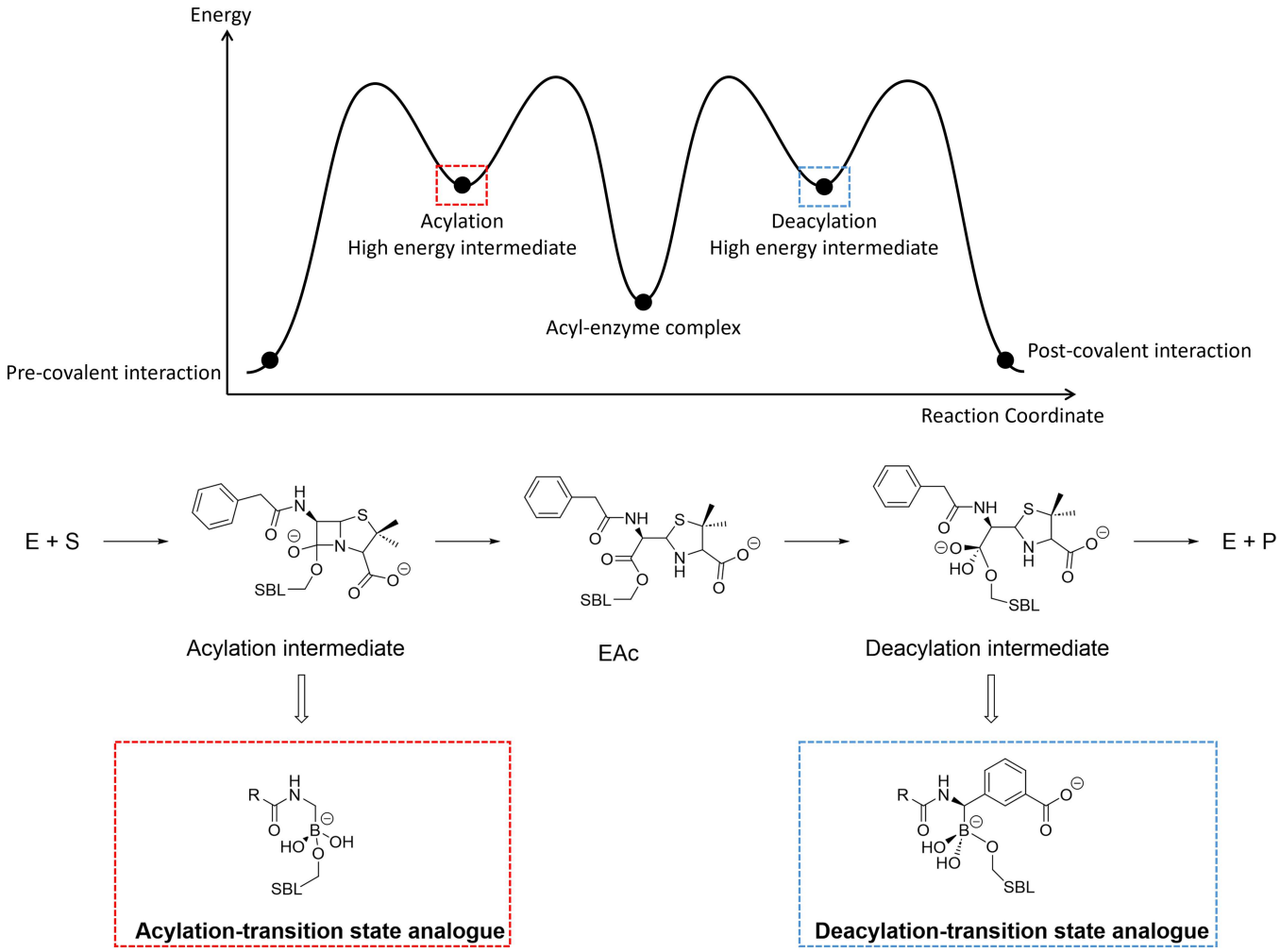

SCHEME 2 | Structural and energetic between two boronic acids acylation and deacylation transition state analogues and the intermediates formed during the β-lactamase-catalyzed hydrolysis of a penicillin. [Color figure can be viewed at wileyonlinelibrary.com]

growing interest translated into broader testing against clinically significant β-lactamases, including those responsible for widespread resistance. Thus, further structural and biochemical analysis of compound **8** were conducted with the clinically relevant class C enzyme ADC-7 [108]. Compound **8** potently inhibited ADC-7 ($K_i = 21$ nM), enhancing ceftazidime activity up to eightfold in *E. coli* DH10B expressing $bla_{ADC\text{-}7}$. Interestingly, in the ADC-7:**8** complex (PDB: 5W13), compound **8** adopted two conformations: one forming hydrogen bonds with N340 and N343, and another engaging S315 [109]. Compound **8** also showed potent activity against class A enzymes SHV-1 and KPC-2 ($IC_{50} = 400$ nM and 600 nM, respectively) [103]. Beyond its β-lactamase inhibitory profile, compound **8** was later also identified as a promising *P. aeruginosa* biofilm inhibitor, suppressing biofilm formation, virulence factors, and quorum sensing-related autoinducer molecules [110].

Among the 10 BATSIs discussed in this subsection (Table 3), compound **8** stands out as the most promising, exhibiting nanomolar inhibitory activity against both class C and class A β-lactamases, including AmpC, ADC-7, SHV-1, and KPC-2. Its potent biochemical profile and ability to enhance β-lactam efficacy, alongside anti-biofilm and anti-virulence effects in *P. aeruginosa*, highlight its therapeutic potential. However, the lack of potency against class B and D combined with a good, yet not exceptional, microbiological profile underscores the need for further scaffold optimization to address target variability.

2.1.2 | *Sulfonylaminomethyl Boronic Acid*

A bioisosteric approach for BATSIs: In 2010, Merck researchers introduced 4,7-dichloro-1-benzothien-2-yl sulfonylaminomethyl boronic acid (compound **11**) as the first BATSI to exhibit inhibitory activity against class D β-lactamases (Figure 8) [111]. Notably, compound **11** inhibited OXA-24/40 with an IC_{50} of 5.6 μM and demonstrated a broader inhibitory profile, showing activity against class A TEM-1 ($IC_{50} = 1.1$ μM) and SHV-5 ($IC_{50} = 0.57$ μM), class C AmpC ($IC_{50} = 1.2$ μM) and P99 ($IC_{50} = 0.62$ μM). Additionally, compound **11** was able to lower the MIC of imipenem against an *A. baumannii* strain overexpressing serine β-lactamases (CL6188), underscoring its potential as a broad-spectrum BLI scaffold.

Shortly after, Eidam et al. introduced a novel series of sulfonamide boronic acids as BLIs, inspired by a bioisosteric approach applied to the acylglycyl boronic acid scaffold presented in section 2.1.1 [112]. Their rationale was based on two key observations: first, in the structure of compound **8**, the

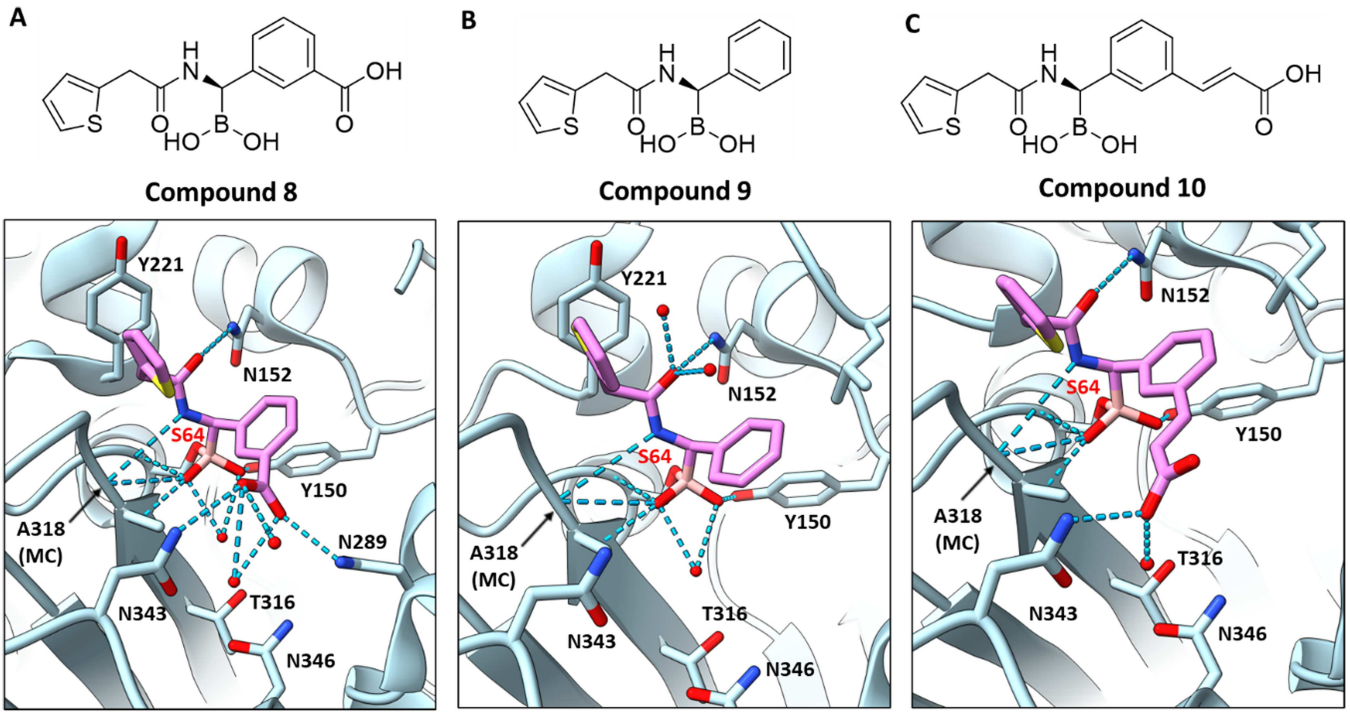

FIGURE 7 | Crystal structures *E. coli* AmpC (UniProt ID: P00811) in complex with: (A) compound **8** (PDB: 1MXO), (B) compound **9** (PDB: 1MY8) and (C) compound **10** (PDB: 2RCX). Color code and graphical conventions are as in Figure 4. [Color figure can be viewed at wileyonlinelibrary.com]

TABLE 3 | Spectrum of activity of acetamido, carboxamido and glycineboronic acid compounds 1-10 against various β-lactamases.

Compound	K_i/IC_{50} (μM)				
Ambler Class	A			C	
β-Lactamase	TEM-1	SHV-1	KPC-2	AmpC	ADC-7
UniProt ID	P62593	P0AD64	Q9F663	P00811	Q6DRA1
1	0.110	—	—	—	—
2	0.006	**0.200**	**0.070**	—	—
3	0.013	—	—	—	—
4	—	—	—	0.150	—
5	—	—	—	0.320	—
6	—	—	—	0.033	—
7	—	—	—	0.200	—
8	—	**0.400**	**0.600**	0.001	0.021
9	—	—	—	0.035	—
10	—	—	—	0.001	—

Note: IC_{50} values are denoted in bold, while K_i are denoted in normal character.

carboxamide oxygen and nitrogen form hydrogen bonds with N152 and the backbone carbonyl of A318 in AmpC; second, noncovalent β-lactamase inhibitors bearing sulfonamide moieties had shown similar interactions within the AmpC active site [113]. Guided by these insights, they synthesized and tested 10 sulfonamide boronic acids, leading to the identification compound **12** (Figure 9), bearing a PenG side chain, which displayed high potency against *E. coli* AmpC (K_i = 70 nM).

Interestingly, the authors observed that replacing a carboxamide with a sulfonamide group in these scaffolds led up to 23-fold improvement in affinity. An important finding from this series was that simpler sulfonamide side chains correlated with higher inhibitory activity; an inverse trend compared to the carboxamide-based boronic acids discussed in Section 2.1.1. These sulfonamide boronic acids exhibited strong synergy with oxyimino- cephalosporins. In strains overproducing class C β-lactamases (*E. coli*, *E. cloacae*, *C. freundii*, *P. aeruginosa*, *K. pneumoniae*), they successfully restored the efficacy of ceftazidime and cefotaxime, reducing significantly MIC values. Later, structural studies of AmpC bound to compound **13** ($K_{i\ AmpC}$ = 1.3 nM) showed that sulfonamide boronic acids maintain important interactions, such as hydrogen bonds between the sulfonamide group and residues N152 and Q120, while adopting

a distinct geometry and polarity compared to carboxamide analogues (Figure 10A) [114]. A similar interaction pattern was observed in the ADC-7:**13** complex, where additional contacts with N221, S320, and T319 were identified (Figure 10B). Compound **13** also demonstrated potent activity against other class C variants, including ADC-7 ($K_i = 160$ nM) and ADC-33 ($K_i = 57$ nM) [115]. These data were also validated in *E. coli* DH10B cells expressing bla_{ADC-7}, where compound **13** reduced the MIC of ceftazidime by up to 64-fold, significantly enhancing its microbiological efficacy. Importantly, representative sulfonamide boronic acids from this series showed no measurable inhibition of α-chymotrypsin or cruzain at 100 μM, supporting the selectivity of this scaffold beyond β-lactamase inhibition. Beyond class C enzymes, **13** also showed activity against class A and D SBLs: **13** inhibited SHV-1 and KPC-2 with IC_{50} values of 430 nM and 200 nM, respectively [103]. Surprisingly, as for compound **11**, its activity has been recently validated against class D OXA-24/40 ($K_i = 4.4$ μM) [115]. However, when **13** was tested in combination with various cephalosporins and carbapenems against *A. baumannii* strains, including OXA-24-expressing isolates (pWH1266) and clinical strains carrying different OXAs, significant MIC improvement was not observed. Similarly, in *A. baumannii* ATCC17978 with an ADC knockout and $bla_{OXA-24/-40}$ constructs, **13** could restore susceptibility levels only negligibly. Additional analogues bearing α-alkyl substitutions (not shown here) were synthesized using the OXA-24/40:**13** crystal structure as a reference, although none outperformed compound **13** (Figure 10C).

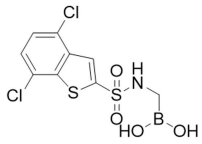

Compound 11

FIGURE 8 | Structure of the α-sulfonylaminomethyl boronic acid **11**.

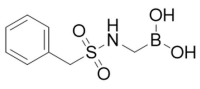

Compound 12

FIGURE 9 | Structure of the α-sulfonylaminomethyl boronic acid **12**.

Eidam et al. further optimized compound **13** scaffold using a fragment-based approach, leading to the development of two of the most potent BATSIs to date: compounds **14** and **15** [114]. Building on previous fragment-screening and defragmentation studies, the authors identified three anionic fragments that occupied the same region as the carboxylate group of compound **13**, but in a more favorable orientation, allowing improved interactions with the backbone amides of G320 [116, 117]. Replacing the carboxylic acid with a tetrazole moiety at the *p*-position of a phenyl ring yielded, amongst others, to **14** (2-chloro-4-tetrazolyl benzene sulfonamide boronic acid) exhibiting an extraordinary 0.2 nM K_i for AmpC and **15** (2-trifluoromethyl-4-tetrazolyl benzene sulfonamide boronic acid), which displayed an even more effective 0.05 nM K_i for the same enzyme (Figure 11). X-ray structures of AmpC in complex with **14** and **15** revealed van der Waals interactions between the trifluoromethyl or chloro substituents and the backbone carbonyls of A318 and T319.

Microbiological testing showed that both compounds, in combination with cefotaxime or ceftazidime, reduced MIC values in 50% of AmpC-overexpressing clinical isolates. Further evaluation of **15** demonstrated a remarkable K_i of 0.45 nM also against the cephalosporinase ADC-7 [118]. When tested in *E. coli* DH10B expressing bla_{ADC-7} and in the MDR clinical strain

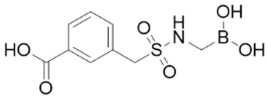

Compound 13

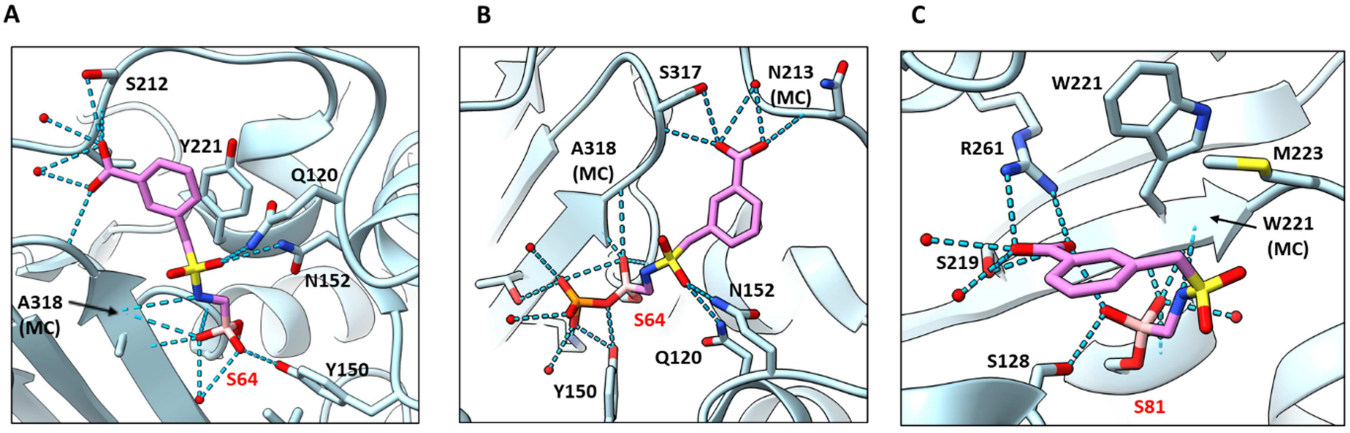

FIGURE 10 | (A) Crystal structures *E. coli* AmpC (UniProt ID: P00811) in complex with compound **13** (PDB: 4E3I). (B) Crystal structures *A. baumannii* ADC-7 (UniProt ID: Q6DRA1) in complex with compound **13** (PDB: 5WAE). (C) Crystal structures *A. baumannii* OXA-24/40 (UniProt ID: Q8RLA6) in complex with compound **13** (PDB: 8CUL). Color code and graphical conventions are as in Figure 4. [Color figure can be viewed at wileyonlinelibrary.com]

A. baumannii M9, **15** lowered CAZ MICs by up to 32-fold and 8-fold, respectively. Moreover, those fragment-optimized sulfonamide boronates retained potent target selectivity, with affinity for AmpC generally 5-6 orders of magnitude greater than the one observed for representative serine proteases.

From the BATSIs described in this subsection, compound **13** emerged as a promising sulfonamide boronic acid inhibitor, showing potent activity against class C β-lactamases and notable synergy with 3rd generation cephalosporins. Its optimized derivative, compound **15**, with picomolar inhibitory affinity and selective inhibition across class Cs, represents one of the most potent BATSI developed to date (Table 4). Despite its impressive performance in vitro against class C, **15** activity is less consistent against class D enzymes and ineffective against metallo-β-lactamases, limiting its potential as a truly broad-spectrum solution.

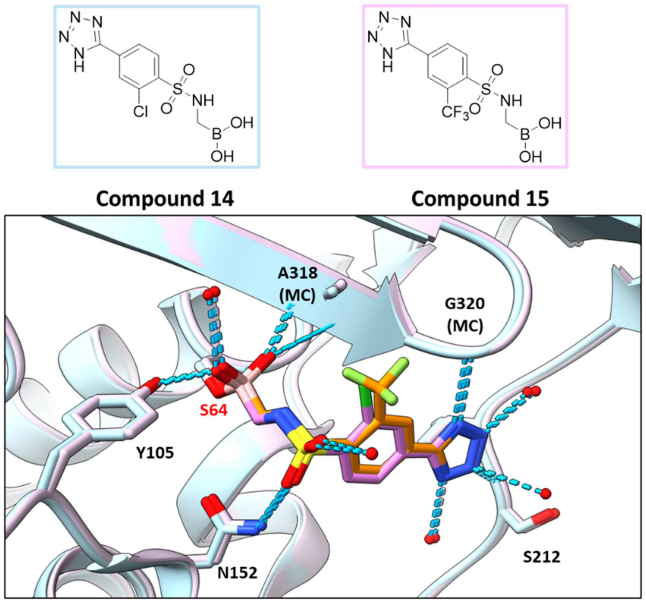

FIGURE 11 | Structural overlay of *Escherichia coli* AmpC (UniProt ID: P00811) in complex with compound **14** (PDB: 4E3N; light-blue ribbon and magenta ligand) and compound **15** (PDB: 4E3M; pink ribbon and orange ligand). The two protein structures were superimposed by Cα-atom alignment. All other color codes and graphical conventions are as described in Figure 4. [Color figure can be viewed at wileyonlinelibrary.com]

2.1.3 | α-/β-Triazolyl Boronic Acids

Click chemistry application for novel BATSIs: To broaden the chemical space and simplify the synthetic pathways, Caselli et al. developed α-amido-β-triazolylethanboronic acids as a novel class of BATSIs [119]. Unlike previous synthetic routes limited by early stage insertion of the *m*-carboxyphenyl group, this approach leveraged the copper-catalyzed azide-alkyne cycloaddition (CuAAC) to install a substituted triazole moiety in the late steps of the synthetic pathway. The triazole moiety was chosen to replace the *m*-carboxybenzyl group due to its strong dipole and preserved aromaticity. Using three different R_1 chains (acetyl, phenylacetyl, and 2-thienyl-2-acetyl groups) Caselli et al. synthesized 14 derivatives, identifying compound **16** and compound **17** as potent inhibitors (Figure 12). For class C, **16** showed K_i values of 140 nM for P99 and 35 nM for PDC-3, while **17** exhibited K_i values of 84 nM and 68 nM, respectively. Moreover, both compounds restored cefotaxime activity in *E. coli* strains overproducing P99 or PDC-3, reducing MICs up to 32-fold. These compounds demonstrated also to be excellent class A inhibitors, exhibiting nanomolar potency against clinically relevant KPC-2 ($IC_{50} = 80$ nM for **16** and $IC_{50} = 40$ nM for **17**) and SHV-1 ($IC_{50} = 130$ nM for **16** and $IC_{50} = 140$ nM for **17**) [103]. Consistent with its favorable biochemical profile against KPC-2 and SHV-1, compound **16** exhibited strong cellular activity in antimicrobial susceptibility assays. In combination with cefepime, and to a lesser extent with ceftazidime, cephalothin, or ertapenem, it restored susceptibility in a broad panel of *E. coli* strains producing KPC, SHV, TEM, and CTX-M β-lactamases, with the cefepime/**16** combination emerging as the most effective overall.

The inhibitory profile for those compounds was supported with structural studies, which revealed key triazole-mediated interactions and conformational flexibility within KPC-2 and SHV-1 active sites (Figure 13). Interestingly, beyond the conserved interactions typically observed for boronic acids bearing a cephalothin-derived R_1 side chain, the triazole scaffold of compound **16** allows the inhibitor to adopt multiple conformations (see Figure 13A) within the KPC-2 active site, enabling a distinctive C–H···O hydrogen-bond interaction with S130 at 2.9 Å.

TABLE 4 | Spectrum of activity of sulfonylaminomethyl boronic acid compounds 11-15 against various β-lactamases.

Compound	K_i/IC_{50} (μM)								
Ambler class	A				C		D		
β-Lactamase UniProt ID	TEM-1 Q6LBN9	SHV-1 P0AD64	SHV-5 P95675	KPC-2 Q9F663	P99 P05364	AmpC P24735* P00811	ADC-7 Q6DRA1	ADC-33 A7Y407	OXA-24/40 Q8RLA6
11	**1.1**	—	**0.570**	—	**0.620**	**1.2***	—	—	**5.6**
12	—	—	—	—	—	0.070	—	—	—
13	—	**0.430**	—	**0.200**	—	0.0013	0.160	0.057	4.4
14	—	—	—	—	—	0.0002	—	—	—
15	—	—	—	—	—	0.00005	0.00045	—	—

Note: For AmpC, UniProt ID P24735 refers to the *Pseudomonas aeruginosa* enzyme, with the corresponding values marked by an asterisk, whereas UniProt ID P00811 refers to *Escherichia coli* AmpC. IC_{50} values are shown in bold, K_i values in regular type, and dashes indicate that no value was reported.

The broad profile of **16** and **17** was further expanded to class C cephalosporinase ADC-7, with K_i values of 44 nM (**16**) and 46 nM (**17**), and also restoring ceftazidime MICs up to 32-fold in *E. coli* strains carrying $bla_{ADC\text{-}7}$ [109]. Crystal structure of ADC-7:**16** and ADC-7:**17** complexes were determined to assess the essential recognition properties for these inhibitor (Figure 14) [108, 109]. As per other similar compounds, the R_1 side chain of both **16** and **17** forms H-bonds through their amide oxygen with the side chain nitrogen of Q120 and N152, while also interacting with the main chain amide nitrogen and oxygen of S315. The first boron hydroxyl group is located within the oxyanion hole forming hydrogen bonding interaction with the main chain oxygens and nitrogens of catalytic S64 and S315, while the second boron hydroxyl group interact through H-bonding with the hydroxy group of Y150 and a water molecule. The R_2 side-chain of **16** and **17** is instead involved in H-bonds through its carboxytriazole group with R340, a characteristic residue from ADC-7.

In another study, the affinity of **16** for MOX-1, a plasmid-mediated CMY-type class C β-lactamase, was evaluated and compared with one of aztreonam (ATM) to gain knowledge for a better design of future inhibitors [120]. Against MOX-1, however, **16** showed weaker affinity ($K_i = 560$ nM) compared to aztreonam ($K_i = 10$ nM), due to tighter binding and structural rearrangements induced by aztreonam sulfonate group. Still, **16** lowered MICs of aztreonam and ceftazidime by 8- to 16-fold in *E. coli* strains overexpressing MOX-1. Compound **16** also demonstrated excellent activity against CTX-M-96, a CTX-M-15-type variant, with an IC_{50} of 2 nM, a value 40 times better than class A carbapenemase KPC-2 [121]. Despite similar acylation and deacylation kinetics across both enzymes, CTX-M-96 binding was stronger, therefore explaining the greater affinity. In the same study, compound **18**, an analogue of **16**, was designed by replacing the thiophene ring with a 5-mercapto-1,3,4-thiadiazol-2-amine moiety to improve its pharmacological properties (Figure 15). Compound **18** exhibited IC_{50} values of 4 nM for

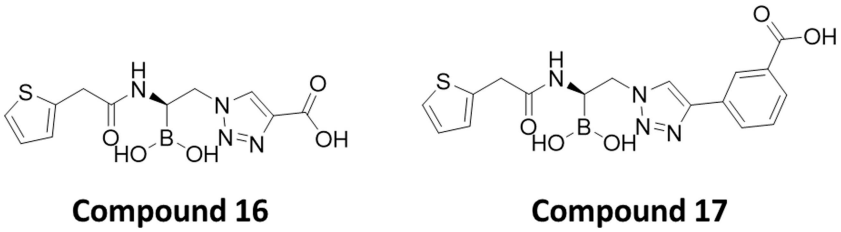

FIGURE 12 | Structures of the α-amido-β-triazolylethanboronic acids **16** and **17**.

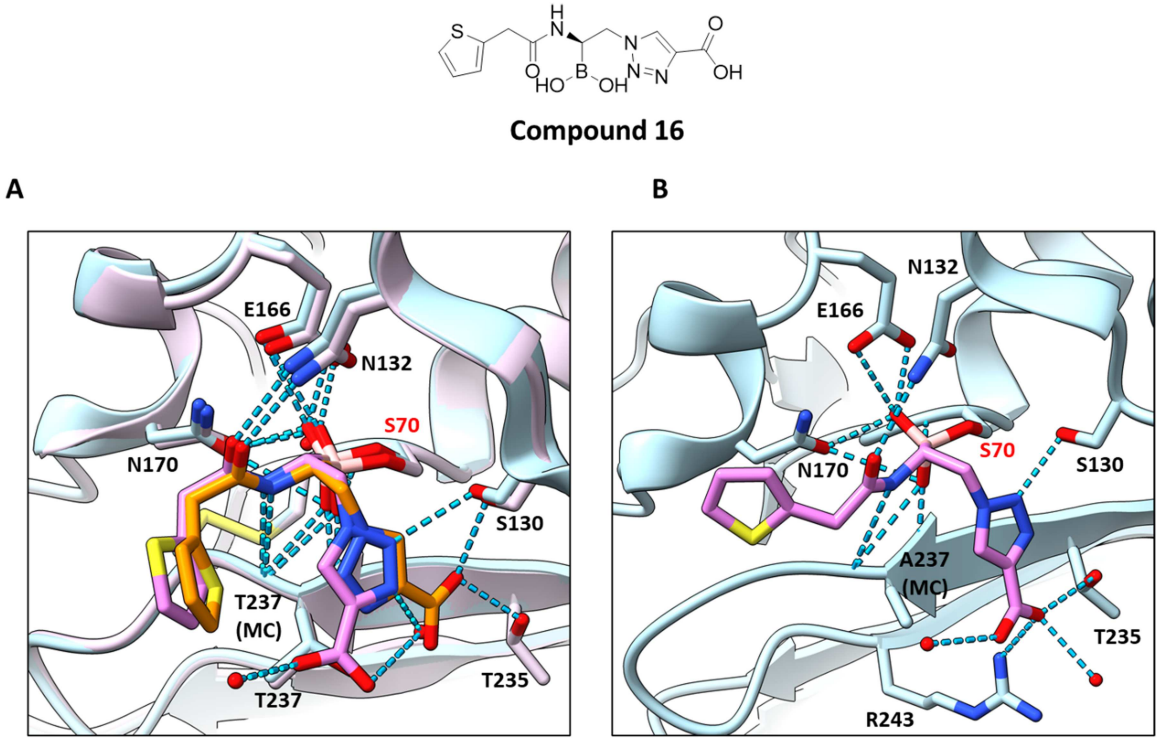

FIGURE 13 | (A) Crystal structures *Klebsiella pneumoniae* KPC-2 (UniProt ID: Q9F663) in complex with compound **16** (PDB: 5EEC). In this case, compounds **16** assumes different conformations, and is presented as a superimposition of orange and pink ligands. (B) Crystal structures *K. pneumoniae* SHV-1 (UniProt ID: P0AD64) in complex with compound **16** (PDB: 5EE8). Color code and graphical conventions are as in Figure 4. [Color figure can be viewed at wileyonlinelibrary.com]

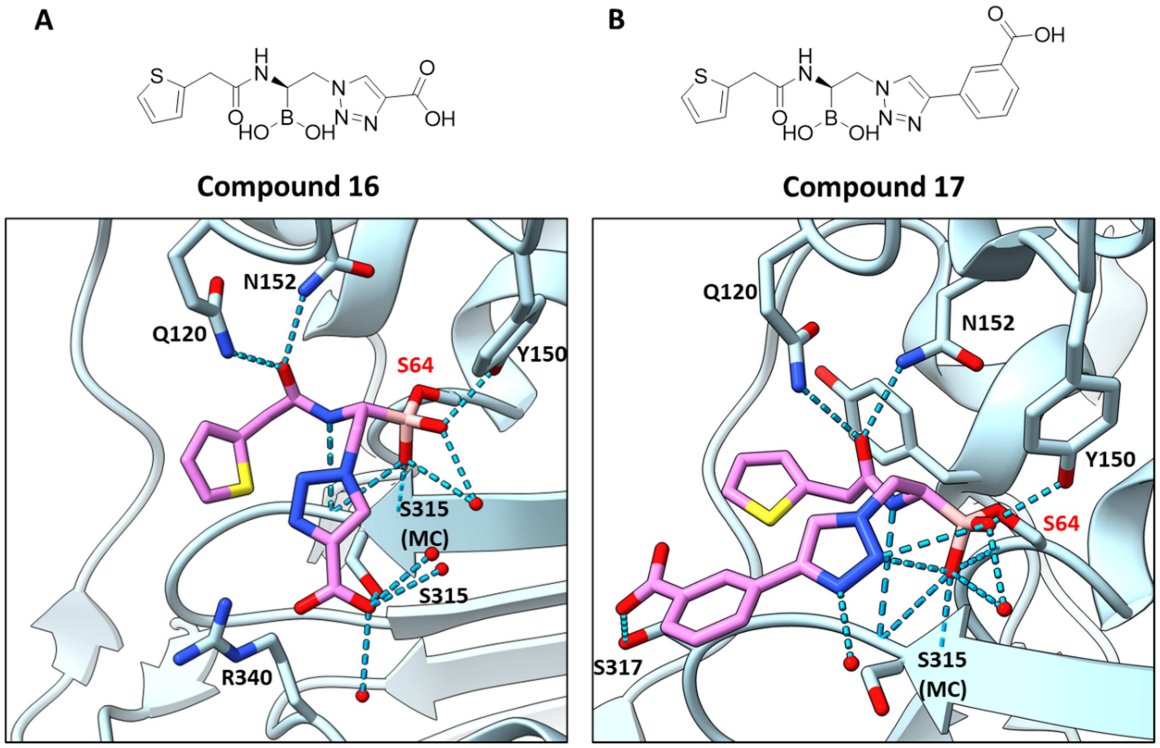

FIGURE 14 | Crystal structures *A. baumannii* ADC-7 (UniProt ID: Q6DRA1) in complex with: (A) compound **16** (PDB: 4U0X). (B) compound **17** (PDB: 5W14). All other color code and graphical conventions are as in Figure 4. [Color figure can be viewed at wileyonlinelibrary.com]

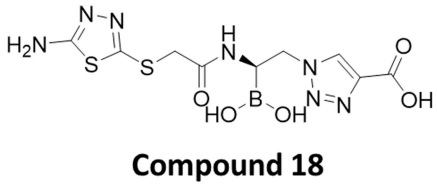

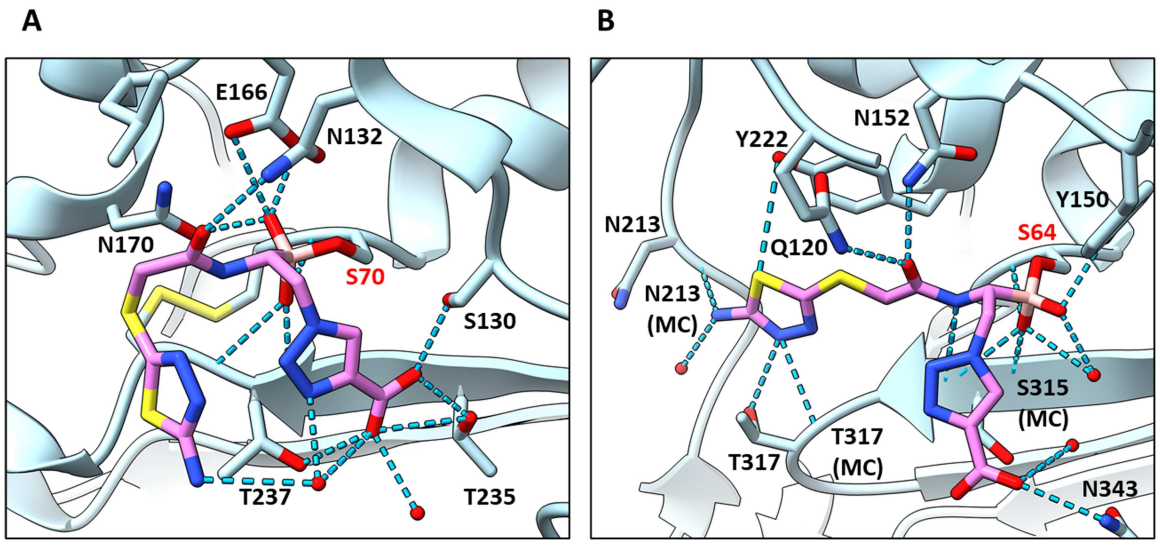

FIGURE 15 | (A) Crystal structures *Klebsiella pneumoniae* KPC-2 (UniProt ID: Q9F663) in complex with compound **18** (PDB: 7UTB). (B) Crystal structures *A. baumannii* ADC-30 (UniProt ID: A7XM81) in complex with compound **18** (PDB: 8FQW). Color code and graphical conventions are as in Figure 4. [Color figure can be viewed at wileyonlinelibrary.com]

CTX-M-96 and 135 nM for KPC-2, though it had slower acylation rates, but similar off rates compared to **16**. Crystal structures of KPC-2 in complex with **16** and **18**, along with docking models of their binding to CTX-M-96, revealed a conserved network of hydrogen bonds involving S70, S130, N132, N170, and S237 with both enzymes (Figure 15A). A follow-up study focused on **18** and **16** activities against ADC-type β-lactamases. Both compounds retained low-nanomolar inhibitory affinity

values against seven ADC variants, with the strongest inhibition against ADC-30 ($K_i = 58$ nM for **18** and $K_i = 28$ nM for **16**) [122]. Moreover, **18** restored susceptibility to multiple cephalosporins, including ceftazidime, cefiderocol, cefotaxime, and ceftolozane, when tested in *E. coli* strains overexpressing various ADCs. Crystal structures of **18** in complex with six ADC variants (herein shown in complex with ADC-30: PDB 8FQW) revealed a consistent binding mode, underscoring the scaffold adaptability despite active site variability (Figure 15B).

Recently, Rojas et al. advanced the development of **16** and **18** by demonstrating potent in vitro bactericidal activity when combined with cefepime [123]. Encouraging results were observed also in vivo, where the cefepime/**18** combination achieved an approximate 3-$\log_{10}$ CFU reduction in lung infection model using male mice infected intranasally with multidrug-resistant KPC-producing *K. pneumoniae* KPC-Kpn-1. Notably, these data demonstrated this combination possess comparable bactericidal activity and in vivo efficacy as the clinically available BL/BLIs ceftazidime-avibactam.

The same group further expanded their library of triazole-based boronic acids by designing a new series of 1,2,3-triazol-1-ylmethaneboronic acids (Figure 16) [124]. Among them, compound **19** exhibited the highest affinity for KPC-2, with an excellent K_i of 1 nM [125]. In addition, when tested in *Klebsiella* strains producing KPC-2, compound **19** reduced cefepime MICs from 32 to 4 μg/mL. Another derivative from this series, compound **20**, was even more effective against KPC-producing *Klebsiella* strains, lowering cefepime MICs to 0.5 μg/mL, although exhibiting a slightly lower affinity for the KPC-2 enzyme ($K_i = 30$ nM). The click-chemistry platform was also applied to design 26 α-triazolylmethaneboronic acids targeting ADC-7 [126]. Herein, structural analysis on compound **21** served as model ($K_i = 6.1$ μM for ADC-7, PDB: 5WAG) to understand the role of the triazole moiety in amide-binding site recognition, therefore indicating α-triazole BATSIs as amide bioisosters active against ADC-7 [118]. The optimization work yielded compound **22**, the most active analogue ($K_i = 90$ nM). Furthermore, at 4 μg/mL, **22** was able to lower ceftazidime MICs by eightfold in *E. coli* overexpressing $bla_{ADC\text{-}7}$ or $bla_{CMY\text{-}2}$, and by twofold in *P. aeruginosa* strains containing the bla_{PDC} gene. Interestingly, the crystal structure of **22** in complex with ADC-7 (PDB: 6TZJ) showed no interaction between the sulfonamide and the enzyme. Instead, a key cation-π interaction was observed between the tolyl group and R340. These results highlight the triazole-based boronates versatility in overcoming class C β-lactamase resistance and demonstrate their promise for broad-spectrum inhibitor development.

Successful application of click chemistry to boronic acids has laid the basis for the development of a plethora of potent BATSIs derived from this versatile reaction (Table 5). Compounds **16** and **18** stand out for their broad-spectrum inhibition,

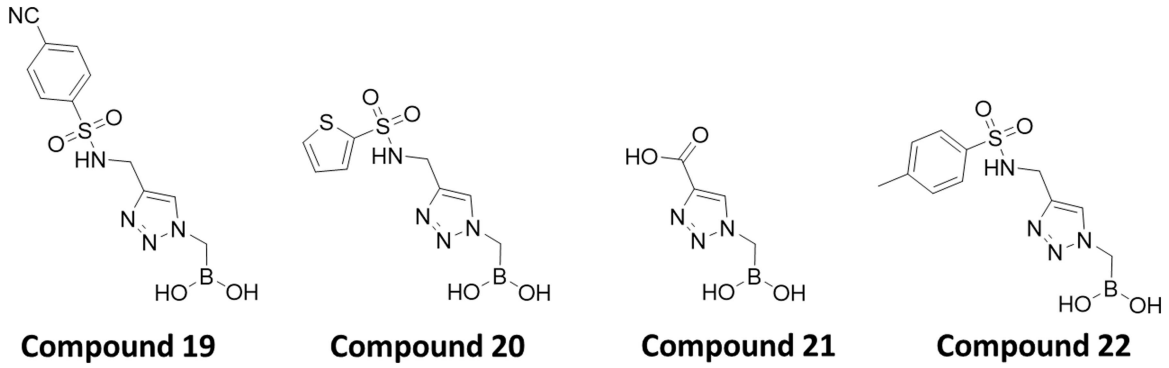

FIGURE 16 | Structure for α-triazolylmethaneboronic acids **19**-**22**.

TABLE 5 | Spectrum of activity of sulfonylaminomethyl boronic acid compounds 16-22 against various β-lactamases.

Compound	K_i/IC_{50} (μM)							
Ambler Class	A			C				
β-Lactamase	SHV-1	KPC-2	CTX-M-96	ADC-7	ADC-30	P99	PDC-3	MOX-1
UniProt ID	P0AD64	Q9F663	Q6ZXB6	Q6DRA1	A7XM81	P05364	P24735	Q51578
16	**0.130**	**0.080**	**0.002**	0.044	0.028	0.140	0.035	0.560
17	**0.140**	**0.040**	—	0.046	—	0.084	0.068	—
18	—	**0.135**	**0.004**	—	0.058	—	—	—
19	—	**0.001**	—	—	—	—	—	—
20	—	**0.030**	—	—	—	—	—	—
21	—	—	—	6.1	—	—	—	—
22	—	—	—	0.090	—	—	—	—

Note: IC_{50} values are denoted in bold, while K_i are denoted in normal character.

low nanomolar potency, and demonstrated in vivo efficacy, particularly against class A and C β-lactamases. However, despite their strong performance, both compounds still fall short in effectively targeting class D and metallo-β-lactamases, underscoring the need for further optimization to achieve truly pan-β-lactamase inhibition.

2.1.4 | *Thiol-Containing Acyclic Boronic Acids*

Thiol insertion to achieve broad-spectrum inhibitors: The BATSIs described in the previous subsections did not hold any potential to target both SBLs and MBLs simultaneously. To address the growing threat posed by MBLs, Wang et al. employed a structure-based design strategy to develop a novel class of thiol-containing acyclic boronic acids as broad-spectrum dual-action inhibitors (Figure 17) [127].

By combining a boronic acid warhead with metal-binding pharmacophores (MBPs), they synthesized (2′S)-(1-(3′-mercapto-2′-methylpropanamido)-methyl)boronic acid (compound **23**) as a prototype dual inhibitor. To validate this design, three control analogues lacking either the thiol or boronic acid groups were also synthesized. Compound **23** demonstrated sub-micromolar activity against VIM-2 ($K_i = 760$ nM), a clinically relevant subclass B1 MBL, and showed promising activity against subclass B2 Sfh-1 ($K_i = 7.34\,\mu$M) and subclass B3 GOB-18 ($K_i = 2.23\,\mu$M). Conversely, compound **23** exhibited poor activity against clinically relevant class B1 NDM-1 ($K_i = 67.13\,\mu$M). For SBLs, **23** inhibited KPC-2 (class A, $K_i = 2.70\,\mu$M) and AmpC (class C, $K_i = 6.46\,\mu$M), but was significantly less effective against TEM-1 (class A, $K_i = 40.97\,\mu$M) and OXA-48 (class D, $K_i = 70.19\,\mu$M). Structural studies of **23** in complex with VIM-2 (Figure 18A) and KPC-2 (Figure 18B) clarified its dual mechanism. In VIM-2, the thiol group acts as a zinc-chelating moiety, displacing the zinc-bridging hydroxide and coordinating both Zn^{2+} ions. The amidocarbonyl and boronic acid groups form stabilizing hydrogen bonds with N233 and R228, respectively. In KPC-2, the boronic acid forms a covalent adduct with S70, typical of BATSIs, while additional stabilizing interactions are formed with T237, N170, E166, and N132.

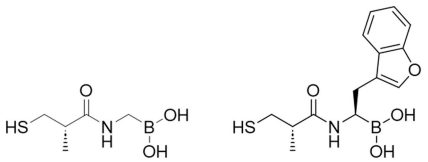

FIGURE 17 | Structure for the (1-(3′-mercaptopropanamido) methyl)boronic acids **23** and **24**.

Guided by these insights, the authors optimized compound **23** model scaffold to develop **24**, a more potent dual-action inhibitor (Table 6). Compound **24** showed improved inhibition of VIM-2 ($K_i = 440$ nM), Sfh-1 ($K_i = 260$ nM), and GOB-18 ($K_i =$ 130 nM). Activity against SBLs also improved, with K_i= values of 610 nM for KPC-2 and 110 nM for AmpC. However, **24,** as the parent compound, retained weak activity against NDM-1 ($K_i =$ 37.95 μM) and class D, in particular OXA-48 ($K_i > 300\,\mu$M). In microbiological assays, both **23** and **24** reduced meropenem MICs against resistant strains, including *E. coli* BAA-2340

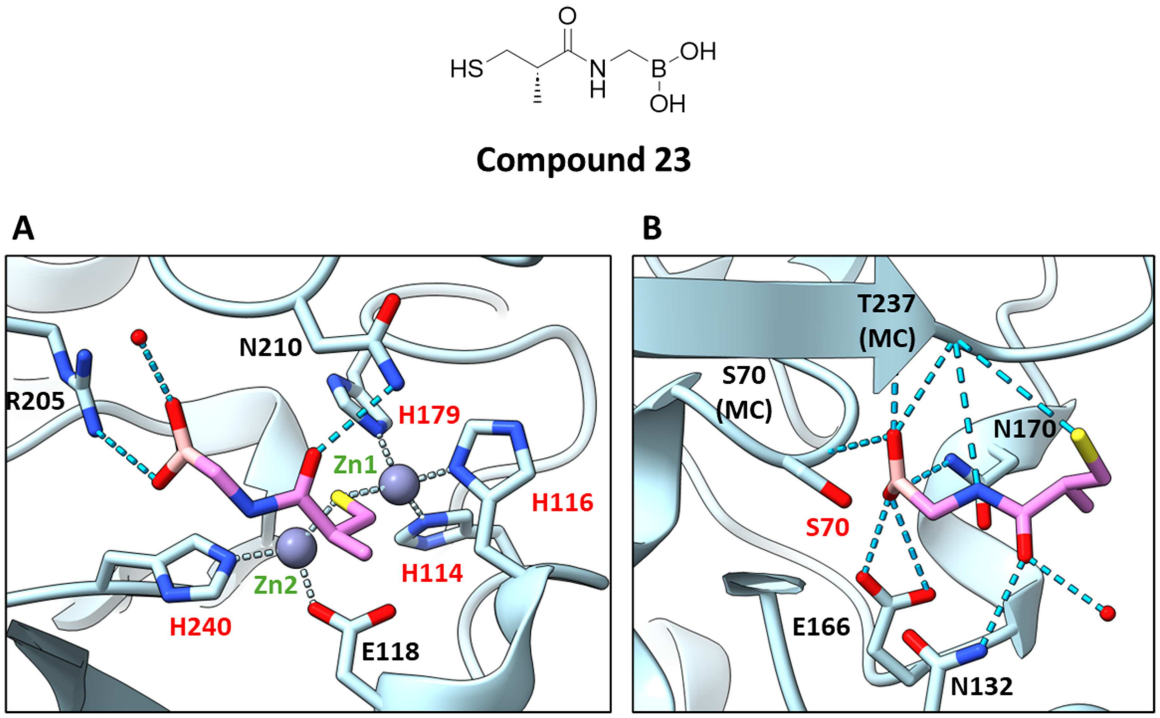

FIGURE 18 | Crystal structures of compound **23** in complex with (A) *Pseudomonas aeruginosa* VIM-2 (UniProt ID: Q9K2N0; PDB: 6J8R) and (B) *Klebsiella pneumoniae* KPC-2 (UniProt ID: Q9F663; PDB: 6J8Q). In VIM-2, the two Zn(II) ions are shown as gray spheres and are coordinated by the indicated catalytic residues. Gray dashed lines represent metal-coordination interactions. Compound **23** chelates the dinuclear metal center through its thiol group. In the deposited KPC-2 structure, compound **23** is not observed as a tetrahedral serine adduct. Residues labeled in red are key catalytic residues. All other color codes and graphical conventions are as in Figure 4. [Color figure can be viewed at wileyonlinelibrary.com]

TABLE 6 | Spectrum of activity of (1-(3′-mercaptopropanamido)methyl)boronic acids 23 and 24 against various β-lactamases.

Compound	K_i (μM)							
Ambler class	A		B1		B2	B3	C	D
β-Lactamase	TEM-1	KPC-2	VIM-2	NDM-1	Sfh-1	GOB-18	AmpC	OXA-48
UniProt ID	P62593	Q9F663	Q9K2N0	C7C422	Q9RMI1	Q4JRB6	P00811	Q6XEC0
23	40.9	2.7	0.760	67.1	7.3	2.2	6.4	70.2
24	—	0.610	0.440	37.9	0.610	0.130	0.110	> 300

expressing bla_{NDM-1}, bla_{KPC-2}, and bla_{AmpC}, highlighting their potential as lead candidates for further development. Notably, representative inhibitors from this series showed no apparent inhibition of human ACE-2 and displayed weak off-target activity across serine hydrolases in both *E. coli* and HEK293T cell lysates, supporting a favorable selectivity profile. Moreover, these compounds potentiated meropenem against clinical isolates without apparent cytotoxicity in HEK293T and MCF-7 cells at concentrations up to 100 μM.

2.2 | Aryl Boronic Acid Derivatives

2.2.1 | *Phenylboronic Derivatives*

From borate ions to template-based discovery: Investigations on the potential inhibitory activity of borate ions/boronic acids against β-lactamases dates back to 1971, when Dobozy et al. discovered that borate ions could reversibly inhibit β-lactamase I (TEM-1) [128]. Kiener and Waley exploited these findings and unveiled the reversible competitive inhibition of a class A β-lactamase from *Bacillus cereus* (K_i = 1.2-4 mM) using boric acid (compound **25**), phenyl boronic acid (compound **26**) and *m*-aminophenylboronic acid (compound **27**) (Chart 3 and Figure 19) [129, 130]. Interestingly, authors debated whether compound **27**, and consequently boronic acid, could be reversible covalent inhibitors for β-lactamases, considering the ability of this class of compounds to form covalent adduct with chymotrypsin and subtilisin, two serine proteases [131–133]. Further studies conducted by Waley's laboratory on aryl boronic acids elucidated the mechanism of binding through a tetrahedral intermediate between a boronic acid and the β-lactamase complex, revealing its covalently and reversible nature [101, 134, 135].

Building on these findings, further evaluation of aryl boronic acids as selective inhibitors against class C β-lactamases led to a remarkable improvement in inhibitory potency (Figure 20). Among 12 compounds tested, 3-iodoacetamidophenylboronic acid (**28**) emerged as the most potent, exhibiting K_i values of 23 μM against AmpC and 2.4 μM against the *Pseudomonas*-derived β-lactamase (PDC) [134]. Microbiological assays confirmed its synergistic activity with cephalosporin C, reducing the MIC up to fourfold against the *P. aeruginosa* strain, a promising indication of its adjuvant potential. While investigating the role of β-lactamases in the hydrolysis and aminolysis of acyclic depsipeptides, Pazhanisamy et al. identified *m*-(dansylamidophenyl)-boronic acid (**29**) as an effective class C β-lactamase inhibitor, with K_i values of 600 nM for P99 and 1.3 μM for AmpC [136–139]. Building on this, Usher et al. applied a structure-based design approach, leading to the discovery of more potent aryl boronic acid inhibitors targeting AmpC [140]. A key insight was the hydrogen bond formed between the boronic acid and the backbone carbonyl of A318, which was shown to stabilize the transition state of the enzyme-inhibitor complex. Starting from the AmpC:**27** crystal structure (PDB: 3BLS, K_i = 7.3 μM for AmpC), a series of analogues were designed through iterative structural modeling, enzymatic assays, and microbiological evaluation [141]. A simple amino-to-nitro substitution yielded *m*-nitrophenylboronic acid (**30**) with improved potency (K_i = 1.7 μM), while the symmetrical 4,4′-biphenyldiboronic acid (**31**) achieved sub-micromolar activity (K_i = 200 nM) against AmpC. Among the reported inhibitors, the benzo[*b*]thiophene-based derivative (compound **43**) stood out as the most potent and will be discussed in detail in Section 2.2.2.

Structure-based and rational design of novel phenyl boronic acid inhibitors: To elucidate whether larger *m*-functionalized aryl boronic acids could access unexploited regions in AmpC, Tondi et al. applied structure-based design combined with parallel synthesis to develop new inhibitors [142]. Out of 28 candidates, compounds **32** and **33** showed markedly improved activity against AmpC, with K_i values of 83 nM and 60 nM, respectively, over 100-fold better than the parent compound **27** (Figure 21). Similar trends were observed for other class C enzymes, including *E. cloacae* P99, with a K_i of 250 nM for compound **32** and a K_i of 450 nM for derivative **33**. However, both compounds showed reduced potency against class A enzymes such as *S. aureus* PC1 and TEM-1, with K_i values in the low micromolar range. As for other boronic acid-based BLIs, compound **32** demonstrated high selectivity for AmpC over other serine proteases showing over 200-fold preference versus chymotrypsin, trypsin and elastase. Both **32** and **33** effectively restored amoxicillin activity against Gram-positive strains like *S. epidermidis* and *S. aureus*, although they had surprisingly limited effects on Gram-negative β-lactamase producers. The crystal structure of AmpC-**32** revealed conserved recognition interactions, particularly quadrupole-dipole contacts between the boronic acid and residues N152 (first phenyl ring) and Y221 (sulfonamide nitrogen), highlighting their importance for future design. To further enhance binding and pharmacokinetics, a small, polar carboxylic acid was introduced at the *para*-position, and the [phenylsulfonyl)thiophene]−2-sulfonamido side chain was kept in *meta* [143]. This led to compound **34**, a validated lead showing strong inhibition of AmpC (K_i = 26 nM) and improved pharmacological properties. The AmpC:**34** complex revealed an additional H-bond interaction with Q120, not seen in AmpC:**32**.

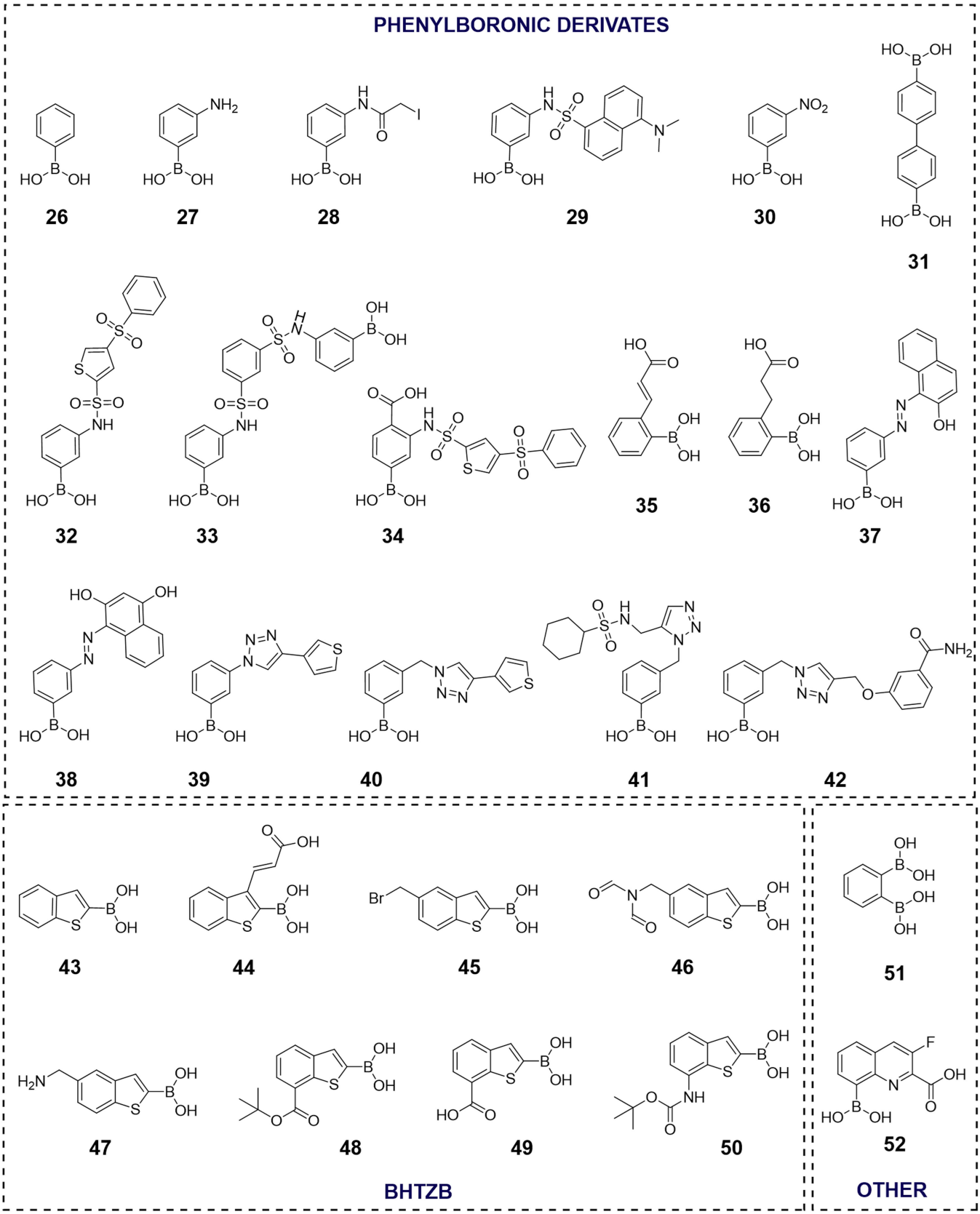

CHART 3 | List of aryl boronic acids presented in Section 2.2. [Color figure can be viewed at wileyonlinelibrary.com]

Later, in a parallel effort to target KPC-2, Celenza et al. used compound **26** ($K_i = 7.6\ \mu M$ for KPC-2) as a model compound for optimization [144]. This led to the development of phenyl boronic acids **35** and **36**, bearing *ortho*-carboxyalkyl groups. Both acted as slow, reversible, time-dependent inhibitors. Their affinities for KPC-2 were improved, with K_i values of 2.43 μM (**35**) and 1.13 μM (**36**), and they restored β-lactam activity in KPC-2-expressing clinical isolates, reducing MICs from 1024 to 0.25 μg/mL, without cytotoxicity. Crystal structures of KPC-2 with **35** and **36** revealed familiar π-stacking interactions with W105, typical of phenyl boronic inhibitors (Figure 22). These analogues also showed activity against class A carbapenemase GES-5 [145]. Specifically, compound **35** inhibited GES-5 with a K_i of 110 nM, and compound **36** displayed an inhibitory affinity of 1.83 μM for the same enzyme, therefore supporting the importance of the carboxylate chain inserted in *o*-position. Interestingly, those analogues revealed modest activity against class C AmpC, displaying a K_i of almost 42 μM for compound **35**, and a K_i of 76 μM for compound **36.** Other compounds mentioned in the article, bearing *meta*-substitutions were inactive against class A, although being effective inhibitors against AmpC, highlighting a key structure-activity relationship.

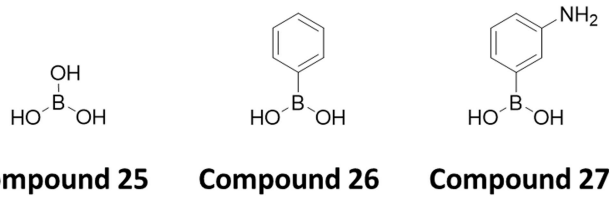

FIGURE 19 | Early compounds used for studying boronic acid properties as BLIs.

Diaza- and triazole-based phenyl boronic acid inhibitors: As per other cases previously described in this review, compound **27** (*m*-aminophenylboronic acid) served as a base for virtual screening models. By exploiting this, Buzzoni et al. developed a new family of phenyl boronic acids featuring *meta*-aza substitutions [146]. Among them, compounds **37** and **38** showed good inhibitory activity against *E. coli* AmpC, with K_i values of 300 nM and 450 nM, respectively (Figure 23). However, their synergy with ceftazidime was modest, reducing the MIC by only twofold in Gram-negative strains overexpressing AmpC.

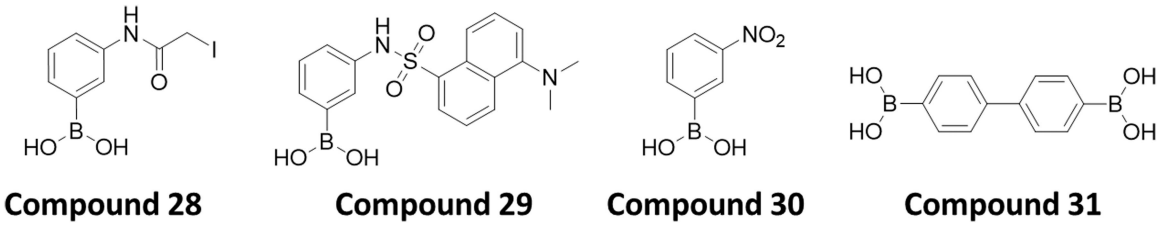

FIGURE 20 | Further derivatization of aryl boronic acids as BLIs leading to nM potency against class C β-lactamases.

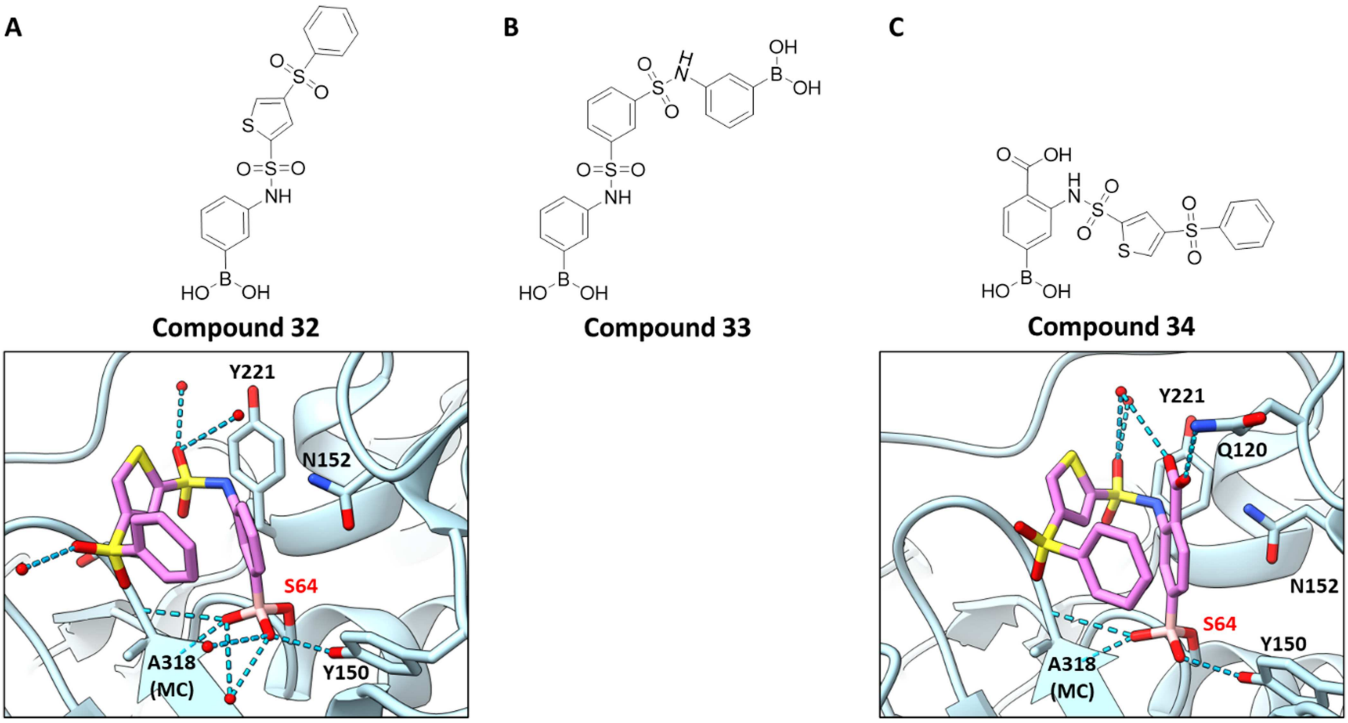

FIGURE 21 | (A) Crystal structures of *E. coli* AmpC (UniProt ID: P00811) in complex with compound **32** (PDB: 1GA9). (B) Structure of compound **33**. (C) Crystal structures of *E. coli* AmpC (UniProt ID: P00811) in complex with compound **34** (PDB: 3BM6) All other color code and graphical conventions are as in Figure 4. [Color figure can be viewed at wileyonlinelibrary.com]

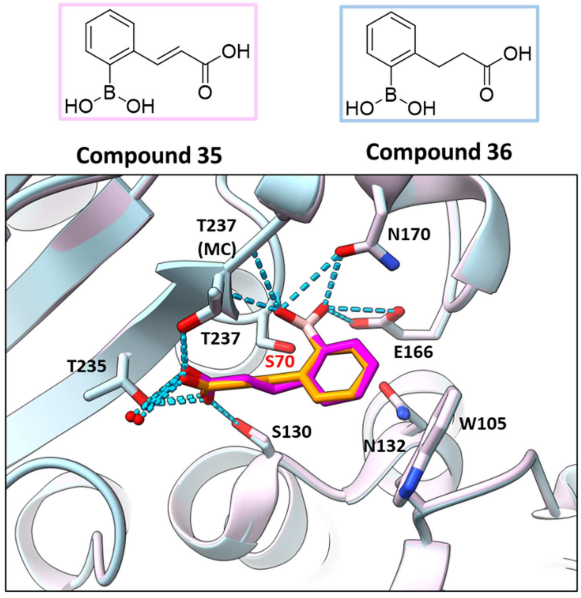

FIGURE 22 | Crystal structures *Escherichia coli* KPC-2 (UniProt ID: A0A0H4IUK8) in complex with compound **35** (PDB: 5LL7, light blue ribbon and ligand in magenta) and compound **36** (PDB: 5MGI, pink ribbon and ligand in orange). In the deposited KPC-2 structures, both compounds are not observed as a tetrahedral serine adduct. All other color code and graphical conventions are as in Figure 4. [Color figure can be viewed at wileyonlinelibrary.com]

E. coli AmpC has often served as a benchmark β-lactamase for evaluating phenyl boronic acid inhibitors. To extend the application of these scaffolds to other SBLs, Zhou et al. designed a series of triazole-based phenyl boronic acids with activity against KPC-2 (Figure 28) [147]. Earlier, compound **30** (*m*-nitrophenylboronic acid) had been reported as one of the first boronates to form a stable acyl-enzyme complex with KPC-2 ($K_M = 1\,\mu M$) [148]. Using this structure and click chemistry strategies, the team synthesized novel triazole analogues to explore structure–activity relationships. Susceptibility testing and *in silico* docking revealed that *meta*-substituted derivatives showed superior KPC-2 inhibition compared to their *para*-substituted counterparts. Building on these findings, a second-generation series of triazole boronates was developed [149]. Compounds **39** and **40** emerged as the most promising, inhibiting KPC-2 with excellent K_i values of 32 and 38 nM, respectively. Moreover, both analogues were able to reverse cefotaxime resistance in KPC-2-producing bacteria, reducing MICs to below 0.06 μg/mL. The study also highlighted the correlation of boronate acidity (pK_a range 5.98–10.0) in predicting KPC-2 binding affinity, suggesting pK_a can be a tunable property in the future development of this class of compounds. Importantly, selected phenylboronic acids from this series were well tolerated in HEK-293 cells, maintaining > 80% viability after 24 h at 5 and 50 μg/mL, both in the presence and absence of cefotaxime.

These compounds were further explored in a notable study by Santi et al., who applied in situ click chemistry to generate novel triazole-based boronates [150]. In this kinetic target-guided synthesis (KTGS) approach, KPC-2 and AmpC served as protein templates to catalyze azide-alkyne cycloadditions.

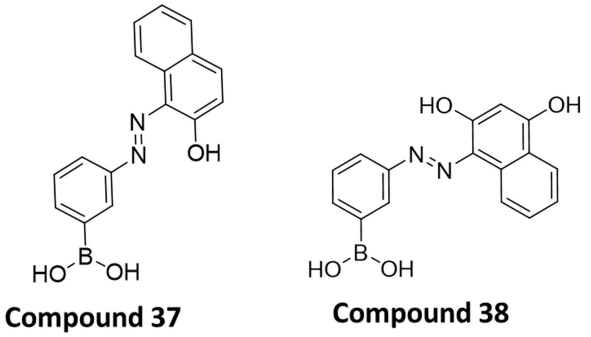

FIGURE 23 | Structures of the *meta*-aza phenylboronic acids **37** and **38**.

Starting with 3-azidomethylphenyl boronic acid and a 90-member alkyne library, the screening yielded compounds **41** and **42** (Figure 24). Notably, compound **41** was the first reported 1,5-disubstituted triazole β-lactamase inhibitor, selected by AmpC and displaying a K_i of 130 nM. Similarly, compound **42** was selected by KPC-2, showing a K_i of 730 nM. While this study marked the first KTGS application to both boronic acids and β-lactamase inhibition, it also outlined limitations and room for further optimization.

This section highlights major advances in aryl and triazole-based boronic acid derivatives, with compounds **34**, **39**, and **40** standing out for their nanomolar inhibition of class C (AmpC) and class A (KPC-2) enzymes, respectively (Table 7). While these inhibitors showcase excellent potency and structure-guided design, many still suffer from limited activity across multiple β-lactamase classes or lack further validation, underscoring the need for broader-spectrum efficacy and translational studies.

2.2.2 | *Benzo[b]Thiophene Derivatives*

As previously described in Section 2.2.1, starting from the crystallographic structure of compound **27** in complex with AmpC, Weston et al. designed a novel class of aryl boronic acids bearing the boronic acid functionality in position 2 of a benzothiophene ring using a structure-based approach [141]. Compound **43** (benzo[*b*]thiophene-2-boronic acid, BZBTH2B), emerged as the best out of 36 commercially available derivatives, exhibiting a strong affinity of ($K_i = 27$ nM) against chromosomally encoded AmpC. When tested in combination with the cephalosporin-derivative ceftazidime, compound **43** was able to potentiate the activity of the β-lactam by up to 64-fold against several resistant strains of bacteria [151]. This promising scaffold was used as model for studies focused on the interaction between AmpC active site and **43**, confirming that this inhibitor acts as acyl-enzyme transition state analogue and forms as a transient covalent bond with the catalytic serine S64 (Figure 25). Interestingly, the unconventional benzothiophene ring revealed a series of unexpected interactions with AmpC, including a π−π interactions with Y221, a π−dipole interactions with N52 and the hydrogen bond between the boronic acid O2 atom and the hydroxyl of Y150 [152]. However, although being one of the first boronic-acid derivative discovered to be active at nM concentration against class C β-lactamases, compounds **43** exhibited poor solubility and permeability to cells.

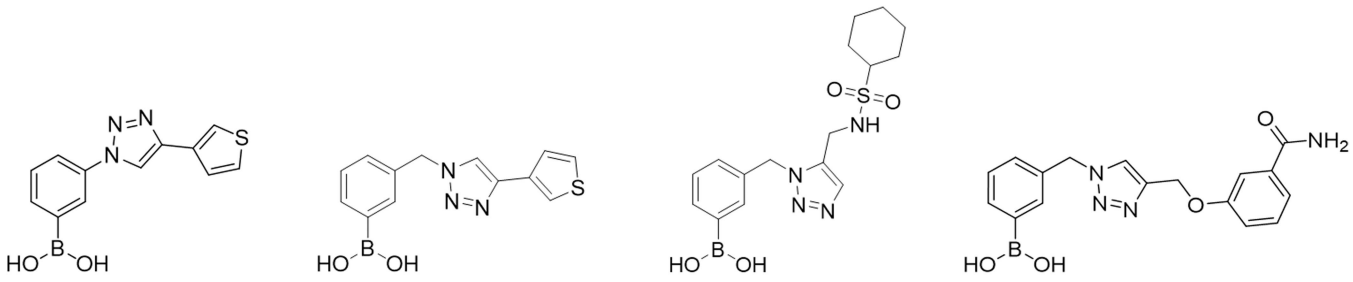

FIGURE 24 | Structures and inhibitory affinity of the triazolyl-based boronic acids **39**-**42**.

TABLE 7 | Spectrum of activity of phenylboronic acid derivatives 28-42 against various β-lactamases.

Compound	K_i (μM)			
Ambler class	A		C	
β-Lactamase	KPC-2	GES-5	AmpC	P99
UniProt ID	Q9F663 A0A0H4IUK8*	Q09HD0	P00811 P24735*	P05364
28	—	—	23	—
29	—	—	1.3	—
30	—	—	1.7	—
31	—	—	0.200	—
32	—	—	0.083	0.250
33	—	—	0.060	0.450
34	—	—	0.026	—
35	2.43*	0.110	42*	—
36	1.13*	1.83	76*	—
37	—	—	0.300	—
38	—	—	0.450	—
39	0.032	—	—	—
40	0.038	—	—	—
41	—	—	0.140	—
42	0.760	—	—	—

Note: For KPC-2, UniProt ID Q9F663 refers to the *Klebsiella pneumoniae* enzyme, whereas A0A0H4IUK8 refers to the *Escherichia coli*-expressed enzyme; values associated with the latter are marked by an asterisk. For AmpC, UniProt ID P24735 refers to the *Pseudomonas aeruginosa* enzyme, with the corresponding values also marked by an asterisk, whereas P00811 refers to *E. coli* AmpC.

Venturelli et al. conducted an in-depth investigation into the impact of C5 substituents on the affinity and pharmacokinetic properties of compound **43** and derivatives [152]. While none of the new compounds surpassed the parent compound in terms of AmpC binding affinity, several displayed significantly improved solubility and permeability. Notably, these derivatives also enhanced the antibacterial activity of ceftazidime against resistant strains. Building on this work, the same group applied structure-based drug design to develop a new derivative, compound **44** (Figure 26) [153]. This molecule features a 2-carboxyvinyl side chain at position 3 of the benzothiophene ring, specifically designed to engage the conserved carboxylate-binding pocket in SBLs. Compound **44** exhibited potent, broad-spectrum inhibition of both class A ($K_i = 40$ nM for both TEM-1 and CTX-M-9) and class C enzymes. The carboxylate moiety enabled critical hydrogen bonding with R276 in CTX-M-9 (PDB: 4LEN) and R244 in TEM-1 (PDB: 1NXY). However, despite its promising enzymatic profile, the compound proved unstable under microbiological assay conditions and could not be evaluated further in cell-based models.

Further derivatization of the benzo[*b*]thiophene-2-boronic acid scaffold (**43**) at C5 and C7 positions led to the development of six compounds with broad-spectrum activity against clinically and epidemiologically relevant β-lactamases from classes A to D (see Figure 26) [154]. Compounds **45**, **46**, and **47**, functionalized at C5, demonstrated a broad-spectrum profile by displaying excellent affinity for class C AmpC and micromolar inhibition of key class A (KPC-2, GES-5), class B (NDM-1, VIM-2), and class D (OXA-24) enzymes. In contrast, compounds **48**, **49**, and **50**, modified at C7, exhibited reduced activity against AmpC, but comparable or improved inhibition across the other classes (Table 8). The loss of AmpC affinity was attributed to steric hindrance from bulkier C7 substituents, which likely disrupted π–π interactions with Y221, a key residue for binding. With the exception of the cyclic boronic acids, presented in the next

section, compounds **45**-**50** (excluding compound **46**) represent the only example of acyclic and phenyl boronic acids active against MBLs, therefore holding promises for future development of broad-spectrum analogues. Importantly, this series of boronic acids was also evaluated for use in phenotypic diagnostic assays, demonstrating strong potential in agar-diffusion combination tests for rapid detection of β-lactamase-producing clinical isolates [155, 156].

Among the boronic acid derivatives evaluated in this subsection, the original compound **43** (benzo[*b*]thiophene-2-boronic acid, BZBTH2B) stands out for its potent nanomolar inhibition of AmpC and its ability to significantly potentiate ceftazidime activity. However, its poor solubility and permeability have limited its therapeutic potential. Subsequent derivatives, including C3-functionalized compound **44** and C5-functionalized analogues **45, 46** and **47**, improved solubility and broadened inhibition profiles across all β-lactamase classes (A–D). Yet, challenges encountered in the refinement process, including metabolic instability and loss of AmpC affinity in C7-substituted variants, highlights the need for further optimization to balance potency, selectivity, and pharmacokinetics for these derivatives.

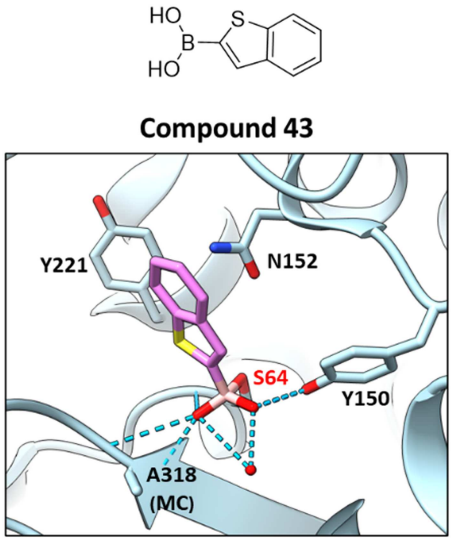

FIGURE 25 | Crystal structures *Escherichia coli* AmpC (UniProt ID: P00811) in complex with compound **43** (PDB: 1C3B). All other color code and graphical conventions are as in Figure 4. [Color figure can be viewed at wileyonlinelibrary.com]

2.2.3 | *Other Aromatic Boronic Acids*

In a recent study, more than 30 aromatic boronic acid derivatives, including *para*-, *meta*-, and *ortho*-phenylenediboronic acids, were systematically evaluated for their class A and C β-lactamase inhibitory activity, with a focus on clinically relevant KPC and AmpC enzymes (Figure 27) [157]. Among them, *ortho*-phenylenediboronic acid (compound **51**) emerged as the most potent compound, significantly restoring carbapenem activity in KPC-producing strains (up to 16-fold MIC reduction) and demonstrating strong synergy in checkerboard assays (Fractional inhibitory concentration (FIC) index: 0.1–0.32). Interestingly, different substitution patterns on the phenylene scaffold conferred distinct activity profiles. *Para*-substituted derivatives effectively potentiated both carbapenems and ceftazidime against KPC and AmpC producers, respectively, while *meta*-substituted analogues were more selective toward ceftazidime/AmpC combinations. Notably, these diboronic acids outperformed simple phenylboronic acid in potency and showed minimal toxicity in human fibroblasts, making them promising scaffolds for further development. However, the introduction of bulky, lipophilic groups (*i.e.* CF_3, I, $SiMe_3$) generally reduced efficacy, suggesting that future optimization should favor hydrophilic modifications, such as amides or peptide-like residues. This study underscores the therapeutic potential of multi-boronate inhibitors and lays a solid foundation for next-generation β-lactamase inhibitors targeting both class A and class C enzymes.

In a continued effort to identify potent β-lactamase inhibitors, a novel class of boron-containing molecules, 2-carboxyquinoline boronic acids, was developed as selective inhibitors of class A carbapenemase KPC-2 (Figure 27) [158]. These compounds were inspired by structural similarities to cephalosporin hydrolytic products and were designed to leverage the unique transition-state mimicry of boronic acids. Among the

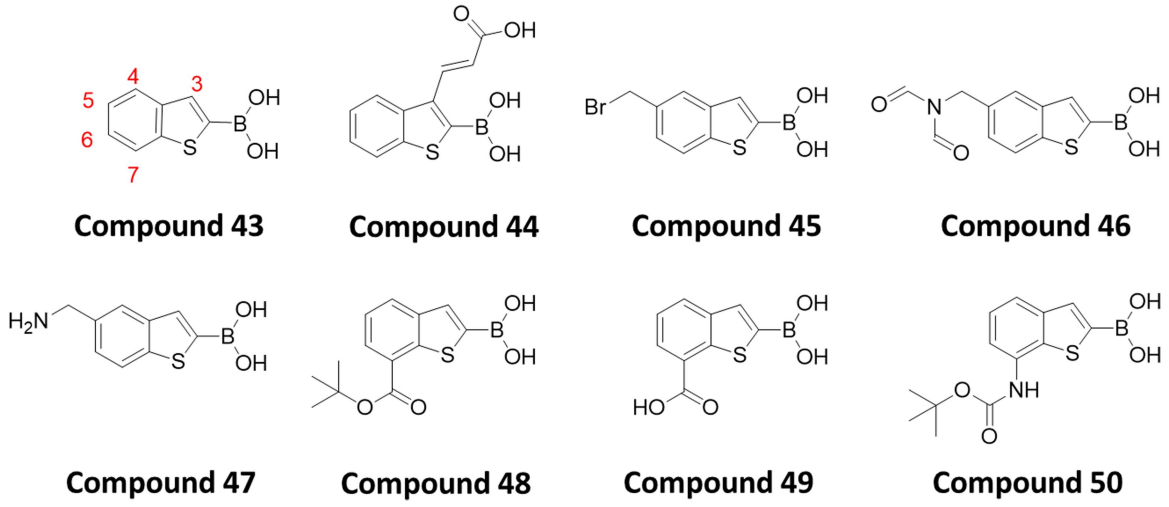

FIGURE 26 | Structures of benzo[b]thiophene-2-boronic acid derivatives **43**-**50**. In the structure of compound **43**, the carbon numberings are displayed in red. [Color figure can be viewed at wileyonlinelibrary.com]

TABLE 8 | Spectrum of activity of benzo[b]thiophene derivatives 43–50 against various β-lactamases.

Compound	K_i (μM)						
Ambler class	A				B	C	D
β-Lactamase	KPC-2	TEM-1	CTX-M-9	GES-5	NDM-1	AmpC	OXA-24/40
UniProt ID	Q9F663	P62593	Q9L5C8	Q09HD0	C7C422	P00811	Q8RLA6
43	—	50	50	—	—	0.027	—
44	—	0.04	0.04	—	—	0.09	—
45	2.8	—	—	8.9	5.9	0.07	67
46	—	—	—	24	—	0.04	—
47	4.4	—	—	15	5.5	0.05	96
48	3.2	—	—	17	3.2	1.3	27
49	4.9	—	—	0.16	3	0.42	16
50	1.4	—	—	5.7	11	1.4	64

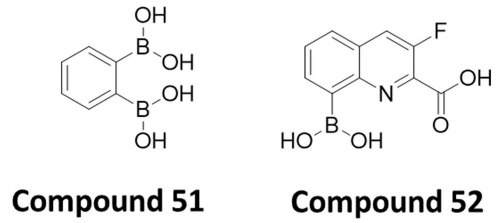

FIGURE 27 | Structures of *ortho*-phenylenediboronic acid **51** and 2-carboxyquinoline boronic acids derivative **52**.

synthesized derivatives, compound **52**, bearing a fluorine at position 3 and a boronic acid at position 8, demonstrated the strongest inhibition, with an excellent IC_{50} of 8.3 nM for KPC-2. For other β-lactamase classes, the authors observed negligible activity against other class A, B, C, and D, although the testing was performed until 2 μM. Importantly, SAR analysis revealed the 2-carboxy, 8-borono, and 3-fluoro substituents are essential for potent inhibition for this scaffold. Molecular docking suggested **52** engages KPC-2 in π–π stacking with W105, a unique interaction absent in other β-lactamases, possibly explaining its selectivity. Importantly, **52** restored the activity of meropenem and ceftazidime up to 256-fold in KPC-2-producing *K. pneumoniae*, and exhibited low cytotoxicity and hemolytic activity, marking it as a promising biocompatible and highly selective inhibitor for the treatment of KPC-driven antibiotic resistance.

2.3 | Cyclic Boronic Acid Derivatives

2.3.1 | *Benzoxaborole Derivatives*

Benzoxaboroles, first identified in the late 1950s, have garnered significant attention in recent decades due to their unique chemical properties, including intrinsic reactivity, metabolic stability, and low toxicity [159]. These attributes have positioned them as promising scaffolds in the development of various therapeutic agents, including dermatological, oncological and antimicrobial agents [91, 160]. Notably, C5-functionalization of the benzoxaborole ring has led to the development of Tavaborole and Crisaborole [161, 162]. Tavaborole (brand name Kerydin) is a topical antifungal agent used for the treatment of onychomycosis and it functions by inhibiting fungal leucyl-tRNA synthetase, thereby disrupting protein synthesis and leading to fungal cell death [161, 162]. Crisaborole, marketed as Eucrisa, is a non-steroidal topical medication approved for the treatment of mild-to-moderate atopic dermatitis [163]. It acts as a phosphodiesterase 4 (PDE4) inhibitor, reducing the production of pro-inflammatory cytokines. Currently, other clinical candidates for this class have been developed as antitrypanosomiasis, antimalaria and antituberculosis drugs.

In 2011, efforts from Anacor and Naeja Pharmaceuticals lead to the development of novel benzoxaborole-based BLIs targeting class C β-lactamases P99 and CMY-2 [164]. Herein, the authors explored benzoxaboroles as boron-containing scaffolds, due to their improved pharmacokinetic properties over classical boronic acids. Through a structure–activity relationship study of C6-substituted benzoxaboroles, the authors identified compound **53** (Chart 4), a pyrazine-substituted benzoxaborole bearing a *p*-carboxylic acid, as a potent and selective inhibitor of class C β-lactamases (Figure 28). Compound **53** exhibited a K_i of 20 nM against P99 and 20 nM for CMY-2. A drastic reduction in the inhibitory affinity was observed for class A TEM-1 (K_i = 20.4 μM) and CTX-M-9a (K_i > 32 μM). Microbiological testing revealed compound **53** restored ceftazidime efficacy in *E. cloacae* and *E. coli* strains overexpressing P99 or CMY-2, reducing MICs from > 128 μg/mL to as low as 0.5–1 μg/mL. In addition, herein it was demonstrated the importance of oxygen-containing linkers at C6. Furthermore, it was observed that small polar groups at the *meta*-position on the phenyl ring optimized binding to class A enzymes, while carboxylates at the *para*-position strongly enhanced class C inhibition.

Based on this work, McKinney et al. reported the rational design, synthesis, and evaluation of over thirty novel benzoxaborole-based derivatives [165]. By integrating crystallographic analysis, computational docking, and SAR optimization, the authors identified a series of promising derivatives, with compound (*rac*)-**54** and the enantiomer (*R*)-**54**, as the most potent broad-spectrum inhibitors of SBLs (Figure 28). Remarkably, compound (*R*)-**54** activity spanned from class A IC_{50} = 26 nM for KPC-2, to class C IC_{50} = 12 nM for P99, and finally to class D IC_{50} = 88 nM for OXA-24/40.

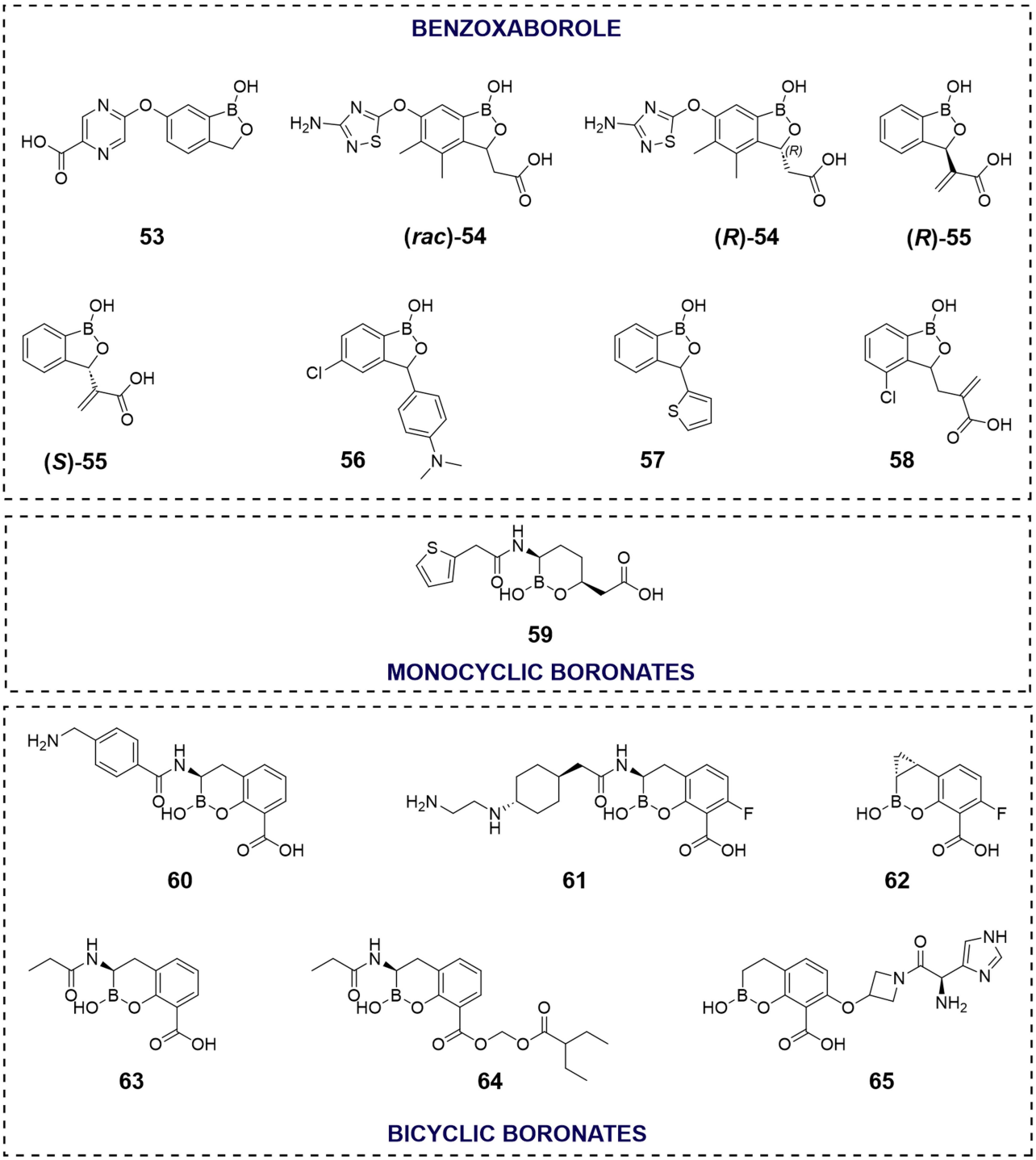

CHART 4 | List of cyclic boronic acids presented in Section 2.3. [Color figure can be viewed at wileyonlinelibrary.com]

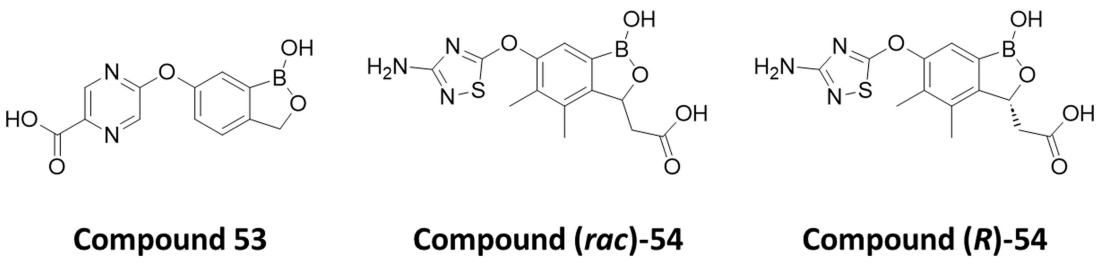

FIGURE 28 | Structures of benzoxaborole-containing derivatives **53**, (*rac*)-**54** and (*R*)-**54**.

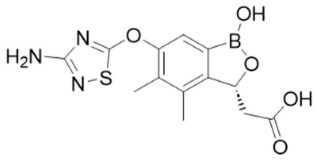

Compound (*R*)-54

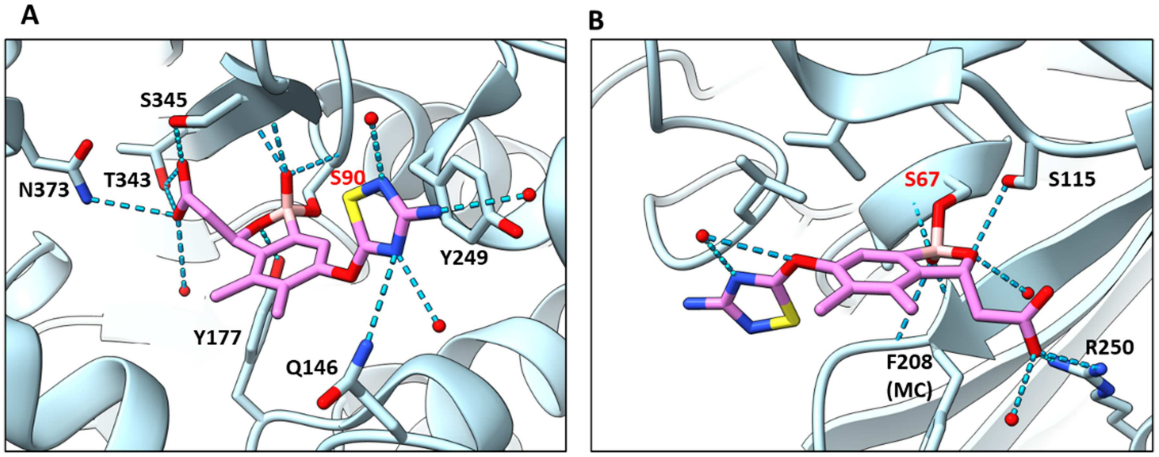

FIGURE 29 | (A) Crystal structures *Pseudomonas aeruginosa* AmpC (UniProt ID: P24735) in complex with compound (*R*)-**54** (PDB: 4WZ4). (B) Crystal structures *P. aeruginosa* OXA-10 (UniProt ID: P14489) in complex with compound (*R*)-**54** (PDB: 4WZ5). All color code and graphical conventions are as in Figure 4. [Color figure can be viewed at wileyonlinelibrary.com]

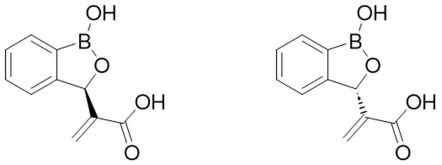

Compound (*R*)-55 Compound (*S*)-55

FIGURE 30 | Structures of chiral 3-substituted benzoxaboroles (*R*)-**55** and (*S*)-**55**.

Both compounds were able to restore ceftazidime efficacy up to 256-fold in *E. coli* and *C. freundii*. However, activity in *K. pneumoniae*, *A. baumannii*, and *P. aeruginosa* remained limited, likely due to poor permeability. Crystallographic studies using compound (*R*)-**54** in complex with AmpC or OXA-10 revealed a similar orientation of the inhibitor in the two enzymes, while confirming key interactions, such as π–π stacking and H-bonding with their respective catalytic residues (Figure 29). Although compound (*rac*)-**54** and (*R*)-**54** outperformed the clinical BLI tazobactam in specific strains, its pharmacokinetic limitations precluded further development without structural refinement.

Later, Xiao et al. described a structure-based design approach to introduce a chiral center in C3 position via asymmetric Morita-Baylis-Hillman reaction and design novel chiral benzoxaboroles [166]. The two most promising enantiomers identified, namely compounds (*R*)-**55** and (*S*)-**55**, demonstrated broad-spectrum inhibitory activity clinically relevant carbapenemases, effectively targeting both MBLs and SBLs (Figure 30). Interestingly, (*R*)-**55** demonstrated a promising affinity for class A KPC-2 ($IC_{50} = 3.1\ \mu M$) and OXA-48 ($IC_{50} = 15.8\ \mu M$), while not exhibiting any activity on class Cs and Bs. A more pronounced activity was observed when (*S*)-**55** was tested against KPC-2 ($IC_{50} = 480\ nM$), OXA-48 ($IC_{50} = 14.1\ \mu M$) and surprisingly MBL VIM-2 ($IC_{50} = 12.1\ \mu M$). Both compounds significantly potentiated meropenem activity against *K. pneumoniae* and *E. coli* isolates producing KPC-2, TEM-1, and AmpC, with the greatest effect observed at an inhibitor concentration of 100 μM [166].

Structural insights from the KPC-2:(*S*)-**55** and the OXA-48:(*R*)-**55** complexes confirmed covalent bond formation between the boron atom and the catalytic S70, consistent with a BATSI mechanism (Figure 31). Notably, the binding mode of these compounds closely resembled that of ring-opened carbapenems, further supporting their BATSI-like behavior. The study also suggested that future optimization should focus on functionalization at the C6 position to enhance potency and spectrum.

The potential of C3-substituted benzoxaboroles as broad-spectrum β-lactamase inhibitors was further investigated, with the identification of compounds **56** and **57** as the most promising candidates (Figure 32) [167]. Compound **56** demonstrated excellent potency, with an IC_{50} of 86 nM against class A KPC-2, and maintained micromolar-level activity against representative enzymes from classes B (Sfh-1, subclass BII), C, and D. Both compounds were able to significantly lower the MICs of meropenem in clinical isolates expressing KPC-2, effectively restoring antibiotic susceptibility. Importantly, neither **56** nor **57** exhibited cytotoxic effects in HEK293T cells at concentrations up to 100 μM. Liang et al. recently continued their promising work on benzoxaboroles as BLIs by optimizing 3-substituted benzoxaboroles through the introduction of a methacrylic acid moieties at the C3 position [168]. Among several analogues synthesized and tested, compound **58** exhibited the best cross-class inhibition, exhibiting

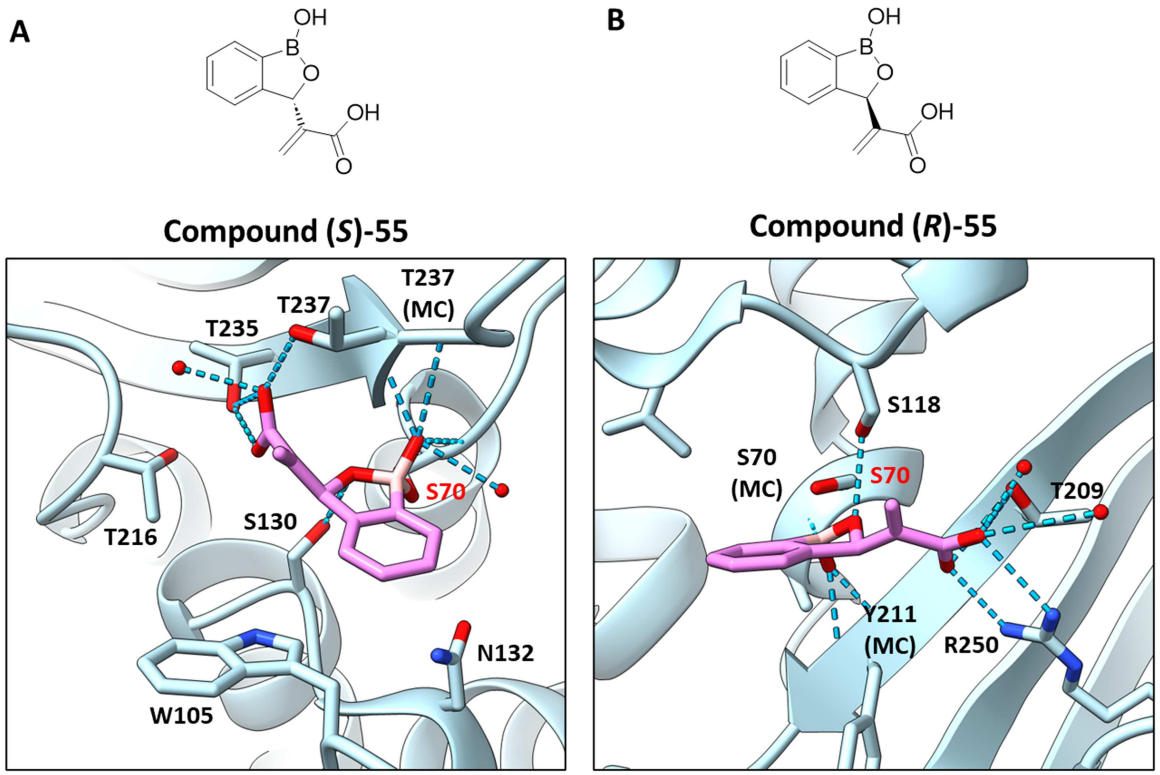

FIGURE 31 | (A) Crystal structures *Klebsiella pneumoniae* KPC-2 (UniProt ID: Q9F663) in complex with compound (*S*)-**55** (PDB: 7E9A). (B) Crystal structures *K. pneumoniae* OXA-48 (UniProt ID: Q6XEC0) in complex with compound (*R*)-**55** (PDB: 7DML). In the deposited OXA-48 structure, compound (*R*)-**55** is not observed as a tetrahedral serine adduct. All color code and graphical conventions are as in Figure 4. [Color figure can be viewed at wileyonlinelibrary.com]

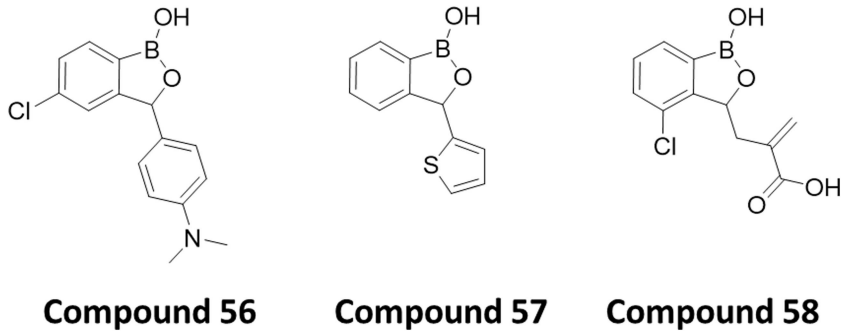

FIGURE 32 | Structures of the benzoxaborole **56, 57** and **58**.

sub-micromolar activity for both SBLs and MBLs (Figure 32). Compound **58** displayed an IC_{50} of 590 nM against KPC-2, an IC_{50} of 470 nM against OXA-48, and IC_{50} of 430 nM for clinically relevant VIM-2. Moreover, compound **58** stood out for its ability to restore meropenem efficacy against multiple multidrug-resistant Gram-negative pathogens. Structural analyses of the VIM-2 and OXA-48 complexes with different analogues revealed binding modes comparable to those of other bicyclic boronates.

Transition of benzoxaboroles into β-lactamase inhibitors, particularly through structure-guided design and functionalization at C3 and C6, has revealed their capacity to selectively and potently inhibit SBLs and, to a lesser extent, MBLs. Among the most notable examples, compounds (*R*)-**54** and **58** stand out for their nanomolar cross-class inhibition, including class D OXA-24/40 and class A KPC-2 (Table 9). However, the overall clinical potential of these agents remains hindered by pharmacokinetic liabilities, particularly limited permeability in Gram-negative strains like *K. pneumoniae* and *P. aeruginosa*, and ability to off-target binding. Future development should focus on improving cell penetration, possibly through tuning polarity or transporter affinity, while retaining key binding features. This class holds promises for next-generation broad-spectrum β-lactamase inhibitors, particularly if such structural optimizations can overcome current barriers to in vivo efficacy.

2.3.2 | *Monocyclic Boronic Acid Derivatives*

The first clinically approved boronic acid as BLI: Monocyclic boronates emerged as a potent class of boron-based BLIs with the development of **vaborbactam** (compound **59**, formerly

TABLE 9 | Spectrum of activity of benzoxaborole derivatives 53-58 against various β-lactamases.

β-lactamase (class, UniProt ID)	IC_{50} (μM)							
	53	**(*S*)-54**	**(*R*)-54**	**(*S*)-55**	**(*R*)-55**	**56**	**57**	**58**
TEM-1 (A, P62593)	20.4	0.01	< 0.005	—	—	1.5	6.9	—
CTX-M-15 (A, A0A223A5J4)	—	< 0.005	< 0.005	—	—	—	—	—
KPC-2 (A, Q9F663)	—	0.041	0.026	0.48	3.08	0.086	0.41	0.59
NDM-1 (B, C7C422)	—	—	—	> 600	550	9.1	22.4	6.8
VIM-2 (B, Q9K2N0)	—	—	—	12.1	> 600	> 100	17.3	0.43
IMP-1 (B, P52699)	—	—	—	142	> 600	—	—	—
Shf-I (B, Q9RMI1)	—	—	—	—	—	3.8	2.5	—
AmpC (C, P24735[a], P00811)	—	< 0.008[a]	0.012[a]	185	134	22.6	18.7	—
CMY-2 (C, Q48434)	0.02	—	—	—	—	—	—	—
P99 (C, P05364)	0.02	0.36	0.067	—	—	—	—	—
OXA-10 (D, P14489)	—	3.1	3.9	—	—	—	—	—
OXA-24/40 (D, Q8RLA6)	—	0.17	0.088	—	—	—	—	—
OXA-48 (D, Q6XEC0)	—	0.21	0.12	14.1	225	2.3	5.4	0.47

Note: The superscript a is referred to the Uniprot ID P24735, reported in the first column.

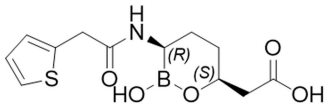

Compound 59

FIGURE 33 | **Vaborbactam** (compound **59**) chemical structure.

RPX7009), a selective inhibitor of class A and C serine β-lactamases (Figure 33) [169]. The design of **vaborbactam** centers on a cyclic α-acylaminoboronic acid scaffold, which promotes a conformationally constrained geometry favorable for enzyme binding [169]. This strategy enhances both potency against SBLs and selectivity over mammalian serine hydrolases, supporting its advancement through preclinical and clinical development. Structurally, **vaborbactam** binds analogously to other boronic acid, through a reversible bond to the catalytic serine residue of β-lactamases, forming a covalent tetrahedral adduct that mimics the transition state of β-lactam hydrolysis. The molecule features a cephalothin R_1 amide side chain moiety, well-characterized for its favorable interactions within SBLs active sites, and a (*S*)-configured carboxymethyl substituent at the 3-position of the boronate ring, a key recognition element for anchoring within the enzyme substrate-binding pocket.

As depicted in Table 10 the spectrum of activity for vaborbactam includes excellent inhibition for class A, including carbapenemases and class C SBLs [88, 169, 170]. However, modest inhibition against class D and only weak activity against class B MBLs limits its scope of inhibition [170, 171]. Moreover, extensive kinetic evaluation and biochemical characterization revealed compound **59** acts as a powerful progressive inactivator of different β-lactamases [171].

Vaborbactam, when combined with β-lactams like cefepime or meropenem, restores antibiotic activity against *Enterobacteriaceae* producing class A and C serine β-lactamases, notably KPC enzymes [169]. Whole-cell assays demonstrate strong correlation with biochemical inhibition data, though factors such as porin loss (e.g., OmpK35/36 mutations) and efflux mechanisms can influence activity [169, 173]. In combination with meropenem, **vaborbactam** demonstrated good in vitro activity also against *Klebsiella* spp. and *Citrobacter* spp. producing KPC enzymes, with less activity in strains lacking porins or overexpressing efflux pumps [173]. Since 2017, Vabomere, a 1:1 combination of meropenem/**vaborbactam**, has been approved for treatment in complicated urinary tract infections, complicated abdominal infections, and hospital-acquired pneumonia [174]. Several excellent reviews and articles cover the extensive microbiological, pharmacological, pharmacokinetic and evolution of resistance for this combination [175–180]. Structural analysis aided to gain understanding for the binding of **vaborbactam** with class A KPC-2 and CTX-M-14 (Figure 34) [181]. Despite their similarity, compound **59** displayed different bindings mode within those enzymes, denoting a rather compact binding in KPC-2.

Despite its approval, vaborbactam remains the only notable example of monocyclic boronic acids, whereas bicyclic boronic acids, presented in the next section, acids have taken a significant advancement due to their cross-class inhibition ability.

2.3.3 | *Bicyclic Boronic Acid Derivatives*

The evolution of benzoxaborinine as potent scaffold for BLIs design: In the last 15 years, Protez Pharmaceuticals first and later Venatorx Pharmaceuticals introduced and evolved bicyclic boronates (2-hydroxy-3,4-dihydro-2H-benzo[*e*] [1,2] oxaborinine) as chemical entity possessing potent cross-class inhibitory properties against β-lactamases [182]. In this context, the benzoxaborinine moiety, described by Ness et al., when they reported that compound **3** might exchange into a cyclic boronate ester, emerged as a key pharmacophore for designing broad-spectrum β-lactamase inhibitors [102]. Seminal studies conducted by Brem et al. and Cahill et al. using different

TABLE 10 | Spectrum of activity of vaborbactam (59) against various β-lactamases.

β-lactamase (class, UniProt ID)	K_i/IC_{50}/K_{iapp} (μM)	β-lactamase (class, UniProt ID)	K_i/IC_{50}/K_{iapp} (μM)
KPC-2 (A, Q9F663)	0.069 (**0.09**)	IMP-1 (B, P52699)	**126**
KPC-3 (A, Q93DC4)	0.050	NDM-1 (B, C7C422)	**631**
BKC-1 (A, A0A0F6QEY8)	0.018	VIM-1 (B, Q5GN09)	**398**
FRI-1 (A, N.A.) [172]	0.17	VIM-2 (B, Q9K2N0)	**316**
SME-2 (A, P52682)	0.042	CphA (B, P26918)	**631**
CTX-M-14 (A, Q9L5C7)	0.033	L1 (B, P52700)	**336**
CTX-M-15 (A, A0A223A5J4)	0.044 (**0.42**)	AmpC (C, P00811)	**5**
SHV-5 (A, P0A3M1)	**0.44**	P99 (C, P05364)	0.053
SHV-12 (A, H6UQL7)	0.029	CMY-2 (C, Q48434)	0.099
TEM-10 (A, Q48388)	0.110	OXA-1 (D, P13661)	**7.9**
TEM-43 (A, O34176)	1.04	OXA-23 (D, Q9L4P2)	66
TEM-116 (A, Q79DR3)	**6**	OXA-48 (D, Q6XEC0)	14

IC_{50} values are denoted in bold, K_i are denoted in normal character, while apparent *K*i (K_{iapp}) values are in italic.

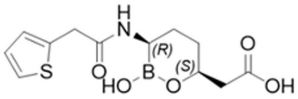

Compound 59

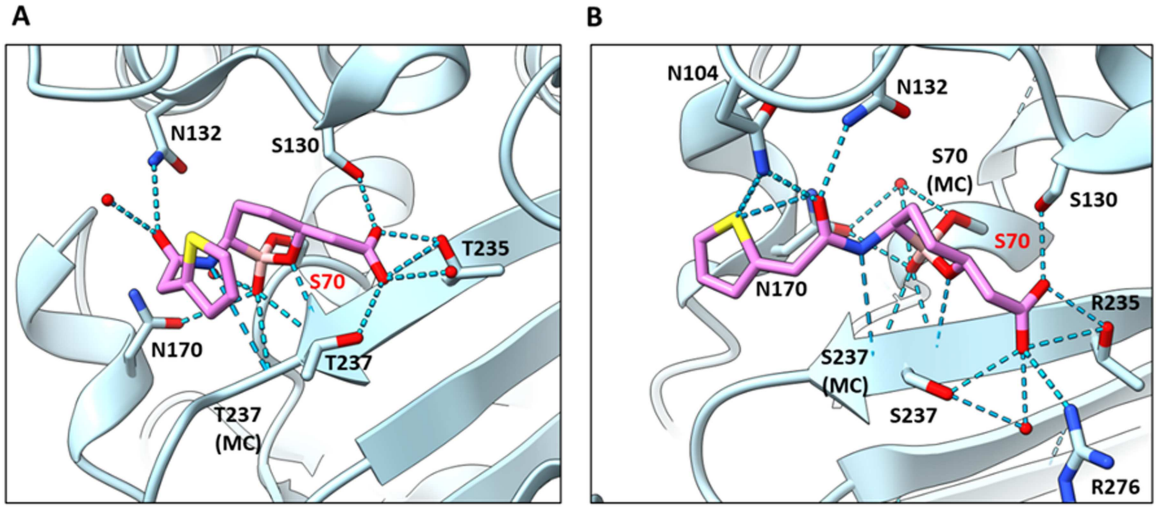

FIGURE 34 | (A) Crystal structures of **Vaborbactam** (**59**) in complex with (A) *Klebsiella pneumoniae* KPC-2 (UniProt ID: Q9F663, PDB: 6V7I) and (B) *E. coli* CTX-M-14 (UniProt ID: Q9L5C7, PDB: 6V7H). All color code and graphical conventions are as in Figure 4. [Color figure can be viewed at wileyonlinelibrary.com]

compounds, including derivative **60**, previously described in Protez's patents, demonstrated bicyclic boronates were able to cross-class inhibition targeting both SBLs and MBLs (Table 11) [39, 183].

Importantly, those reports demonstrated bicyclic boronic acids were able to mimic the common tetrahedral intermediate observed in the β-lactam hydrolysis process catalyzed by SBLs and MBLs (see Scheme 1). Surprisingly, it was also reported an inhibitory activity against PBP 5 (dacA from *E. coli*), a non-essential PBP via the same mechanism. When tested in combination with meropenem against different strains of Enterobacterales overexpressing MBLs and SBLs, compound **60** could reduce the MIC up to 128-fold and did not exhibit any cytotoxicity in human HEK293 cells.

Efforts aimed to exploit the versatility of biciclyc boronates lead to the development of **taniborbactam** (compound **61**, VNRX-5133), a potent β-lactamase inhibitor with a partial broad-spectrum scope (Figure 35) [182, 184]. Belonging to the class of compound synthesized by Protez/Venatorx, **taniborbactam** scaffold maintains the pharmacophore 2-hydroxy-3,4-dihydro-2H-benzo[*e*] [1,2] oxaborinine framework and the carboxylic group in position 8, while the 4-(aminomethyl) benzamido

TABLE 11 | Spectrum of activity of compound 60 against various β-lactamases.

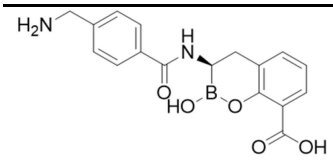

Compound 60

β-lactamase (class, UniProt ID)	IC_{50} (μM)
KPC-2 (A, Q9F663)	0.030
CTX-M-15 (A, A0A223A5J4)	0.013
TEM-1 (A, P62593)	0.003
TEM-116 (A, Q79DR3)	0.003
IMP-1 (B, P52699)	1
NDM-1 (B, C7C422)	0.029
VIM-1 (B, Q5GN09)	0.085
VIM-2 (B, Q9K2N0)	0.003
CphA (B, P26918)	> 100
AmpC (C, P00811)	0.12
OXA-23 (D, Q9L4P2)	3.3
OXA-48 (D, Q6XEC0)	2.6

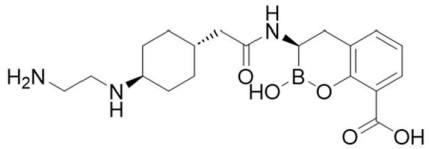

Compound 61

FIGURE 35 | **Taniborbactam** (compound **61**) structure.

group of compound **60** is replaced by an aliphatic cyclohexyl and a flexible ethylene diamino group [182]. Those moieties were observed to play a pivotal role in improving compound **61** affinity for different BLs and its microbiological profile, by improving physicochemical properties and permeability for Gram-negative outer membrane [182].

Unsurprisingly, structural studies confirmed compound **61** behave analogously to other boronic acids, employing its tetrahedral form, hybridized sp^3, to mimic the high-energy tetrahedral intermediate of the β-lactam hydrolysis process [184]. In SBLs, such as CTX-M-15 and OXA-10, **taniborbactam** forms the canonical covalent bond with the S70, and its boron-bound hydroxyl mimics the oxyanion, while interacting with key residues including N132, N104, T235, and T237 (Figure 36A,B). In MBLs, such as VIM-2 and NDM-1, the boron atom coordinates with the active-site zinc ions (Zn1 and Zn2), with additional stabilizing hydrogen bonds formed by the amine side chain and conserved residues, including E149 (Figure 36C,D).

An interesting phenomenon was observed in the crystal structure in complex with NDM-1, where **taniborbactam** assumes a tricyclic form due to rearrangement of the acylamino side-chain carbonyl group with boron combined with the associated loss of water/hydroxide (Figure 36D) [184]. Compared to previous boronic acid presented herein, **taniborbactam** demonstrated a superior cross-class inhibitory profile as BLI (Table 12) [182, 184, 185]. Biochemically, **taniborbactam** displays nanomolar-range inhibition against many clinically relevant β-lactamases. It effectively inhibits class A carbapenemases (e.g., KPC-2), class C cephalosporinases (e.g., AmpC), and even class D OXA-48 [185, 186]. More notably, **taniborbactam** demonstrates potent activity against class B1 MBLs (e.g., NDM and VIM), a feature not achieved by monocyclic inhibitors, such as **vaborbactam** [184]. Moreover, its fast-on/slow-off kinetics favor prolonged engagement with the enzyme, enhancing its stability and efficacy in vivo [182].

In microbiological assays, **taniborbactam** (compound **61**) displayed potent synergistic activity when combined with cefepime or meropenem [174, 182, 185, 187, 188]. Notably, cefepime/**taniborbactam** achieved MIC values as low as 0.12–1 μg/mL against Enterobacterales producing class A (e.g., KPC), class C (e.g., CMY-2), and class D (e.g., OXA-48/163) β-lactamases, while also significantly lowering MICs against MBL producers, particularly those overexpressing NDM-1, NDM-5, and VIM-2 [185, 187, 188]. Importantly, this BL/BLI combination restored cefepime activity against resistant strains of *E. coli* and *K. pneumoniae*, including MDR isolates, with ≥ 512-fold reductions in MIC observed [187, 188]. Moreover, **taniborbactam** was highly effective in in vivo infection models and exhibited remarkable target specificity, with also no cytotoxicity in mammalian cell lines (HeLa, MRC-5, 3T3) [185]. No intrinsic antibacterial activity was observed as well as off-target effects in a 129-assay pharmacological panel, except for the intended β-lactamase inhibition [182, 187]. Currently, in phase III, Cefepime–**taniborbactam** demonstrated superiority to meropenem for the treatment of cUTI, with a safety profile similar to that of meropenem [52, 189]. An increasing number of report and reviews and articles are covering the extensive microbiological, pharmacological, pharmacokinetic and evolution of resistance for this combination [189–191].

Addressing the need for next-generation BLIs with ultrabroad-spectrum activity, **Xeruborbactam** (compound **62,** QPX7728), developed by Qpex Biopharma, emerged as a groundbreaking compound (Figure 37) [192]. Derived from oxaborinin scaffold [102], **Xeruborbactam** was rationally engineered to overcome the limitations of earlier boronic acid-based inhibitors, such as vaborbactam, lacking activity against class B and D enzymes [192]. **Xeruborbactam** was optimized to fine-tune the inhibitor spectrum, metabolic stability, and permeability, with decoration, such as the incorporation of a cyclopropane ring to increase conformational rigidity, and the insertion of electron-withdrawing substituents (fluorine) proving to improve binding interactions and reduce metabolic liability. These refinements yielded a molecule with enhanced bioavailability, stability, and potency, suitable for both intravenous and oral administration [192]. The structural basis for this potent broad-spectrum inhibitor are in line with previous boronic acid BLIs, therefore supporting **Xeruborbactam** mimics the tetrahedral transition state of β-lactam hydrolysis by forming a covalent adduct with the catalytic serine in SBLs. Other relevant interaction for the stability of this compound includes CH–π contacts between the electron-deficient aromatic ring (bearing the fluorine, carboxylate, and boronate substituents) and side chains such as Y211,

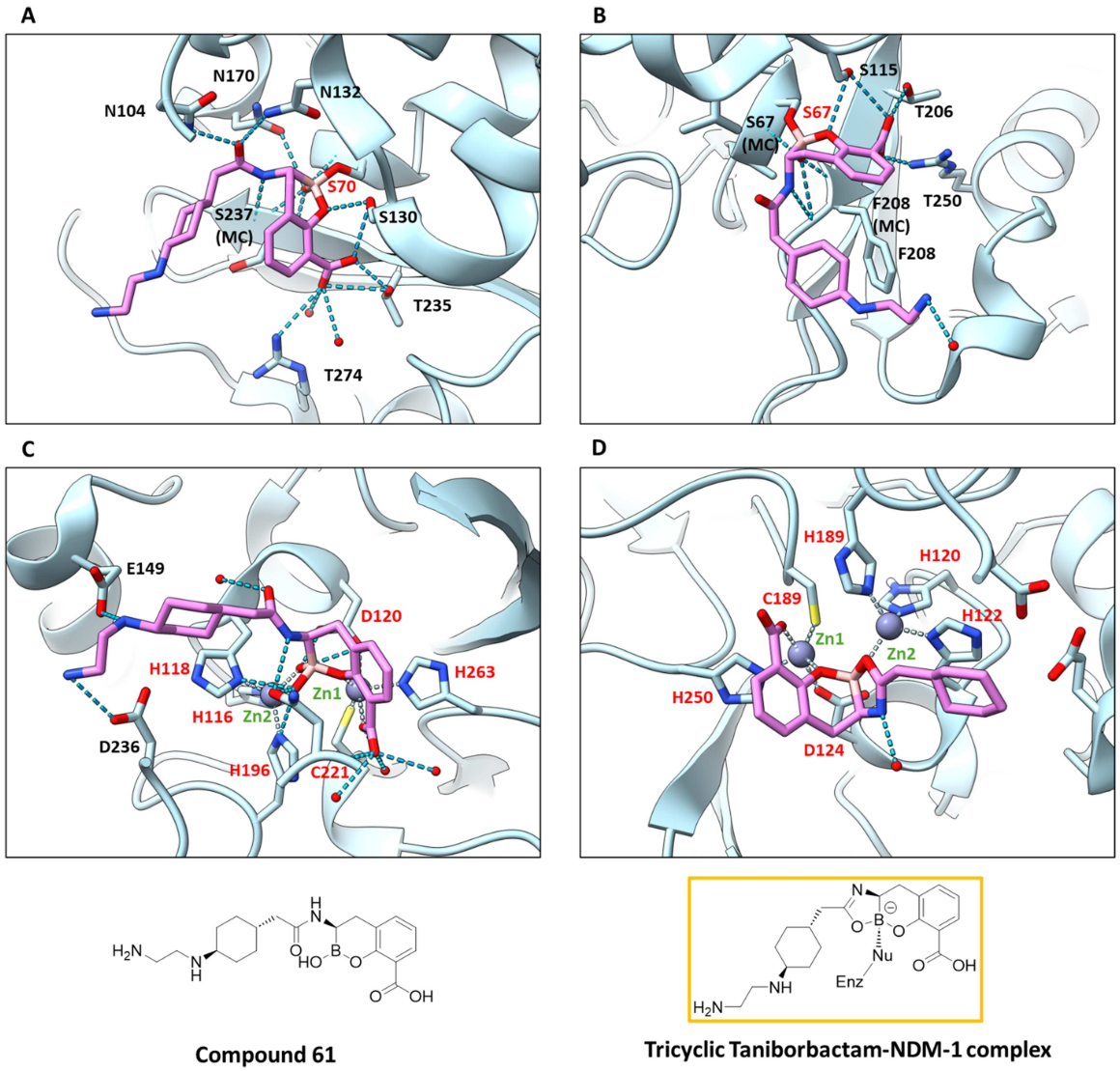

FIGURE 36 | Crystal structures of **taniborbactam** (**61**) in complex with: (A) *Escherichia coli* CTX-M-15 (UniProt ID: A0A223A5J4; PDB: 6SP6); (B) *Pseudomonas aeruginosa* OXA-10 (UniProt ID: P14489; PDB: 6RTN); (C) *P. aeruginosa* VIM-2 (UniProt ID: Q9K2N0; PDB: 6SP7); and (D) *Klebsiella pneumoniae* NDM-1 (UniProt ID: C7C422; PDB: 6RMF). In the VIM-2 and NDM-1 complexes, Zn(II) ions are shown as gray spheres and are coordinated by the indicated catalytic residues, while gray dashed lines denote metal-coordination interactions. The unexpected tricyclic taniborbactam adduct observed in the NDM-1 complex is shown in the orange box. All other color codes and graphical conventions are as in Figure 4. [Color figure can be viewed at wileyonlinelibrary.com]

I102, and L247 (OXA-48), while the cyclopropane group engages in hydrophobic interactions with W105 and V120. These interactions are key to the inhibitor tight binding and its marked stereoselectivity, indeed the (3*R*,4*S*)-stereoisomer is far more potent than its enantiomer. In MBLs, compound **62** binds by coordinating Zn1 through the tetrahedral boronate and engaging Zn2 via its carboxylate and phenolic oxygens. This dual-zinc coordination mimics the tetrahedral intermediate formed during β-lactam hydrolysis and is highly conserved among MBLs.

The biochemical profile of compound **62** revealed excellent inhibitory properties for all classes of β-lactamases, while retaining the canonical mechanism of action observed in other bicyclic boronates (Table 13) [192, 193]. Thus, **xeruborbactam** display sub-nM inhibition for carbapenemases, cephalosporinases and nM activity against MBLs and class D [88].

More remarkably, further characterization on **xeruborbactam** microbiological profile revealed its ability to restore the activity of a wide range of intravenous (i.e., meropenem, ceftazidime, cefepime) and oral (e.g., ceftibuten, tebipenem) β-lactam antibiotics against strains harboring ESBLs, AmpC-type cephalosporinases, KPC, OXA, and NDM/VIM carbapenemases [193–199]. The meropenem/**xeruborbactam** combination exhibits particularly attractive microbiological profiles in carbapenem-resistant Enterobacterales, even in the presence of multiple resistance mechanisms [199]. Compound **62** has demonstrated excellent pharmacokinetic properties, with high metabolic stability, low clearance, and good oral bioavailability [193–195, 197, 198]. In preclinical models, **xeruborbactam** was effective in restoring β-lactam efficacy in infection models involving resistant *E. coli*, *K. pneumoniae*, and *P. aeruginosa*. The compound does not inhibit human serine or metalloproteases, except cathepsin A, which remains under evaluation.

Holding great promises, **xeruborbactam** is currently undergoing Phase I clinical trials in combination with the β-lactam QPX2014 (structure not yet disclosed), showing promise as a versatile, pan-β-lactamase inhibitor for treating severe infections caused by MDR Gram-negative pathogens. Lately, given the oral bioavailability of **xeruborbactam** is limited to only 20% in monkeys (50% in rats and dogs), an orally bioavailable prodrug of compound **62**, named QPX7831, has been developed to reach optimal properties across all key attributes [200].

The collective efforts from Burns and others at Venatorx Pharmaceuticals lead to the development of **ledaborbactam** (VNRX-5236, compound **63**) and its orally bioavailable prodrug **ledaborbactam etzadroxil** (VNRX-7145, compound **64**), two potent bicyclic boron-based BLIs (Figure 38) [201]. Interestingly, **ledaborbactam** and its prodrug compound **64** demonstrated potent inhibitory affinity for Ambler class A, C, and D β-lactamases and to be capable of restoring antibacterial activity of the 3rd generation oral cephalosporin ceftibuten [202]. From a biochemical point of view, **ledaborbactam** inhibits class A KPC-2 ($IC_{50} = 80$ nM), SHV-5 ($IC_{50} = 126$ nM) and CTX-M-15 ($IC_{50} = 20$ nM), class C P99 ($IC_{50} = 14$ nM) and CMY-2 ($IC_{50} = 10$ nM) and class D OXA-48 ($IC_{50} = 317$ nM) [201, 202].

TABLE 12 | Spectrum of activity of taniborbactam (61) against various β-lactamases.

β-lactamase (class, UniProt ID)	K_i/IC_{50} (μM)
KPC-2 (A, Q9F663)	0.004
CTX-M-15 (A, A0A223A5J4)	0.017
SHV-5 (A, P0A3M1)	0.003
TEM-116 (A, Q79DR3)	**0.12**
IMP-1 (B, P52699)	**2.51**
NDM-1 (B, C7C422)	**0.01**
VIM-1 (B, Q5GN09)	**0.0079**
VIM-2 (B, Q9K2N0)	**0.0005**
CphA (B, P26918)	**2.51**
L1 (B, P52700)	**> 10**
AmpC (C, P00811)	**0.032**
OXA-48 (D, Q6XEC0)	**0.42**

IC_{50} values are denoted in bold, while K_i are denoted in normal character.

The well-characterized microbiological profile demonstrates that, in combination with ceftibuten, compound **63** possess potent in vitro activity ($MIC_{90} \leq 2$ mg/L) and effectively restores β-lactam efficacy in multidrug-resistant urinary and systemic infection models [201, 203, 204]. It shows consistent activity against Enterobacterales strains producing ESBLs, KPCs, AmpC, and OXA-48-like enzymes, even in isolates resistant to commonly prescribed oral agents, such as nitrofurantoin or fosfomycin [202–205]. *In vivo*, the ceftibuten/**64** combination provides robust protection in murine models of septicemia and urinary tract infection, supporting its continued development as an oral treatment for resistant Gram-negative infections [206]. Currently, Ceftibuten/**64** combination has completed Phase I and is moving to the next phases.

Recently, **KSP-1007** (compound **65**) was reported by Sumitomo Pharma and Kitasato University as a novel bicyclic boronate BLI developed to address the critical need for effective therapies against carbapenem-resistant Gram-negative bacteria [207]. Chemically, **KSP-1007** features a benzoxaborinine-8-carboxylic acid core, with a single functionalization in position 7, that being a 1-[(2*R*)−2-amino-2-(1*H*-imidazol-4-yl)acetyl]azetidin-3-yl}oxy) moiety. Biochemically, **KSP-1007** demonstrates low

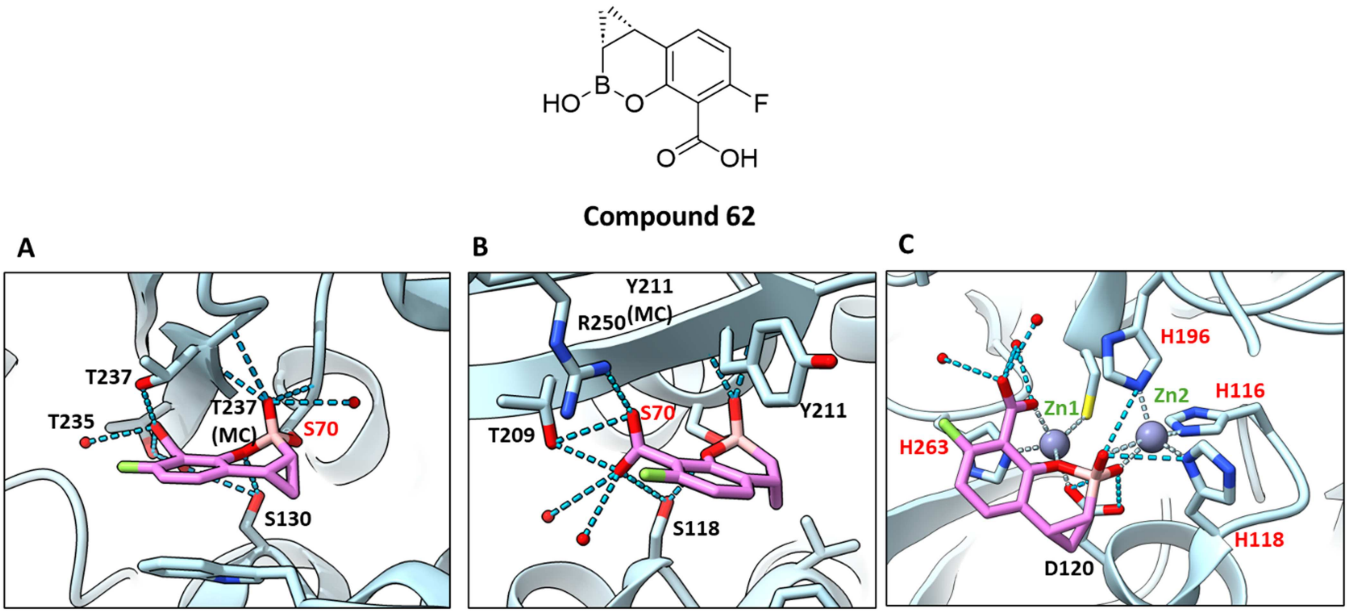

FIGURE 37 | Crystal structures of **xeruborbactam** (**62**) in complex with: (A) *Klebsiella pneumoniae* KPC-2 (UniProt ID: Q9F663; PDB: 6V1J); (B) *K. pneumoniae* OXA-48 (UniProt ID: Q6XEC0; PDB: 6V1O); and (C) *Pseudomonas aeruginosa* VIM-2 (UniProt ID: Q9K2N0; PDB: 6V1P). In the VIM-2 complex, the two Zn(II) ions are shown as gray spheres and are coordinated by the indicated catalytic residues, while gray dashed lines denote metal-coordination interactions. All other color codes and graphical conventions are as in Figure 4. [Color figure can be viewed at wileyonlinelibrary.com]

TABLE 13 | Spectrum of activity of xeruborbactam (62) against various β-lactamases.

β-lactamase (class, UniProt ID)	K_i (μM)
KPC-2 (A, Q9F663)	0.0019
CTX-M-14 (A, Q9L5C7)	0.00029
SHV-12 (A, H6UQL7)	0.00074
TEM-10 (A, Q48388)	0.00066
IMP-1 (B, P52699)	0.22
NDM-1 (B, C7C422)	0.032
VIM-1 (B, Q5GN09)	0.008
AmpC (C, P00811)	0.0085
OXA-48 (D, Q6XEC0)	0.00028

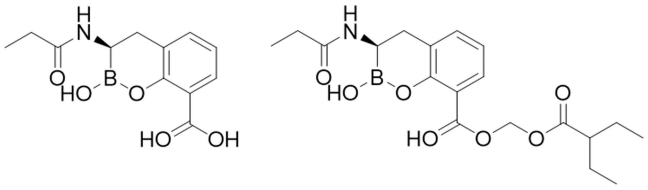

Compound 63 Compound 64

FIGURE 38 | **Ledaborbactam** (compound **63**) and its etzadroxil prodrug (compound **64)** structures.

apparent inhibition constants (K_{iapp}) across all four Ambler classes of β-lactamases, including KPCs, OXA-48-like, NDM, and IMP variants (Table 14).

TABLE 14 | Spectrum of activity of KSP-1007 (65) against various β-lactamases.

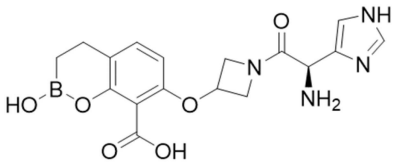

Compound 65

β-lactamase (class, UniProt ID)	K_{iapp} (μM)
KPC-2 (A, Q9F663)	0.00146
KPC-3 (A, Q93DC4)	0.00219
CTX-M-14 (A, Q9L5C7)	0.000153
CTX-M-15 (A, A0A223A5J4)	0.000066
SHV-5 (A, P0A3M1)	0.127
SHV-12 (A, H6UQL7)	0.053
TEM-10 (A, Q48388)	0.0069
IMP-1 (B, P52699)	0.512
NDM-1 (B, C7C422)	0.126
VIM-1 (B, Q5GN09)	0.350
VIM-2 (B, Q9K2N0)	1.21
PDC-11 (C, D0EJY2)	0.00079
OXA-23 (D, Q9L4P2)	0.00407
OXA-48 (D, Q6XEC0)	0.000861

Only apparent K_i (K_{iapp}) values were reported for this compound.

Notably, it displays stronger inhibition of carbapenemases than **taniborbactam** and remains active in the presence of human plasma, indicating limited interference from protein binding, an issue that compromises other inhibitors. Microbiologically, **KSP-1007** significantly potentiates meropenem activity, reducing MIC values by ≥ 8-fold across a wide spectrum of carbapenemase-producing pathogens. *In vitro*, meropenem/**KSP-1007** outperformed or matched investigational and approved agents like cefepime/**taniborbactam**, cefiderocol, and aztreonam/avibactam, particularly against challenging strains harboring MBLs or PBP3 mutations. It showed strong bactericidal activity (MBC/MIC ≤ 4) and demonstrated superior efficacy in murine systemic and urinary tract infection models. Unlike other BL/BLI combinations, MEM/**KSP-1007** also displayed promising activity against cefiderocol-resistant *A. baumannii* and was unaffected by serum protein binding, reinforcing its potential as a broad-spectrum, next-generation carbapenem-based therapeutic. More recently, Takemoto et al. further characterized the pharmacological behavior of **KSP-1007** in combination with meropenem in a neutropenic murine thigh infection model using carbapenemase-producing Enterobacterales and *A. baumannii* [208]. Their results identified the percentage of the dosing interval during which the free **KSP-1007** concentration remained above a threshold concentration (%fT > CT) as a key PK/PD index, with activity being enhanced by more frequent dosing and showing limited dependence on peak exposure. Importantly, the MEM/**KSP-1007** combination retained bactericidal efficacy against highly resistant strains, and preliminary lung infection data indicated good pulmonary penetration, with epithelial lining fluid/plasma AUC ratios of 68%–100%, further supporting the clinical development of compound **65** as a meropenem partner against carbapenemase-producing Gram-negative pathogens.

3 | Conclusions

In this review, we have presented the historical development of boronic acid-based β-lactamase inhibitors, from the earliest reports in the '70 up to the most recent advancements. Initial doubts and concerns about boron-based compounds have been progressively addressed through extensive studies demonstrating their potent inhibitory activity alongside favorable selectivity profiles and low toxicity [92]. This progress has been made possible by the unique properties of boron, an electron-deficient atom that is not commonly recognized by bacterial resistance mechanisms. The electrophilicity of boron, combined with the overall architecture of boronic acids, promotes the formation of a reversible covalent bond with the nucleophilic catalytic serine residue of SBLs or, in the case of MBLs, with a hydroxide ion in their active site. Once bound to these targets, boronic acids undergo a structural transformation from a trigonal planar, sp^2-hybridized state to a tetrahedral, sp^3-hybridized intermediate. This rearrangement effectively mimics the tetrahedral intermediate of β-lactam hydrolysis, thereby inhibiting β-lactamase activity with high potency. This mode of action has guided the design of tailored inhibitors over the years, with the 65 compounds presented herein representing some of the most

representative examples of boron-based BLIs. While the vast majority of early reports focused on phenylboronic acid derivatives, the field emphasis subsequently shifted toward acyclic boronic acids and, more recently, toward cyclic boronates. This evolution reflects significant progress in boron chemistry, including the incorporation of stereogenic carbon centers adjacent to the boron pharmacophore, the advent of click chemistry, and the growing expertise in synthesizing complex bicyclic boronates, all of which collectively enable fine-tuning of both potency and selectivity. Today, boronic acids have become a flexible and chemically tractable scaffold for developing BLIs with sub-nanomolar potency, broad spectrum of activity across multiple Ambler classes, and desirable selectivity profiles. Nevertheless, to date, **vaborbactam** (**59**), in combination with meropenem (Vabomere), stands as the only clinically approved representative, a powerful combination against KPC-producing Enterobacterales. The impressive progress made with bicyclic boronates, as discussed in Section 2.3-3. has fostered a growing pipeline of new BATSIs, including **taniborbactam** (**61**), **xeruborbactam** (**62**), **ledaborbactam** (**63**), and **KSP1007** (**65**). Importantly, these compounds collectively demonstrate broad spectrum activity against MBLs, and class D OXA-type β-lactamases, a feature largely missing from the acyclic boronic acids (described in Section 2.1) and phenylboronic acids (described in Section 2.2), which predominantly target class A and C β-lactamases. While most boronic acids do not exhibit intrinsic antibacterial activity, their potent synergy with β-lactams, desirable PK/PD properties, and strong barrier to resistance, stemming from their unique mechanisms of action, make them exceptionally attractive as combination therapy components. Yet, when compared to other classes of β-lactamase inhibitors, boronic acids still harbor significant untapped potential, especially considering the opportunity to modify and fine-tune their structures in the vicinity of the boron pharmacophore. This versatility is exemplified by the design of novel acyclic compounds, which enable extensive structure-activity relationship optimization to maximize binding affinities and spectrum of activity. Nevertheless, the growing class of cyclic boronic acids holds the scepter for the promising avenue to develop broad-spectrum BLIs. The continued expansion and optimization of their spectrum of activity, combined with their favorable safety profiles, hold great promise for extending the utility of β-lactam antibiotics in the face of evolving resistance mechanisms. At the bacterial level, most boronic acid-based BLIs discussed in this review have been developed and evaluated against clinically relevant Gram-negative pathogens, particularly β-lactamase-producing Enterobacterales such as *K. pneumoniae*, *E. coli*, *E. cloacae*, *C. freundii*, and *S. marcescens*, as well as *P. aeruginosa* and *A. baumannii*. Nevertheless, the antibacterial potential of boronic acid scaffolds is not restricted to Gram-negative bacteria, as selected inhibitors have also shown activity against Gram-positive pathogens and *Mycobacterium tuberculosis* [209, 210]. In the organisms considered here, boronic acid-based BLIs have restored the activity of partner β-lactams against strains producing class A and C enzymes and, for newer bicyclic boronates, selected class D carbapenemases and MBLs. However, broad-spectrum in this context primarily refers to β-lactamase class coverage rather than uniform activity against all bacterial species, since microbiological efficacy also depends on the partner antibiotic, membrane permeability, efflux, target alterations, and the overall resistance background of each strain. Moreover, the effects of these inhibitors and their combinations on the intestinal microbiome remain insufficiently characterized and represent an important area for future investigation. As we move forward, the rational design of new compounds, supported by growing structural and biochemical knowledge, will remain a key strategy for delivering broad-spectrum, clinically relevant BLIs. Furthermore, innovative techniques, such as kinetic target-guided synthesis or the exploration of large libraries of fragments made accessible through click chemistry, may enable the discovery of previously unforeseen and potent compounds. Together, this review aims to underscore the significance of boronic acid-based inhibitors as powerful tools in the ongoing battle against antimicrobial resistance.

Acknowledgments

Funded by the European Union. The views and opinions expressed are, however, those of the author(s) only and do not necessarily reflect those of the European Union or other granting authority. Neither the European Union nor the granting authority can be held responsible for them. This project has received funding from the European Union's Horizon Europe research and innovation programme under the Marie Sklodowska-Curie grant agreement no. 101068156. Further information can be found on the website: https://www.bliss.unimore.it/ (accessed on 08 June, 2026). This study was also supported by funds provided by the European Union—NextGenerationEU, Mission 4, Component 2, Investment 1.1—PRIN 2022—CUP E53D23001480006, Project Number: 2022WBPFSC. Also, PRD2026 (Financial contribution from the PRD2026 from the Department of Life Sciences, University of Modena and Reggio Emilia, Italy is gratefully acknowledged. This research was also supported by the National Institute of Allergy and Infectious Diseases of the National Institutes of Health (NIH) under award number R01AI072219 (to R.A.B., F.P., and E.C.) and in part by funds and/or facilities provided by the Cleveland Department of Veterans Affairs, Award Number I01BX001974 to R.A.B. from the Biomedical Laboratory Research and Development Service of the VA Office of Research and Development. The content is solely the responsibility of the authors and does not necessarily represent the official views of the NIH or the Department of Veterans Affairs. Open access publishing facilitated by Universita degli Studi di Modena e Reggio Emilia, as part of the Wiley - CRUI-CARE agreement.

Data Availability Statement

Data sharing not applicable to this article as no data sets were generated or analyzed during the current study.

References

1. J. H. Kwon and W. G. Powderly, "The Post-Antibiotic Era Is Here," *Science* 373, no. 6554 (2021): 471.

2. M. Naghavi, S. E. Vollset, K. S. Ikuta, et al., "Global Burden of Bacterial Antimicrobial Resistance 1990–2021: A Systematic Analysis With Forecasts to 2050," *Lancet* 404, no. 10459 (2024): 1199–1226.

3. A. P. Magiorakos, A. Srinivasan, R. B. Carey, et al., "Multidrug-Resistant, Extensively Drug-Resistant and Pandrug-Resistant Bacteria: An International Expert Proposal for Interim Standard Definitions for Acquired Resistance," *Clinical Microbiology and Infection* 18, no. 3 (2012): 268–281.

4. A. Bharadwaj, A. Rastogi, S. Pandey, S. Gupta, and J. S. Sohal, "Multidrug-Resistant Bacteria: Their Mechanism of Action and Prophylaxis," *BioMed Research International* 2022, no. 1 (2022): 5419874.

5. C. Bartal, K. V. I. Rolston, and L. Nesher, "Carbapenem-Resistant *Acinetobacter baumannii*: Colonization, Infection and Current

Treatment Options," *Infectious Diseases and Therapy* 11, no. 2 (2022): 683–694.

6. C. J. L. Murray, K. S. Ikuta, F. Sharara, et al., "Global Burden of Bacterial Antimicrobial Resistance in 2019: A Systematic Analysis," *Lancet* 399, no. 10325 (2022): 629–655.

7. H. Sati, E. Carrara, A. Savoldi, et al., "The WHO Bacterial Priority Pathogens List 2024: A Prioritisation Study to Guide Research, Development, and Public Health Strategies Against Antimicrobial Resistance," *Lancet Infectious Diseases* 25 (2025): 1033–1043.

8. R. A. Bonomo, E. M. Burd, J. Conly, et al., "Carbapenemase-Producing Organisms: A Global Scourge," *Clinical Infectious Diseases* 66, no. 8 (2018): 1290–1297.

9. E. Tacconelli, E. Carrara, A. Savoldi, et al., "Discovery, Research, and Development of New Antibiotics: The WHO Priority List of Antibiotic-Resistant Bacteria and Tuberculosis," *Lancet Infectious Diseases* 18, no. 3 (2018): 318–327.

10. L. M. C. Jacobs, P. Consol, and Y. Chen, "Drug Discovery in the Field of β-Lactams: An Academic Perspective," *Antibiotics (USSR)* 13, no. 1 (2024): 59.

11. E. Y. Klein, I. Impalli, S. Poleon, et al., "Global Trends in Antibiotic Consumption During 2016–2023 and Future Projections Through 2030," *Proceedings of the National Academy of Sciences* 121, no. 49 (2024): e2411919121.

12. E. Sauvage, F. Kerff, M. Terrak, J. A. Ayala, and P. Charlier, "The Penicillin-Binding Proteins: Structure and Role in Peptidoglycan Biosynthesis," *FEMS Microbiology Reviews* 32, no. 2 (2008): 234–258.

13. A. Zapun, C. Contreras-Martel, and T. Vernet, "Penicillin-Binding Proteins and β-Lactam Resistance," *FEMS Microbiology Reviews* 32, no. 2 (2008): 361–385.

14. V. Villamil, L. S. Brusoni, F. Prati, E. Caselli, and N. Santi, "Boronate-Based Inhibitors of Penicillin-Binding Proteins: An Underestimated Avenue for Antibiotic Discovery?," *Pharmaceuticals* 18, no. 9 (2025): 1325.

15. D. P. M. Sethuvel, Y. D. Bakthavatchalam, M. Karthik, et al., "β-Lactam Resistance in ESKAPE Pathogens Mediated Through Modifications in Penicillin-Binding Proteins: An Overview," *Infectious Diseases and Therapy* 12, no. 3 (2023): 829–841.

16. E. M. Darby, E. Trampari, P. Siasat, et al., "Molecular Mechanisms of Antibiotic Resistance Revisited," *Nature Reviews Microbiology* 21, no. 5 (2023): 280–295.

17. J. M. A. Blair, M. A. Webber, A. J. Baylay, D. O. Ogbolu, and L. J. V. Piddock, "Molecular Mechanisms of Antibiotic Resistance," *Nature Reviews Microbiology* 13, no. 1 (2015): 42–51.

18. J. M. Munita and C. A. Arias, "Mechanisms of Antibiotic Resistance," *Microbiology Spectrum* 4, no. 2 (2016): 10.1128/microbiolspec.vmbf-0016-2015.

19. A. J. Baylay, L. J. V. Piddock, and M. A. Webber, *Molecular Mechanisms of Antibiotic Resistance—Part I* (John Wiley & Sons, 2019), 1–26.

20. L. K. R. Sharkey and A. J. O'Neill, "Molecular Mechanisms of Antibiotic Resistance—Part II," in *Bacterial Resistance to Antibiotics—From Molecules to Man* (John Wiley & Sons, 2019), 27–50.

21. L. Fernández and R. E. W. Hancock, "Adaptive and Mutational Resistance: Role of Porins and Efflux Pumps in Drug Resistance," *Clinical Microbiology Reviews* 25, no. 4 (2012): 661–681.

22. K. Bush, "Past and Present Perspectives on β-Lactamases," *Antimicrobial Agents and Chemotherapy* 62, no. 10 (2018): e01076-18, https://doi.org/10.1128/aac.01076-01018.

23. K. Bush and P. A. Bradford, "β-Lactams and β-Lactamase Inhibitors: An Overview," *Cold Spring Harbor Perspectives in Medicine* 6, no. 8 (2016): a025247.

24. J. F. Fisher and S. Mobashery, "β-Lactam Resistance Mechanisms: Gram-Positive Bacteria and Mycobacterium Tuberculosis," *Cold Spring Harbor Perspectives in Medicine* 6, no. 5 (2016): a025221.

25. N. Kaderabkova, M. Bharathwaj, R. C. D. Furniss, D. Gonzalez, and T. Palmer, "Mavridou DAIYR. The Biogenesis of β-Lactamase Enzymes," *Microbiology* 168, no. 8 (2022): 001217.

26. L. J. González, G. Bahr, T. G. Nakashige, E. M. Nolan, R. A. Bonomo, and A. J. Vila, "Membrane Anchoring Stabilizes and Favors Secretion of New Delhi Metallo-β-Lactamase," *Nature Chemical Biology* 12, no. 7 (2016): 516–522.

27. L. Capodimonte, F. Meireles, G. Bahr, et al., "OXA β-Lactamases From Acinetobacter spp. Are Membrane Bound and Secreted Into Outer Membrane Vesicles," *mBio* 16, no. 2 (2025): 0334324.

28. C. L. Tooke, P. Hinchliffe, E. C. Bragginton, et al., "β-Lactamases and β-Lactamase Inhibitors in the 21st Century," *Journal of Molecular Biology* 431, no. 18 (2019): 3472–3500.

29. S. Ghafourian, N. Sadeghifard, S. Soheili, and Z. Sekawi, "Extended Spectrum Beta-Lactamases: Definition, Classification and Epidemiology," *Current Issues in Molecular Biology* 17, no. 1 (2015): 11–21.

30. A. M. Queenan and K. Bush, "Carbapenemases: The Versatile β-Lactamases," *Clinical Microbiology Reviews* 20, no. 3 (2007): 440–458.

31. B. G. Hall and M. Barlow, "Revised Ambler Classification of β-Lactamases," *Journal of Antimicrobial Chemotherapy* 55, no. 6 (2005): 1050–1051.

32. R. P. Ambler, "The Structure of B-Lactamases," *Philosophical Transactions of the Royal Society of London B, Biological Sciences* 289, no. 1036 (1980): 321–331.

33. R. F. Pratt, "β-Lactamases: Why and How," *Journal of Medicinal Chemistry* 59, no. 18 (2016): 8207–8220.

34. M. Barlow and B. G. Hall, "Phylogenetic Analysis Shows That the OXA B-Lactamase Genes Have Been on Plasmids for Millions of Years," *Journal of Molecular Evolution* 55, no. 3 (2002): 314–321.

35. R. I. Aminov, "A Brief History of the Antibiotic Era: Lessons Learned and Challenges for the Future," *Frontiers in Microbiology* 1 (2010): 2010.

36. G. Bahr, L. J. González, and A. J. Vila, "Metallo-β-lactamases in the Age of Multidrug Resistance: From Structure and Mechanism to Evolution, Dissemination, and Inhibitor Design," *Chemical Reviews* 121, no. 13 (2021): 7957–8094.

37. M. F. Tioni, L. I. Llarrull, A. A. Poeylaut-Palena, et al., "Trapping and Characterization of a Reaction Intermediate in Carbapenem Hydrolysis by *B. cereus* Metallo-β-lactamase," *Journal of the American Chemical Society* 130, no. 47 (2008): 15852–15863.

38. S. M. Drawz and R. A. Bonomo, "Three Decades of β-Lactamase Inhibitors," *Clinical Microbiology Reviews* 23, no. 1 (2010): 160–201.

39. J. Brem, R. Cain, S. Cahill, et al., "Structural Basis of Metallo-β-Lactamase, Serine-β-Lactamase and Penicillin-Binding Protein Inhibition by Cyclic Boronates," *Nature Communications* 7, no. 1 (2016): 12406.

40. J. M. Frère, B. Joris, and G. D. Shockman, "Penicillin-Sensitive Enzymes in Peptidoglycan Biosynthesis," *CRC Critical Reviews in Microbiology* 11, no. 4 (1984): 299–396.

41. C. Contreras-Martel, A. Amoroso, E. C. Y. Woon, et al., "Structure-Guided Design of Cell Wall Biosynthesis Inhibitors That Overcome β-Lactam Resistance in *Staphylococcu aureus* (MRSA)," *ACS Chemical Biology* 6, no. 9 (2011): 943–951.

42. K. Bush and G. A. Jacoby, "Updated Functional Classification of β-Lactamases," *Antimicrobial Agents and Chemotherapy* 54, no. 3 (2010): 969–976.

43. F. Brunetti, S. H. Marshall, C. R. Bethel, et al., "Standardized Numbering and Alignment of the KPC Family of β-Lactamases," *Antimicrobial Agents and Chemotherapy* 70, no. 7 (2026): e01868-01825.

44. K. Bush, "Bench-To-Bedside Review: The Role of β-Lactamases in Antibiotic-Resistant Gram-Negative Infections," *Critical Care* 14, no. 3 (2010): 224.

45. T. Palzkill, "Metallo-β-Lactamase Structure and Function," *Annals of the New York Academy of Sciences* 1277, no. 1 (2013): 91–104.

46. S. Zhang, X. Liao, T. Ding, and J. Ahn, "Role of β-Lactamase Inhibitors as Potentiators in Antimicrobial Chemotherapy Targeting Gram-Negative Bacteria," *Antibiotics (USSR)* 13, no. 3 (2024): 260.

47. J.-D. Docquier and S. Mangani, "An Update on β-lactamase Inhibitor Discovery and Development," *Drug Resistance Updates* 36 (2018): 13–29.

48. L. M. Lima, B. N. M. Silva, G. Barbosa, and E. J. Barreiro, "-Lactam Antibiotics: An Overview From a Medicinal Chemistry Perspective," *European Journal of Medicinal Chemistry* 208 (2020): 112829.

49. C. González-Bello, D. Rodríguez, M. Pernas, Á. Rodríguez, and E. Colchón, "β-Lactamase Inhibitors To Restore the Efficacy of Antibiotics Against Superbugs," *Journal of Medicinal Chemistry* 63, no. 5 (2020): 1859–1881.

50. Z. Iqbal, J. Sun, H. Yang, et al., "Recent Developments to Cope the Antibacterial Resistance via β-Lactamase Inhibition," *Molecules* 27, no. 12 (2022): 3832.

51. D. Carcione, C. Siracusa, A. Sulejmani, V. Leoni, and J. Intra, "Old and New Beta-Lactamase Inhibitors Molecular Structure Mechanism of Action and Clinical Use," *Antibiotics (USSR)* 10, no. 8 (2021): 995.

52. A. Katsarou, P. Stathopoulos, I. D. Tzvetanova, C.-M. Asimotou, and M. E. Falagas, "β-Lactam/β-Lactamase Inhibitor Combination Antibiotics Under Development," *Pathogens* 14, no. 2 (2025): 168.

53. M. Sargianou, P. Stathopoulos, C. Vrysis, I. D. Tzvetanova, and M. E. Falagas, "New β-Lactam/β-Lactamase Inhibitor Combination Antibiotics," *Pathogens* 14, no. 4 (2025): 307.

54. K. M. Papp-Wallace, "The Latest Advances in β-lactam/β-Lactamase Inhibitor Combinations for the Treatment of Gram-Negative Bacterial Infections," *Expert Opinion on Pharmacotherapy* 20, no. 17 (2019): 2169–2184.

55. J. Crandon and D. Nicolau, "In Vitro Activity of Cefepime/AAI101 and Comparators Against Cefepime Non-Susceptible Enterobacteriaceae," *Pathogens* 4, no. 3 (2015): 620–625.

56. A. Matagne, M. F. Ghuysen, and J. M. Frère, "Interactions Between Active-Site-Serine β-lactamases and Mechanism-Based Inactivators: A Kinetic Study and an Overview," *Biochemical Journal* 295, no. 3 (1993): 705–711.

57. C. L. Tooke, P. Hinchliffe, M. Beer, et al., "Tautomer-Specific Deacylation and Ω-Loop Flexibility Explain the Carbapenem-Hydrolyzing Broad-Spectrum Activity of the KPC-2 β-Lactamase," *Journal of the American Chemical Society* 145, no. 13 (2023): 7166–7180.

58. K. M. Papp-Wallace, C. R. Bethel, J. Caillon, et al., "Beyond Piperacillin-Tazobactam: Cefepime and AAI101 as a Potent β-Lactam −β-Lactamase Inhibitor Combination," *Antimicrobial Agents and Chemotherapy* 63, no. 5 (2019): e00105-19, https://doi.org/10.1128/aac.00105-00119.

59. K. Coleman, "Diazabicyclooctanes (DBOs): A Potent New Class of Non-β-Lactam β-Lactamase Inhibitors," *Current Opinion in Microbiology* 14, no. 5 (2011): 550–555.

60. A. Bonnefoy, "In Vitro Activity of AVE1330A, an Innovative Broad-Spectrum on-β-Lactam β-Lactamase Inhibitor," *Journal of Antimicrobial Chemotherapy* 54, no. 2 (2004): 410–417.

61. D. E. Ehmann, H. Jahić, P. L. Ross, et al., "Avibactam Is a Covalent, Reversible, Non–β-Lactam β-Lactamase Inhibitor," *Proceedings of the National Academy of Sciences* 109, no. 29 (2012): 11663–11668.

62. N. P. Krishnan, N. Q. Nguyen, K. M. Papp-Wallace, R. A. Bonomo, and F. van den Akker, "Inhibition of Klebsiella β-Lactamases (SHV-1 and KPC-2) by Avibactam: A Structural Study," *PLoS One* 10, no. 9 (2015): e0136813.

63. S. D. Lahiri, S. Mangani, H. Jahić, et al., "Molecular Basis of Selective Inhibition and Slow Reversibility of Avibactam Against Class D Carbapenemases: A Structure-Guided Study of OXA-24 and OXA-48," *ACS Chemical Biology* 10, no. 2 (2015): 591–600.

64. D. E. Ehmann, H. Jahić, P. L. Ross, et al., "Kinetics of Avibactam Inhibition Against Class A, C, and D β-Lactamases," *Journal of Biological Chemistry* 288, no. 39 (2013): 27960–27971.

65. J. A. Karlowsky, K. M. Kazmierczak, B. L. M. de Jonge, M. A. Hackel, D. F. Sahm, and P. A. Bradford, "In Vitro Activity of Aztreonam-Avibactam Against Enterobacteriaceae and *Pseudomonas aeruginosa* Isolated by Clinical Laboratories in 40 Countries From 2012 to 2015," *Antimicrobial Agents and Chemotherapy* 61, no. 9 (2017): e00472-17, https://doi.org/10.1128/aac.00472-00417.

66. M. A. Powles, A. Galgoci, A. Misura, et al., "In Vivo Efficacy of Relebactam (MK-7655) in Combination With Imipenem-Cilastatin in Murine Infection Models," *Antimicrobial Agents and Chemotherapy* 62, no. 8 (2018): e02577-17, https://doi.org/10.1128/aac.02577-02517.

67. K. M. Papp-Wallace, M. D. Barnes, J. Alsop, et al., "Relebactam Is a Potent Inhibitor of the KPC-2 β-Lactamase and Restores Imipenem Susceptibility in KPC-Producing Enterobacteriaceae," *Antimicrobial Agents and Chemotherapy* 62, no. 6 (2018): e00174-18, https://doi.org/10.1128/aac.00174-00118.

68. M. C. Canver, M. J. Satlin, L. F. Westblade, et al., "Activity of Imipenem-Relebactam and Comparator Agents Against Genetically Characterized Isolates of Carbapenem-Resistant Enterobacteriaceae," *Antimicrobial Agents and Chemotherapy* 63, no. 9 (2019): e00672-19, https://doi.org/10.1128/aac.00672-00619.

69. A. Morinaka, Y. Tsutsumi, M. Yamada, et al., "OP0595, a New Diazabicyclooctane: Mode of Action as a Serine β-Lactamase Inhibitor, Antibiotic and β-Lactam 'Enhancer'," *Journal of Antimicrobial Chemotherapy* 70, no. 10 (2015): 2779–2786.

70. D. M. Livermore, S. Mushtaq, M. Warner, A. Vickers, and N. Woodford, "In Vitro Activity of Cefepime/Zidebactam (WCK 5222) Against Gram-Negative Bacteria," *Journal of Antimicrobial Chemotherapy* 72, no. 5 (2017): 1373–1385.

71. H. S. Sader, R. E. Mendes, L. R. Duncan, C. G. Carvalhaes, and M. Castanheria, "Antimicrobial Activity of Cefepime/Zidebactam (WCK 5222), a β-Lactam/β-Lactam Enhancer Combination, Against Clinical Isolates of Gram-Negative Bacteria Collected Worldwide (2018–19)," *Journal of Antimicrobial Chemotherapy* 77, no. 10 (2022): 2642–2649.

72. A. M. King, D. T. King, S. French, et al., "Structural and Kinetic Characterization of Diazabicyclooctanes as Dual Inhibitors of Both Serine-β-Lactamases and Penicillin-Binding Proteins," *ACS Chemical Biology* 11, no. 4 (2016): 864–868.

73. T. F. Durand-Réville, S. Guler, J. Comita-Prevoir, et al., "ETX2514 Is a Broad-Spectrum β-Lactamase Inhibitor for the Treatment of Drug-Resistant Gram-Negative Bacteria Including *Acinetobacter baumannii*," *Nature Microbiology* 2, no. 9 (2017): 17104.

74. A. B. Shapiro, "Kinetics of Sulbactam Hydrolysis by β-Lactamases, and Kinetics of β-Lactamase Inhibition by Sulbactam," *Antimicrobial Agents and Chemotherapy* 61, no. 12 (2017): e01612-17, https://doi.org/10.1128/aac.01612-01617.

75. K. M. Papp-Wallace, S. M. McLeod, and A. A. Miller, "Durlobactam, a Broad-Spectrum Serine β-lactamase Inhibitor, Restores Sulbactam Activity Against Acinetobacter Species," supplement, *Clinical Infectious Diseases* 76, no. Suppl_2 (2023): S194–S201.

76. T. F. Durand-Réville, J. Comita-Prevoir, J. Zhang, et al., "Discovery of an Orally Available Diazabicyclooctane Inhibitor (ETX0282) of Class A, C, and D Serine β-Lactamases," *Journal of Medicinal Chemistry* 63, no. 21 (2020): 12511–12525.

77. A. A. Miller, A. B. Shapiro, S. M. McLeod, et al., "In Vitro Characterization of ETX1317, a Broad-Spectrum β-Lactamase Inhibitor That Restores and Enhances β-Lactam Activity Against Multi-Drug-Resistant Enterobacteriales, Including Carbapenem-Resistant Strains," *ACS Infectious Diseases* 6, no. 6 (2020): 1389–1397.

78. A. J. Fratoni, A. V. Berry, X. Liu, et al., "Imipenem/Funobactam (Formerly XNW4107) In Vivo Pharmacodynamics Against Serine Carbapenemase-Producing Gram-Negative Bacteria: A Novel Modelling Approach for Time-Dependent Killing," *Journal of Antimicrobial Chemotherapy* 78, no. 9 (2023): 2343–2353.

79. Y. Li, M. Yan, F. Xue, et al., "In Vitro and In Vivo Activities of a Novel β-Lactamase Inhibitor Combination Imipenem/XNW4107 Against Recent Clinical Gram-Negative Bacilli From China," *Journal of Global Antimicrobial Resistance* 31 (2022): 1–9.

80. Z. Huang, X. Yang, Y. Jin, et al., "First-In-Human Study to Evaluate the Safety, Tolerability, and Population Pharmacokinetic/Pharmacodynamic Target Attainment Analysis of FL058 Alone and in Combination With Meropenem in Healthy Subjects," *Antimicrobial Agents and Chemotherapy* 68, no. 1 (2023): e01330-01323.

81. D. T. Davies, S. Leiris, M. Zalacain, et al., "Discovery of ANT3310, a Novel Broad-Spectrum Serine β-Lactamase Inhibitor of the Diazabicyclooctane Class, Which Strongly Potentiates Meropenem Activity Against Carbapenem-Resistant Enterobacterales and *Acinetobacter baumanni*i," *Journal of Medicinal Chemistry* 63, no. 24 (2020): 15802–15820.

82. A. B. Shapiro and N. Gao, "Interactions of the Diazabicyclooctane Serine β-Lactamase Inhibitor ETX1317 With Target Enzymes," *ACS Infectious Diseases* 7, no. 1 (2021): 114–122.

83. Z. Huang, X. Bian, Y. Li, et al., "In Vitro Pharmacokinetics/Pharmacodynamics of FL058 (a Novel Beta-Lactamase Inhibitor) Combined With Meropenem Against Carbapenemase-Producing Enterobacterales," *Frontiers in Pharmacology* 15 (2024): 2024.

84. Z. Tan, Y. Lin, J. Fan, et al., "FL058, a Novel β-Lactamase Inhibitor, Increases the Anti-Mycobacterium Abscessus Activity of Imipenem," *International Journal of Antimicrobial Agents* 65, no. 2 (2025): 107414.

85. M. Zalacain, P. Achard, A. Llanos, et al., "Meropenem-ANT3310, a Unique β-Lactam-β-Lactamase Inhibitor Combination With Expanded Antibacterial Spectrum Against Gram-Negative Pathogens Including Carbapenem-Resistant *Acinetobacter baumannii*," *Antimicrobial Agents and Chemotherapy* 68, no. 3 (2024): e01120-e01123.

86. K. M. Papp-Wallace, A. R. Mack, M. A. Taracila, and R. A. Bonomo, "Resistance to Novel β-Lactam–β-Lactamase Inhibitor Combinations," *Infectious Disease Clinics of North America* 34, no. 4 (2020): 773–819.

87. A. Krajnc, P. A. Lang, T. D. Panduwawala, J. Brem, and C. J. Schofield, "Will Morphing Boron-Based Inhibitors Beat the β-lactamases?," *Current Opinion in Chemical Biology* 50 (2019): 101–110.

88. E. Lence and C. González-Bello, "Bicyclic Boronate β-Lactamase Inhibitors: The Present Hope Against Deadly Bacterial Pathogens," *Advanced Therapeutics* 4, no. 5 (2021): 2000246.

89. E. Caselli, R. A. Powers, L. C. Blasczcak, C. Y. Wu, F. Prati, and B. K. Shoichet, "Energetic, Structural, and Antimicrobial Analyses of Beta-Lactam Side Chain Recognition by Beta-Lactamases," *Chemistry & Biology* 8, no. 1 (2001): 17–31.

90. W. Yang, X. Gao, and B. Wang, "Boronic Acid Compounds as Potential Pharmaceutical Agents," *Medicinal Research Reviews* 23, no. 3 (2003): 346–368.

91. Z. Huang, L. Bai, J. Liu, and Y. Luo, "Boron-Containing Compounds as Antimicrobial Agents to Tackle Drug-Resistant Bacteria," *Pharmaceutical Fronts* 06, no. 04 (2024): e336–e354.

92. M. P. Silva, L. Saraiva, M. Pinto, and M. E. Sousa, "Boronic Acids and Their Derivatives in Medicinal Chemistry: Synthesis and Biological Applications," *Molecules* 25, no. 18 (2020): 4323.

93. R. J. Grams, W. L. Santos, I. R. Scorei, et al., "The Rise of Boron-Containing Compounds: Advancements in Synthesis, Medicinal Chemistry, and Emerging Pharmacology," *Chemical Reviews* 124, no. 5 (2024): 2441–2511.

94. K. Bush and P. A. Bradford, "Interplay Between β-Lactamases and New β-Lactamase Inhibitors," *Nature Reviews Microbiology* 17, no. 5 (2019): 295–306.

95. T. Hillyer and W. S. Shin, "Meropenem/Vaborbactam—A Mechanistic Review for Insight into Future Development of Combinational Therapies," *Antibiotics (USSR)* 13, no. 6 (2024): 472.

96. R. Martin and J. B. Jones, "Rational Design and Synthesis of a Highly Effective Transition State Analog Inhibitor of the RTEM-1 β-Lactamase," *Tetrahedron Letters* 36, no. 46 (1995): 8399–8402.

97. N. C. J. Strynadka, R. Martin, S. E. Jensen, M. Gold, and J. B. Jones, "Structure-Based Design of a Potent Transition State Analogue for TEM-1 β-lactamase," *Nature Structural & Molecular Biology* 3, no. 8 (1996): 688–695.

98. N. C. J. Strynadka, H. Adachi, S. E. Jensen, et al., "Molecular Structure of the Acyl-Enzyme Intermediate in β-Lactam Hydrolysis at 1.7 Å Resolution," *Nature* 359, no. 6397 (1992): 700–705.

99. R. Martin, M. Gold, and J. B. Jones, "Inhibition of the RTEM-1 β-Lactamase by Boronic Acids," *Bioorganic & Medicinal Chemistry Letters* 4, no. 10 (1994): 1229–1234.

100. N. C. J. Strynadka, S. E. Jensen, K. Johns, et al., "Structural and Kinetic Characterization of a β-Lactamase-Inhibitor Protein," *Nature* 368, no. 6472 (1994): 657–660.

101. J. E. Baldwin, T. D. W. Claridge, A. E. Derome, B. D. Smith, M. Twyman, and S. G. Waley, "Direct Observation of a Tetrahedral Boronic acid–β-Lactamase Complex Using 11B NMR Spectroscopy," *Journal of the Chemical Society. Chemical Communications* no. 8 (1991): 573–574.

102. S. Ness, R. Martin, A. M. Kindler, et al., "Structure-Based Design Guides the Improved Efficacy of Deacylation Transition State Analogue Inhibitors of TEM-1 β-Lactamase," *Biochemistry* 39, no. 18 (2000): 5312–5321.

103. L. J. Rojas, M. A. Taracila, K. M. Papp-Wallace, et al., "Boronic Acid Transition State Inhibitors Active Against KPC and Other Class A β-Lactamases: Structure-Activity Relationships as a Guide to Inhibitor Design," *Antimicrobial Agents and Chemotherapy* 60, no. 3 (2016): 1751–1759.

104. Y. Chen, B. Shoichet, and R. Bonnet, "Structure, Function, and Inhibition Along the Reaction Coordinate of CTX-M β-Lactamases," *Journal of the American Chemical Society* 127, no. 15 (2005): 5423–5434.

105. R. A. Powers and B. K. Shoichet, "Structure-Based Approach for Binding Site Identification on AmpC β-Lactamase," *Journal of Medicinal Chemistry* 45, no. 15 (2002): 3222–3234.

106. F. Morandi, E. Caselli, S. Morandi, et al., "Nanomolar Inhibitors of AmpC β-Lactamase," *Journal of the American Chemical Society* 125, no. 3 (2003): 685–695.

107. S. Morandi, F. Morandi, E. Caselli, B. K. Shoichet, and F. Prati, "Structure-Based Optimization of Cephalothin-Analogue Boronic Acids as Beta-Lactamase Inhibitors," *Bioorganic & Medicinal Chemistry* 16, no. 3 (2008): 1195–1205.

108. R. A. Powers, H. C. Swanson, M. A. Taracila, et al., "Biochemical and Structural Analysis of Inhibitors Targeting the ADC-7 Cephalosporinase of *Acinetobacter baumannii*," *Biochemistry* 53, no. 48 (2014): 7670–7679.

109. E. Caselli, C. Romagnoli, R. A. Powers, et al., "Inhibition of Acinetobacter-Derived Cephalosporinase: Exploring the Carboxylate Recognition Site Using Novel β-Lactamase Inhibitors," *ACS Infectious Diseases* 4, no. 3 (2018): 337–348.

110. S. Peppoloni, E. Pericolini, B. Colombari, et al., "The β-Lactamase Inhibitor Boronic Acid Derivative SM23 as a New Anti-*Pseudomonas aeruginosa* Biofilm," *Frontiers in Microbiology* 11 (2020): 35.

111. Q. Tan, A. M. Ogawa, R. E. Painter, Y.-W. Park, K. Young, and F. P. DiNinno, "4,7-Dichloro Benzothien-2-yl Sulfonylaminomethyl Boronic Acid: First Boronic Acid-Derived Beta-Lactamase Inhibitor With Class A, C, and D Activity," *Bioorganic & Medicinal Chemistry Letters* 20, no. 8 (2010): 2622–2624.

112. O. Eidam, C. Romagnoli, E. Caselli, et al., "Design, Synthesis, Crystal Structures, and Antimicrobial Activity of Sulfonamide Boronic Acids as β-Lactamase Inhibitors," *Journal of Medicinal Chemistry* 53, no. 21 (2010): 7852–7863.

113. R. A. Powers, F. Morandi, and B. K. Shoichet, "Structure-Based Discovery of a Novel, Noncovalent Inhibitor of AmpC β-Lactamase," *Structure* 10, no. 7 (2002): 1013–1023.

114. O. Eidam, C. Romagnoli, G. Dalmasso, et al., "Fragment-Guided Design of Subnanomolar β-Lactamase Inhibitors Active In Vivo," *Proceedings of the National Academy of Sciences* 109, no. 43 (2012): 17448–17453.

115. M. L. Introvigne, T. J. Beardsley, M. C. Fernando, et al., "Sulfonamidoboronic Acids as "Cross-Class" Inhibitors of an Expanded-Spectrum Class C Cephalosporinase, ADC-33, and a Class D Carbapenemase, OXA-24/40: Strategic Compound Design to Combat Resistance in *Acinetobacter baumanni*i," *Antibiotics (USSR)* 12, no. 4 (2023): 644.

116. K. Babaoglu and B. K. Shoichet, "Deconstructing Fragment-Based Inhibitor Discovery," *Nature Chemical Biology* 2, no. 12 (2006): 720–723.

117. D. G. Teotico, K. Babaoglu, G. J. Rocklin, R. S. Ferreira, A. M. Giannetti, and B. K. Shoichet, "Docking for Fragment Inhibitors of AmpC β-Lactamase," *Proceedings of the National Academy of Sciences* 106, no. 18 (2009): 7455–7460.

118. A. A. Bouza, H. C. Swanson, K. A. Smolen, et al., "Structure-Based Analysis of Boronic Acids as Inhibitors of Acinetobacter-Derived Cephalosporinase-7, a Unique Class C β-Lactamase," *ACS Infectious Diseases* 4, no. 3 (2018): 325–336.

119. E. Caselli, C. Romagnoli, R. Vahabi, M. A. Taracila, R. A. Bonomo, and F. Prati, "Click Chemistry in Lead Optimization of Boronic Acids as β-Lactamase Inhibitors," *Journal of Medicinal Chemistry* 58, no. 14 (2015): 5445–5458.

120. T. Ishikawa, N. Furukawa, E. Caselli, et al., "Insights Into the Inhibition of MOX-1 β-Lactamase by S02030, a Boronic Acid Transition State Inhibitor," *Frontiers in Microbiology* 12 (2021): 720036.

121. T. A. Alsenani, M. M. Rodríguez, B. Ghiglione, et al., "Boronic Acid Transition State Inhibitors as Potent Inactivators of KPC and CTX-M β-Lactamases: Biochemical and Structural Analyses," *Antimicrobial Agents and Chemotherapy* 67, no. 1 (2023): e00930.

122. R. A. Powers, C. M. June, M. C. Fernando, et al., "Synthesis of a Novel Boronic Acid Transition State Inhibitor, MB076: A Heterocyclic Triazole Effectively Inhibits Acinetobacter-Derived Cephalosporinase Variants With an Expanded-Substrate Spectrum," *Journal of Medicinal Chemistry* 66, no. 13 (2023): 8510–8525.

123. L. J. Rojas, T. B. Nielsen, P. Pantapalangkoor, et al., "Restoring Cefepime Activity Against Multidrug-Resistant KPC-Producing *Klebsiella pneumoniae* by Combination With Boronic Acid Inhibitors, MB076 and S02030," *Antimicrobial Agents and Chemotherapy* 69, no. 3 (2025): e00964-00924.

124. C. Romagnoli, E. Caselli, and F. Prati, "Synthesis of [(1,2,3-Triazol-1-yl)Methyl]boronic Acids Through Click Chemistry: Easy Access to a Potential Scaffold for Protease Inhibitors," *European Journal of Organic Chemistry* 2015, no. 5 (2015): 1075–1083.

125. M. L. Introvigne, M. A. Taracila, F. Prati, E. Caselli, and R. A. Bonomo, "α-Triazolylboronic Acids: A Promising Scaffold for Effective Inhibitors of KPCs," *ChemMedChem* 15, no. 14 (2020): 1283–1288.

126. E. Caselli, F. Fini, M. L. Introvigne, et al., "1,2,3-Triazolylmethaneboronate: A Structure Activity Relationship Study of a Class of β-Lactamase Inhibitors Against *Acinetobacter baumannii* Cephalosporinase," *ACS Infectious Diseases* 6, no. 7 (2020): 1965–1975.

127. Y.-L. Wang, S. Liu, Z.-J. Yu, et al., "Structure-Based Development of (1-(3′-Mercaptopropanamido)Methyl)Boronic Acid Derived Broad-Spectrum, Dual-Action Inhibitors of Metallo- and Serine-β-Lactamases," *Journal of Medicinal Chemistry* 62, no. 15 (2019): 7160–7184.

128. O. Dobozy, I. Mile, and I. V. Ferencz, "Effect of Electrolytes on the Activity and Iodine Sensitivity of Penicillinase From *B. cereus*," *Acta biochimica et biophysica; Academiae Scientiarum Hungaricae* 6, no. 2 (1971): 97–105.

129. P. A. Kiener and S. G. Waley, "Reversible Inhibitors of Penicillinases," *Biochemical Journal* 169, no. 1 (1978): 197–204.

130. S. J. Cartwright and S. G. Waley, "Purification of β-lactamases by Affinity Chromatography on Phenylboronic Acid-Agarose," *Biochemical Journal* 221, no. 2 (1984): 505–512.

131. D. A. Matthews, R. A. Alden, J. J. Birktoft, S. T. Freer, and J. Kraut, "X-Ray Crystallographic Study of Boronic Acid Adducts With Subtilisin BPN′ (Novo). A Model for the Catalytic Transition State," *Journal of Biological Chemistry* 250, no. 18 (1975): 7120–7126.

132. R. N. Lindquist and C. Terry, "Inhibition of Subtilisin by Boronic Acids, Potential Analogs of Tetrahedral Reaction Intermediates," *Archives of Biochemistry and Biophysics* 160, no. 1 (1974): 135–144.

133. M. Philipp and S. Maripuri, "Inhibition of Subtilisin by Substituted Arylboronic Acids," *FEBS Letters* 133, no. 1 (1981): 36–38.

134. T. Beesley, N. Gascoyne, V. Knott-Hunziker, et al., "The Inhibition of Class Cβ-Lactamases by Boronic Acids," *Biochemical Journal* 209, no. 1 (1983): 229–233.

135. I. E. Crompton, B. K. Cuthbert, G. Lowe, and S. G. Waley, "β-Lactamase Inhibitors. The Inhibition of Serine β-Lactamases by Specific Boronic Acids," *Biochemical Journal* 251, no. 2 (1988): 453–459.

136. S. Pazhanisamy and R. F. Pratt, "Beta.-Lactamase-Catalyzed Aminolysis of Depsipeptides: Proof of the Nonexistence of a Specific D-Phenylalanine/Enzyme Complex by Double-Label Isotope Trapping," *Biochemistry* 28, no. 17 (1989): 6870–6875.

137. S. Pazhanisamy, C. P. Govardhan, and R. F. Pratt, "Beta.-Lactamase-Catalyzed Aminolysis of Depsipeptides: Amine Specificity and Steady-State Kinetics," *Biochemistry* 28, no. 17 (1989): 6863–6870.

138. S. Pazhanisamy and R. F. Pratt, "Beta.-Lactamase-Catalyzed Aminolysis of Depsipeptides: Peptide Inhibition and a New Kinetic Mechanism," *Biochemistry* 28, no. 17 (1989): 6875–6882.

139. M. Dryjanski and R. F. Pratt, "Steady-State Kinetics of the Binding of Beta-Lactams and Penicilloates to the Second Binding Site of the Enterobacter Cloacae P99 Beta-Lactamase," *Biochemistry* 34, no. 11 (1995): 3561–3568.

140. K. C. Usher, L. C. Blaszczak, G. S. Weston, B. K. Shoichet, and S. J. Remington, "Three-Dimensional Structure of AmpC β-Lactamase From *Escherichia coli* Bound to a Transition-State Analogue: Possible Implications for the Oxyanion Hypothesis and for Inhibitor Design," *Biochemistry* 37, no. 46 (1998): 16082–16092.

141. G. S. Weston, J. Blázquez, F. Baquero, and B. K. Shoichet, "Structure-Based Enhancement of Boronic Acid-Based Inhibitors of AmpC β-Lactamase," *Journal of Medicinal Chemistry* 41, no. 23 (1998): 4577–4586.

142. D. Tondi, R. A. Powers, E. Caselli, et al., "Structure-Based Design and in-Parallel Synthesis of Inhibitors of AmpC Beta-Lactamase," *Chemistry & Biology* 8, no. 6 (2001): 593–611.

143. D. Tondi, S. Calò, B. K. Shoichet, and M. P. Costi, "Structural Study of Phenyl Boronic Acid Derivatives as Ampc Beta-Lactamase Inhibitors," *Bioorganic & Medicinal Chemistry Letters* 20, no. 11 (2010): 3416–3419.

144. G. Celenza, M. Vicario, P. Bellio, et al., "Phenylboronic Acid Derivatives as Validated Leads Active in Clinical Strains Overexpressing KPC-2: A Step Against Bacterial Resistance," *ChemMedChem* 13, no. 7 (2018): 713–724.

145. P. Linciano, M. Vicario, I. Kekez, et al., "Phenylboronic Acids Probing Molecular Recognition Against Class A and Class C β-Lactamases," *Antibiotics (USSR)* 8, no. 4 (2019): 171.

146. V. Buzzoni, J. Blazquez, S. Ferrari, S. Calò, A. Venturelli, and M. P. Costi, "Aza-Boronic Acids as Non-Beta-Lactam Inhibitors of AmpC-Beta-Lactamase," *Bioorganic & Medicinal Chemistry Letters* 14, no. 15 (2004): 3979–3983.

147. J. Zhou, P. Stapleton, S. Haider, and J. Healy, "Boronic Acid Inhibitors of the Class A β-Lactamase KPC-2," *Bioorganic & Medicinal Chemistry* 26, no. 11 (2018): 2921–2927.

148. W. Ke, C. R. Bethel, K. M. Papp-Wallace, et al., "Crystal Structures of KPC-2 β-Lactamase in Complex With 3-Nitrophenyl Boronic Acid and the Penam Sulfone PSR-3-226," *Antimicrobial Agents and Chemotherapy* 56, no. 5 (2012): 2713–2718.

149. J. Zhou, P. Stapleton, F. H. Xavier-Junior, et al., "Triazole-Substituted Phenylboronic Acids as Tunable Lead Inhibitors of KPC-2 Antibiotic Resistance," *European Journal of Medicinal Chemistry* 240 (2022): 114571.

150. N. Santi, A. Piccirilli, F. Corsini, et al., "Discovery of Boronic Acids-Based β-Lactamase Inhibitors Through In Situ Click Chemistry," *International Journal of Molecular Sciences* 26, no. 9 (2025): 4182.

151. R. A. Powers, J. Blázquez, G. S. Weston, B. K. Shoichet, M.-I. Morosini, and F. Baquero, "The Complexed Structure and Antimicrobial Activity of a Non-β-Lactam Inhibitor of AmpC β-Lactamase," *Protein Science* 8, no. 11 (1999): 2330–2337.

152. A. Venturelli, D. Tondi, L. Cancian, et al., "Optimizing Cell Permeation of an Antibiotic Resistance Inhibitor for Improved Efficacy," *Journal of Medicinal Chemistry* 50, no. 23 (2007): 5644–5654.

153. D. Tondi, A. Venturelli, R. Bonnet, C. Pozzi, B. K. Shoichet, and M. P. Costi, "Targeting Class A and C Serine β-Lactamases With a Broad-Spectrum Boronic Acid Derivative," *Journal of Medicinal Chemistry* 57, no. 12 (2014): 5449–5458.

154. M. Santucci, F. Spyrakis, S. Cross, et al., "Computational and Biological Profile of Boronic Acids for the Detection of Bacterial Serine- and metallo-β-lactamases," *Scientific Reports* 7, no. 1 (2017): 17716.

155. G. Gupta, V. Tak, and P. Mathur, "Detection of AmpC β Lactamases in Gram-Negative Bacteria," *Journal of Laboratory Physicians* 6, no. 01 (2014): 001–006.

156. D. J. Diekema and M. A. Pfaller, "Rapid Detection of Antibiotic-Resistant Organism Carriage for Infection Prevention," *Clinical Infectious Diseases* 56, no. 11 (2013): 1614–1620.

157. K. Joanna, C. Piotr, D. Krzysztof, et al. "Aromatic Diboronic Acids as Effective KPC/AmpC Inhibitors." (2023).

158. Z. Ma, G. Cui, L. Dou, F. Chen, and H. Xie, "2-Carboxyquinoline Boronic Acids as Highly Potent KPC Inhibitors," *ChemMedChem* 20, no. 7 (2025): e202400901.

159. H. R. Snyder, A. J. Reedy, and W. J. Lennarz, "Synthesis of Aromatic Boronic Acids. Aldehydo Boronic Acids and a Boronic Acid Analog of Tyrosine1," *Journal of the American Chemical Society* 80 (1958): 835–838.

160. A. Adamczyk-Woźniak, K. M. Borys, and A. Sporzyński, "Recent Developments in the Chemistry and Biological Applications of Benzoxaboroles," *Chemical Reviews* 115, no. 11 (2015): 5224–5247.

161. S. J. Baker, Y.-K. Zhang, T. Akama, et al., "Discovery of a New Boron-Containing Antifungal Agent, 5-Fluoro-1,3-Dihydro-1-Hydroxy-2,1- Benzoxaborole (AN2690), for the Potential Treatment of Onychomycosis," *Journal of Medicinal Chemistry* 49, no. 15 (2006): 4447–4450.

162. F. L. Rock, W. Mao, A. Yaremchuk, et al., "An Antifungal Agent Inhibits an Aminoacyl-tRNA Synthetase by Trapping tRNA in the Editing Site," *Science* 316, no. 5832 (2007): 1759–1761.

163. T. Akama, S. J. Baker, Y.-K. Zhang, et al., "Discovery and Structure–Activity Study of a Novel Benzoxaborole Anti-Inflammatory Agent (AN2728) for the Potential Topical Treatment of Psoriasis and Atopic Dermatitis," *Bioorganic & Medicinal Chemistry Letters* 19, no. 8 (2009): 2129–2132.

164. Y. Xia, K. Cao, Y. Zhou, et al., "Synthesis and Sar of Novel Benzoxaboroles as a New Class of β-Lactamase Inhibitors," *Bioorganic & Medicinal Chemistry Letters* 21, no. 8 (2011): 2533–2536.

165. D. C. McKinney, F. Zhou, C. J. Eyermann, et al., "4,5-Disubstituted 6-Aryloxy-1,3-Dihydrobenzo[c][1,2]Oxaboroles Are Broad-Spectrum Serine β-Lactamase Inhibitors," *ACS Infectious Diseases* 1, no. 7 (2015): 310–316.

166. Y.-C. Xiao, X.-P. Chen, J. Deng, et al., "Design and Enantioselective Synthesis of 3-(α-Acrylic Acid) Benzoxaboroles to Combat Carbapenemase Resistance," *Chemical Communications* 57, no. 62 (2021): 7709–7712.

167. Y.-H. Yan, Z.-F. Li, X.-L. Ning, et al., "Discovery of 3-aryl Substituted Benzoxaboroles as Broad-Spectrum Inhibitors of Serine- and Metallo-β-Lactamases," *Bioorganic & Medicinal Chemistry Letters* 41 (2021): 127956.

168. G.-Q. Liang, Y.-Y. Jiang, C.-L. Han, et al., "Discovery of 3-Methacylic Acid Substituted Benzoxaboroles as Dual Metallo- and Serine-β-Lactamase Inhibitors," *European Journal of Medicinal Chemistry* 293 (2025): 117723.

169. S. J. Hecker, K. R. Reddy, M. Totrov, et al., "Discovery of a Cyclic Boronic Acid β-Lactamase Inhibitor (RPX7009) With Utility vs Class A Serine Carbapenemases," *Journal of Medicinal Chemistry* 58, no. 9 (2015): 3682–3692.

170. G. W. Langley, R. Cain, J. M. Tyrrell, et al., "Profiling Interactions of Vaborbactam With Metallo-β-Lactamases," *Bioorganic & Medicinal Chemistry Letters* 29, no. 15 (2019): 1981–1984.

171. R. Tsivkovski and O. Lomovskaya, "Biochemical Activity of Vaborbactam," *Antimicrobial Agents and Chemotherapy* 64, no. 2 (2020): e01935-19, https://doi.org/10.1128/aac.01935-01919.

172. L. Dortet, L. Poirel, S. Abbas, S. Oueslati, and P. Nordmann, "Genetic and Biochemical Characterization of FRI-1, a Carbapenem-Hydrolyzing Class A β-Lactamase From *Enterobacter cloacae*," *Antimicrobial Agents and Chemotherapy* 59, no. 12 (2015): 7420–7425.

173. O. Lomovskaya, D. Sun, D. Rubio-Aparicio, et al., "Vaborbactam: Spectrum of Beta-Lactamase Inhibition and Impact of Resistance Mechanisms on Activity in Enterobacteriaceae," *Antimicrobial Agents and Chemotherapy* 61, no. 11 (2017): e01443-17, https://doi.org/10.1128/aac.01443-01417.

174. L. Principe, T. Lupia, L. Andriani, et al., "Microbiological, Clinical, and PK/PD Features of the New Anti-Gram-Negative Antibiotics: β-Lactam/β-Lactamase Inhibitors in Combination and Cefiderocol—An All-Inclusive Guide for Clinicians," *Pharmaceuticals* 15, no. 4 (2022): 463.

175. R. M. Burgos, M. J. Biagi, K. A. Rodvold, and L. H. Danziger, "Pharmacokinetic Evaluation of Meropenem and Vaborbactam for the Treatment of Urinary Tract Infection," *Expert Opinion on Drug Metabolism & Toxicology* 14, no. 10 (2018): 1007–1021.

176. L. A. H. O. Petty, T. S. Patel, J. M. Pogue, and K. S. Kaye, "Overview of Meropenem-Vaborbactam and Newer Antimicrobial Agents for the Treatment of Carbapenem-Resistant Enterobacteriaceae," *Infection and Drug Resistance* 11 (2018): 1461–1472.

177. S. C. J. Jorgensen and M. J. Rybak, "Meropenem and Vaborbactam: Stepping Up the Battle Against Carbapenem-Resistant Enterobacteriaceae," *Pharmacotherapy: Journal of Human Pharmacology and Drug Therapy* 38, no. 4 (2018): 444–461.

178. G. G. Zhanel, C. K. Lawrence, H. Adam, et al., "Imipenem–Relebactam and Meropenem–Vaborbactam: Two Novel Carbapenem-β-Lactamase Inhibitor Combinations," *Drugs* 78, no. 1 (2018): 65–98.

179. S. Dhillon, "Meropenem/Vaborbactam: A Review in Complicated Urinary Tract Infections," *Drugs* 78, no. 12 (2018): 1259–1270.

180. D. Sun, D. Rubio-Aparicio, K. Nelson, M. N. Dudley, and O. Lomovskaya, "Meropenem-Vaborbactam Resistance Selection, Resistance Prevention, and Molecular Mechanisms in Mutants of KPC-Producing *Klebsiella pneumoniae*," *Antimicrobial Agents and Chemotherapy* 61, no. 12 (2017): e01694-17, https://doi.org/10.1128/aac.01694-01617.

181. O. A. Pemberton, R. Tsivkovski, M. Totrov, O. Lomovskaya, and Y. Chen, "Structural Basis and Binding Kinetics of Vaborbactam in Class A β-Lactamase Inhibition," *Antimicrobial Agents and Chemotherapy* 64, no. 10 (2020): aac.00398-20, https://doi.org/10.1128/aac.00398-00320.

182. B. Liu, R. E. L. Trout, G.-H. Chu, et al., "Discovery of Taniborbactam (VNRX-5133): A Broad-Spectrum Serine- and Metallo-β-Lactamase Inhibitor for Carbapenem-Resistant Bacterial Infections," *Journal of Medicinal Chemistry* 63, no. 6 (2020): 2789–2801.

183. S. T. Cahill, R. Cain, D. Y. Wang, et al., "Cyclic Boronates Inhibit All Classes of β-Lactamases," *Antimicrobial Agents and Chemotherapy* 61, no. 4 (2017): e02260-16, https://doi.org/10.1128/aac.02260-02216.

184. A. Krajnc, J. Brem, P. Hinchliffe, et al., "Bicyclic Boronate VNRX-5133 Inhibits Metallo- and Serine-β-Lactamases," *Journal of Medicinal Chemistry* 62, no. 18 (2019): 8544–8556.

185. J. C. Hamrick, J.-D. Docquier, T. Uehara, et al., "VNRX-5133 (Taniborbactam), a Broad-Spectrum Inhibitor of Serine- and Metallo-β-Lactamases, Restores Activity of Cefepime in Enterobacterales and *Pseudomonas aeruginosa*," *Antimicrobial Agents and Chemotherapy* 64, no. 3 (2020): e01963-19, https://doi.org/10.1128/aac.01963-01919.

186. C. L. Tooke, P. Hinchliffe, A. Krajnc, et al., "Cyclic Boronates as Versatile Scaffolds for KPC-2 β-Lactamase Inhibition," *RSC Medicinal Chemistry* 11, no. 4 (2020): 491–496.

187. T. Uehara, C. L. Chatwin, B. Miller, et al., "Spectrum of Cefepime-Taniborbactam Coverage Against 190 β-Lactamases Defined in Engineered Isogenic *Escherichia coli* Strains," *Antimicrobial Agents and Chemotherapy* 69, no. 5 (2025): e01699-01624.

188. J. A. Karlowsky, M. G. Wise, M. A. Hackel, et al., "Cefepime–Taniborbactam Activity Against Antimicrobial-Resistant Clinical Isolates of Enterobacterales and *Pseudomonas aeruginosa*: GEARS Global Surveillance Programme 2018–22," *Journal of Antimicrobial Chemotherapy* 79, no. 12 (2024): 3116–3131.

189. F. M. Wagenlehner, L. B. Gasink, P. C. McGovern, et al., "Cefepime–Taniborbactam in Complicated Urinary Tract Infection," *New England Journal of Medicine* 390, no. 7 (2024): 611–622.

190. G. G. Zhanel, C. Mansour, S. Mikolayanko, et al., "Cefepime–Taniborbactam: A Novel Cephalosporin/β-Lactamase Inhibitor Combination," *Drugs* 84, no. 10 (2024): 1219–1250.

191. M. Hackel, M. G. Wise, G. Moeck, and D. F. Sahm, "P-1514. Cefepime-Taniborbactam Exhibits Limited Cross-Resistance With Ceftazidime-Avibactam and Ceftolozane-Tazobactam Against Carbapenem-Nonsusceptible Enterobacterales and Multidrug-Resistant *Pseudomonas aeruginosa* From the United States 2018–2022," *suppl, Open Forum Infectious Diseases* 12, no. S1 (2025): ofae631.1683.

192. S. J. Hecker, K. R. Reddy, O. Lomovskaya, et al., "Discovery of Cyclic Boronic Acid QPX7728, an Ultrabroad-Spectrum Inhibitor of Serine and Metallo-β-Lactamases," *Journal of Medicinal Chemistry* 63, no. 14 (2020): 7491–7507.

193. R. Tsivkovski, M. Totrov, and O. Lomovskaya, "Biochemical Characterization of QPX7728, a New Ultrabroad-Spectrum Beta-Lactamase Inhibitor of Serine and Metallo-Beta-Lactamases," *Antimicrobial Agents and Chemotherapy* 64, no. 6 (2020): e00130-20, https://doi.org/10.1128/aac.00130-00120.

194. K. Nelson, D. Rubio-Aparicio, D. Sun, M. Dudley, and O. Lomovskaya, "In Vitro Activity of the Ultrabroad-Spectrum-Beta-Lactamase Inhibitor QPX7728 Against Carbapenem-Resistant Enterobacterales With Varying Intrinsic and Acquired Resistance Mechanisms," *Antimicrobial Agents and Chemotherapy* 64, no. 8 (2020): e00757-20, https://doi.org/10.1128/aac.00757-00720.

195. O. Lomovskaya, R. Tsivkovski, K. Nelson, et al., "Spectrum of Beta-Lactamase Inhibition by the Cyclic Boronate QPX7728, an Ultrabroad-Spectrum Beta-Lactamase Inhibitor of Serine and Metallo-Beta-Lactamases: Enhancement of Activity of Multiple Antibiotics Against Isogenic Strains Expressing Single Beta-Lactamases," *Antimicrobial Agents and Chemotherapy* 64, no. 6 (2020): e00212-20, https://doi.org/10.1128/aac.00212-00220.

196. O. Lomovskaya, K. Nelson, D. Rubio-Aparicio, R. Tsivkovski, D. Sun, and M. N. Dudley, "Impact of Intrinsic Resistance Mechanisms on Potency of QPX7728, a New Ultrabroad-Spectrum Beta-Lactamase Inhibitor of Serine and Metallo-Beta-Lactamases in Enterobacteriaceae, *Pseudomonas aeruginosa*, and *Acinetobacter baumannii*," *Antimicrobial Agents and Chemotherapy* 64, no. 6 (2020): e00552-20, https://doi.org/10.1128/aac.00552-00520.

197. O. Lomovskaya, D. Rubio-Aparicio, K. Nelson, et al., "In Vitro Activity of the Ultrabroad-Spectrum Beta-Lactamase Inhibitor QPX7728 in Combination With Multiple Beta-Lactam Antibiotics Against *Pseudomonas aeruginosa*," *Antimicrobial Agents and Chemotherapy* 65, no. 6 (2021): e00210-21, https://doi.org/10.1128/aac.00210-00221.

198. O. Lomovskaya, D. Rubio-Aparicio, R. Tsivkovski, J. Loutit, and M. Dudley, "The Ultrabroad-Spectrum Beta-Lactamase Inhibitor QPX7728 Restores the Potency of Multiple Oral Beta-Lactam Antibiotics Against Beta-Lactamase-Producing Strains of Resistant Enterobacterales," *Antimicrobial Agents and Chemotherapy* 66, no. 2 (2022): e02168-02121.

199. O. Lomovskaya, M. Castanheira, J. Lindley, et al., "In Vitro Potency of Xeruborbactam in Combination With Multiple β-Lactam Antibiotics in Comparison With Other β-Lactam/β-Lactamase Inhibitor (BLI) Combinations Against Carbapenem-Resistant and Extended-Spectrum β-Lactamase-Producing Enterobacterales," *Antimicrobial Agents and Chemotherapy* 67, no. 11 (2023): e00440-00423.

200. K. R. Reddy, J. Parkinson, M. Sabet, et al., "Selection of QPX7831, an Orally Bioavailable Prodrug of Boronic Acid β-Lactamase Inhibitor QPX7728," *Journal of Medicinal Chemistry* 64, no. 23 (2021): 17523–17529.

201. R. E. Trout, A. Zulli, E. Mesaros, et al., "Discovery of VNRX-7145 (VNRX-5236 Etzadroxil): An Orally Bioavailable β-Lactamase Inhibitor for Enterobacterales Expressing Ambler Class A, C, and D Enzymes," *Journal of Medicinal Chemistry* 64, no. 14 (2021): 10155–10166.

202. C. L. Chatwin, J. C. Hamrick, R. Trout, et al., "Microbiological Characterization of VNRX-5236, a Broad-Spectrum β-Lactamase Inhibitor for Rescue of the Orally Bioavailable Cephalosporin Ceftibuten as a Carbapenem-Sparing Agent Against Strains of Enterobacterales Expressing Extended-Spectrum β-Lactamases and Serine Carbapenemases," *Antimicrobial Agents and Chemotherapy* 65, no. 8 (2021): 0055221, https://doi.org/10.1128/aac.00552-00521.

203. C. L. Myers, A. Stevenson, B. Miller, D. M. Daigle, T. Uehara, and D. C. Pevear, "Cefepime–Taniborbactam and Ceftibuten–Ledaborbactam Maintain Activity Against KPC Variants That Lead to Ceftazidime–Avibactam Resistance," *Antimicrobial Agents and Chemotherapy* 69, no. 3 (2025): e01511–e01524.

204. J. A. Karlowsky, M. A. Hackel, and D. F. Sahm, "In Vitro Activity of Ceftibuten/VNRX-5236 Against Urinary Tract Infection Isolates of Antimicrobial-Resistant Enterobacterales," *Antimicrobial Agents and Chemotherapy* 66, no. 1 (2022): e01304–e01321.

205. R. E. Mendes, P. R. Rhomberg, A. A. Watters, and M. Castanheira, "In Vitro Activity of the Orally Bioavailable ceftibuten/VNRX-7145 (VNRX-5236 Etzadroxil) Combination Against a Challenge Set of Enterobacterales Pathogens Carrying Molecularly Characterized β-Lactamase Genes," *Journal of Antimicrobial Chemotherapy* 77, no. 3 (2022): 689–694.

206. A. J. Fratoni, L. M. Avery, D. P. Nicolau, and T. E. Asempa, "In Vivo Pharmacokinetics and Pharmacodynamics of Ceftibuten/Ledaborbactam, a Novel Oral β-Lactam/β-Lactamase Inhibitor Combination," *Journal of Antimicrobial Chemotherapy* 78, no. 1 (2023): 93–100.

207. K. Takemoto, R. Nakayama, K. Fujimoto, et al., "In Vitro and In Vivo Activities of KSP-1007, a Broad-Spectrum Inhibitor of Serine- and Metallo-β-Lactamases, in Combination With Meropenem Against Carbapenem-Resistant Gram-Negative Bacteria," *Antimicrobial Agents and Chemotherapy* 68, no. 6 (2024): e01602–e01623.

208. K. Takemoto, M. Kamada, K. Matsushita, H. Matsui, J. Hidaka, and H. Hanaki, "Pharmacokinetics/Pharmacodynamics of KSP-1007 in Combination With Meropenem Against Carbapenemase-Producing Gram-Negative Bacteria in a Neutropenic Murine Thigh Infection Model," *Antimicrobial Agents and Chemotherapy* 70, no. 4 (2026): e01852.

209. S. G. Kurz, S. Hazra, C. R. Bethel, et al., "Inhibiting the β-Lactamase of *Mycobacterium tuberculosis* (Mtb) With Novel Boronic Acid Transition-State Inhibitors (BATSIs)," *ACS Infectious Diseases* 1, no. 6 (2015): 234–242.

210. V. T. Nguyen, B. T. Birhanu, V. Miguel-Ruano, et al., "Restoring Susceptibility to β-Lactam Antibiotics in Methicillin-Resistant *Staphylococcus aureus*," *Nature Chemical Biology* 21, no. 4 (2025): 482–489.